Official Journal of the ISRS/AAO

NOVEMBER 2006
Volume 22 (Suppl) • Number 9

Journal of Refractive Surgery®

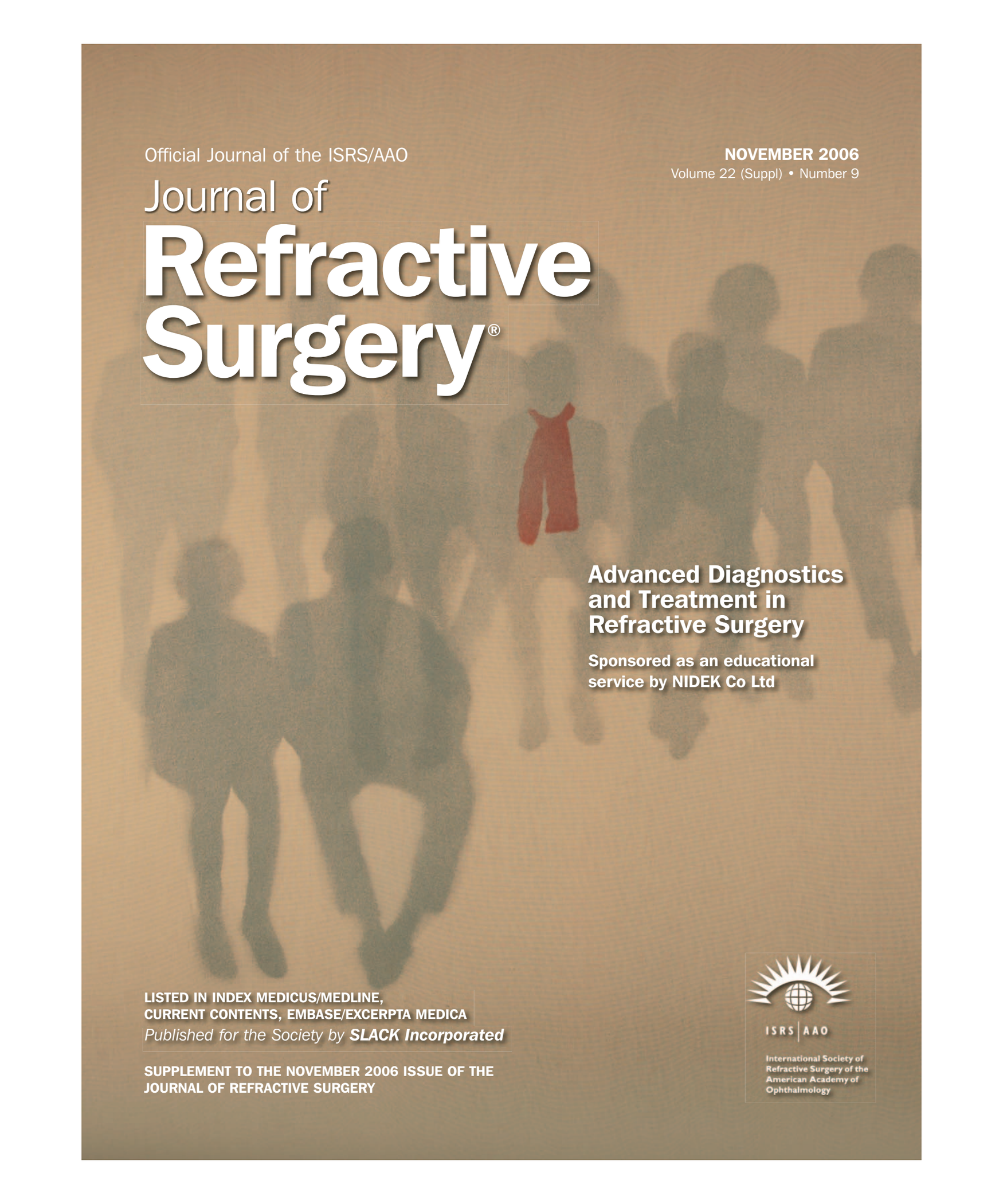

Advanced Diagnostics and Treatment in Refractive Surgery

Sponsored as an educational service by NIDEK Co Ltd

LISTED IN INDEX MEDICUS/MEDLINE, CURRENT CONTENTS, EMBASE/EXCERPTA MEDICA

Published for the Society by ***SLACK Incorporated***

SUPPLEMENT TO THE NOVEMBER 2006 ISSUE OF THE JOURNAL OF REFRACTIVE SURGERY

ISRS | AAO

International Society of Refractive Surgery of the American Academy of Ophthalmology

NOVEMBER 2006
Volume 22 (Suppl) • Number 9

Official Journal of the ISRS/AAO

Journal of Refractive Surgery®

Advanced Diagnostics and Treatment In Refractive Surgery

Paul Dougherty, MD, Guest Editor

GUEST EDITORIAL

S1012 **Introduction to Advanced Diagnostics and Treatment in Refractive Surgery**
Paul Dougherty, MD, Guest Editor

OPD-SCAN DIAGNOSIS

S1014 **Measurement of Combined Corneal, Internal, and Total Ocular Optical Quality Analysis in Anterior Segment Pathology With the OPD-Scan and OPD-Station**
Damien Gatinel, MD; Thanh Hoang-Xuan, MD

S1021 **Precision of NIDEK OPD-Scan Measurements**
Mike P. Holzer, MD; Susanne Goebels; Gerd U. Auffarth, MD

S1024 **Wavefront Analysis in Asian-Brazilians**
Eliane Mayumi Nakano, MD; Harkaran Bains, MD; Kozo Nakano, MD; Celso Nakano, MD; Waldir Portellinha, MD; Marivaldo Oliveira, MD; Lenio Alvarenga, MD

S1027 **Comparison of Measurement of Pupil Sizes Among the Colvard Pupillometer, Procyon Pupillometer, and NIDEK OPD-Scan**
Claire McDonnell, MCOptom; Martina Rolincova, MSc; Jan Venter, MD

S1031 **Optical Quality Analysis After Surface Excimer Laser Ablation: The Relationship Between Wavefront Aberration and Subepithelial Haze**
Yan Wang, MD; Jichang He, PhD; Kanxing Zhao, MD, PhD; Ying Jin, MD; Tong Zuo, OD; Wei Wang, PhD

S1037 **Precision of Higher Order Aberration Repeatability With NIDEK OPD-Scan Retinoscopic Aberrometry**
Jackson Barreto, Jr, MD; Marcelo V. Netto, MD; Alberto Cigna, MD; Samir Bechara, MD; Newton Kara-José, MD

CONFOCAL MICROSCOPY

S1041 **Clinical Use of In Vivo Confocal Microscopy Through Focusing in Corneal Refractive Surgery**
Li Ying, MD, PhD; Zhang Xiao; Zhong Liuxueying; Jin Yumei

S1047 **Corneal Diabetic Neuropathy: A Confocal Microscopy Study**
Edoardo Midena, MD; Erica Brugin, MD; Alessandra Ghirlando, MD; Marco Sommavilla, MD; Angelo Avogaro, MD

CUSTOMIZED LASIK

S1053 **Improvement of Best Spectacle-corrected Visual Acuity After LASIK in Highly Myopic Eyes With Reduced Preoperative Best Spectacle-corrected Visual Acuity**
Rui He, MB; Min Qu, MM; Yi Fen, MM; Shun Yu, MB

S1056 **Optical Factors in Increased Best Spectacle-corrected Visual Acuity After LASIK**
Uzeyir Erdem, MD; Orkun Muftuoglu, MD

HYPEROPIA, ASTIGMATISM, AND PRESBYOPIA

S1069 **LASIK Using the NIDEK EC-5000 for the Correction of Hyperopic Astigmatism**
Mahmoud M. Ismail, MD, PhD

S1073 **Correction of High Astigmatism: Case Studies Using the Mixed-cylinder Approach**
Hamza N. Khan, MD, MPH, FRCSC; Geoffrey B. Kaye, MBChB, FCS(SA), FRCSC; Jean Luc Febbraro, MD

CATARACT INCISIONS

S1079 **Corneal Astigmatism, High Order Aberrations, and Optical Quality After Cataract Surgery: Microincision Versus Small Incision**
Ke Yao, MD; Xiajing Tang, MD; Panpan Ye, MD

S1083 **Changes in Corneal Astigmatism and High Order Aberrations After Clear Corneal Tunnel Phacoemulsification Guided by Corneal Topography**
Yongxiang Jiang, PhD; Qihua Le, PhD; Jin Yang, MD; Yi Lu, MD

NEW TECHNIQUES

S1089 **Automated Visual Axis Alignment for Refractive Excimer Laser Ablation**
Omid Kermani, MD

Introduction to Advanced Diagnostics and Treatment in Refractive Surgery

Paul Dougherty, MD, Guest Editor

Welcome to the latest edition of the NIDEK-sponsored supplement to the *Journal of Refractive Surgery*. I have been given the honor once again by George O. Waring III, MD, Editor-in-Chief, to edit these varied, but very interesting and important articles. These articles have been produced by some of the most recognized international leaders in refractive surgery together with less well-known surgeons from virtually every continent in the world. Articles such as these that are produced in countries where the newest refractive technology is available and not subject to United States Food and Drug Administration review provide a glimpse into the future of our practices here in the States.

This supplement is sponsored by NIDEK Co Ltd. Although this company is based in Gamagori, Japan, it truly has a global perspective when it comes to ophthalmology and refractive surgery. This company, founded by visionary engineer and entrepreneur Hideo Ozawa, has a tremendous commitment to refractive surgery. Sponsorship of these supplements on a yearly basis demonstrates the commitment that this company has to educating surgeons and bringing refractive surgery technology into the 21st century.

I am amazed by the fact that there are many more similarities than differences in practice styles when I talk with surgeons from Asia, Europe, and South America. The techniques and technology I encounter in my discussions with surgeons in China demonstrate that the surgeons in this supposedly "emerging" economy have access to more advanced technology than we have in the supposedly "developed" United States. The articles in this supplement reflect how flat the refractive surgery world has become.

Although NIDEK has been hampered by slow regulatory approvals in the United States, it is the leader worldwide in developing new and unique diagnostic and therapeutic technologies for use in vision correction. Surgeons in the United States will soon have access to many of the wonderful technologies described herein, including hyperopic, aspheric, and customized treatments with the NIDEK laser. As a US investigator for some of these technologies, I have had the opportunity to experience the fantastic outcomes and high level of patient satisfaction with these technologies.

This supplement is comprised of a variety of topics from surgeons from all over the world including Brazil, Canada, China, Egypt, France, Italy, Germany, Japan, Turkey, the United Kingdom, and the United States. The supplement is broken down into six sections including OPD-Scan Diagnosis; Confocal Microscopy; Customized LASIK; Hyperopia, Astigmatism, and Presbyopia; Cataract Incisions; and New Techniques.

Outcomes from topography-guided (CATz) and whole-eye wavefront-guided (OPDCAT) treatments are discussed in a number of articles in this supplement. Although "optical zones" used with the newer CATz and OPDCAT software of 4.5 to 5.5 mm (combined with transition zones out to 10 mm) seem smaller than other lasers, the newer ablation profiles result in some of the largest effective optical zones and best quality of vision in the industry. With NAVEX technology, traditional definitions of optical and transition zones need to be cast aside as the two zones seamlessly join into one another to create a functional optical zone of up to 10 mm.

The articles that appear within this supplement are not formally peer reviewed. However, each paper was editorially reviewed by Dr Waring and myself. Because of this, these articles are published as a supplement to the *Journal of Refractive Surgery* with "S" pagination. In the past 10 years, the NIDEK supplement to the Journal has eminated from an international symposium sponsored by NIDEK and thus was designated as "Proceedings." This year, the papers are culled from submissions by users and were not presented at a meeting.

From Dougherty Laser Vision, Camarillo, Calif.

Correspondence: Paul Dougherty, MD, Dougherty Laser Vision, 1821 Daily Dr, Camarillo, CA 93101. Tel: 805.987.5300; Fax: 805.987.5330; E-mail: info@doughertylaservision.com

I extend special thanks to three individuals who helped me with the production of this supplement: Rich Bains, special consultant to NIDEK, for all of his hard work in collecting and doing the initial edit of these manuscripts (I am convinced that Rich's other occupation is that of clairvoyant, given his ability to edit text from such a wide variety of authors); Dr George Waring for his invitation to again be the guest editor as well as his mentoring over the past few years; and Aileen Wiegand, the managing editor of the *Journal of Refractive Surgery*, who does an amazing job of organizing and editing the manuscripts and keeping the supplement on time.

The process of working with surgeons from around the world to put together this supplement has been both stimulating and fun. I am sure you will find the following articles informative and thought provoking.

Measurement of Combined Corneal, Internal, and Total Ocular Optical Quality Analysis in Anterior Segment Pathology With the OPD-Scan and OPD-Station

Damien Gatinel, MD; Thanh Hoang-Xuan, MD

ABSTRACT

PURPOSE: To show the clinical use of the NIDEK OPD-Scan wavefront aberrometer and OPD-Station software in anterior segment surgery and pathology.

METHODS: Case examples are presented along with discussion about the relevant clinical data obtained from the OPD-Scan and OPD-Station software.

RESULTS: Six case examples including cataract surgery, secondary IOL implantation, phakic intraocular lens surgery, pterygium surgery, contact lens fitting, and multifocal ablations are discussed.

CONCLUSIONS: A complete understanding of the optics of the eye facilitates a better clinical comprehension of a variety of conditions in anterior segment surgery and pathology. [*J Refract Surg*. 2006;22:S1014-S1020.]

Wavefront aberrometers are increasingly used in mainstream ophthalmology. Wavefront aberrometers provide the critical first step in the measurement and correction of the spherical and cylindrical components of the refractive error in addition to the higher order aberrations of the visual system that affect visual performance. The ability to acquire a more detailed measurement of the optics of the eye may allow for achieving optical visual outcomes beyond those currently seen using conventional subtractive or additive refractive surgical procedures.[1,2]

Wavefront aberrometers are tools to diagnose visual complaints of optical origin. Hence, the use of wavefront sensors should not be restricted to the field of wavefront-guided laser correction but should be used in any clinical situation that requires precise assessment of the optical quality of the eye. The crystalline lens and the cornea contribute to the optical quality of the eye by balancing their respective aberrations in normal eyes.[3,4] The recent introduction of aspheric intraocular lenses (IOLs) to reduce the total spherical aberration and improve the optical quality of the pseudophakic eye is one potential application of aberrometry. Ideally, one may want to quantify the aberrations of the cataractous eye preoperatively to select the best IOL shape that would compensate for the corneal spherical aberration. This would require precise measurements of the preoperative corneal spherical aberration. Wavefront aberrometry could also be used postoperatively to determine the induced aberrations and their effect on visual quality. However, only a few aberrometers exist that can separately quantify the aberrations of the anterior corneal surface and internal optics of the eye.

In this article, we describe the use of one such aberrometer, the NIDEK OPD-Scan with OPD-Station software (NIDEK Co Ltd, Gamagori, Japan), in anterior segment surgery and pathology, separate from its use in customized ablations, and show its application as an "everyday practice tool."

From the Rothschild Foundation, YAP-HP Bichat Claude Bernard Hospital, Paris VII University, Paris, France.

The authors have no financial interest in the materials presented herein.

Correspondence: Damien Gatinel, MD, 25 rue Manin, 75019 Paris, France. E-mail: gatinel@aol.com

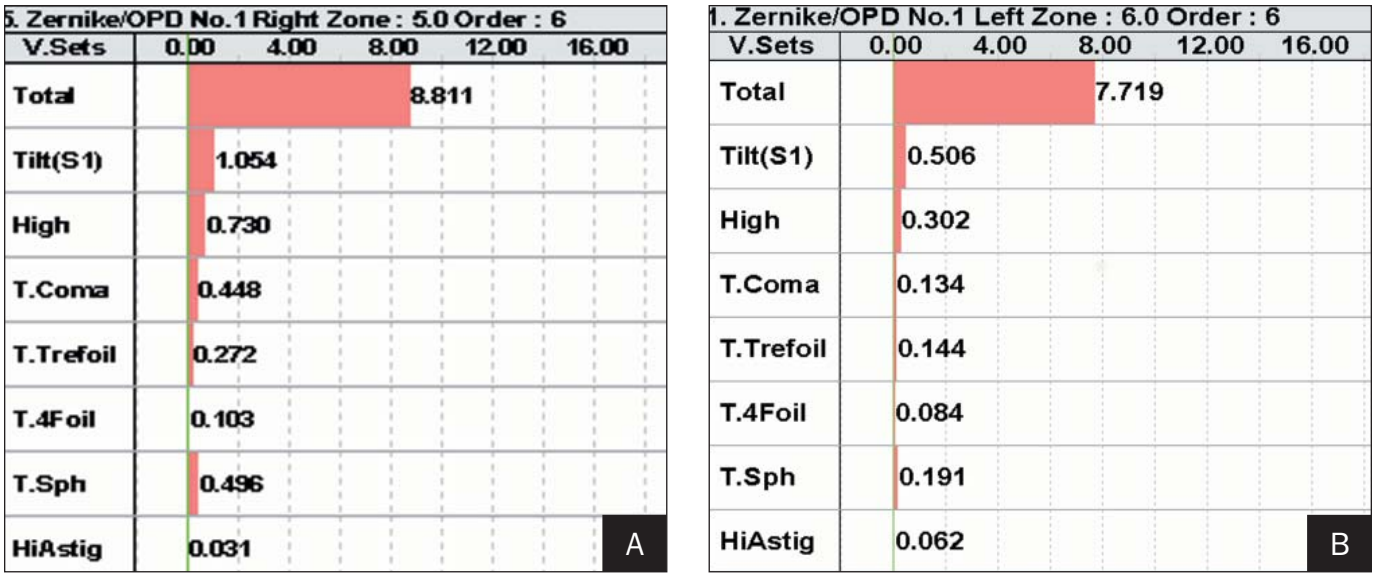

Figure 1. *Case 1.* Zernike analysis of the aberrations of the **A**) right and **B)** left eye out to the sixth order. Root-mean-square values in microns are shown for a 5-mm pupil. Aberrations for the entire eye are tabulated for the total aberrations (Total); tilt; higher-order aberration (High); total coma aberration (T. Coma); total trefoil (T. Trefoil); total quadrafoil (T. 4Foil); total spherical aberration (T. Sph); and higher order astigmatism (HiAstig).

PATIENTS AND METHODS

Six patients undergoing anterior segment surgery are used to illustrate the use of the NIDEK OPD-Scan with OPD-Station software as an aid in clinical assessment, diagnosis, and treatment planning. The OPD-Scan is a multifunction instrument that combines Placido-based corneal topography with wavefront aberrometry of the entire eye. This wavefront measuring apparatus is based on retinoscopic principles that use a slit of infrared light to scan along all 360° meridians over a 6-mm pupil. The timing and scan rate of the reflected light are analyzed with an array of photodetectors to determine the wavefront aberrations along each meridian.

In addition to the determination of an accurate refraction,[5] the OPD-Scan provides a complete set of maps, including four different corneal topography maps, local refractive power of the entire eye due to aberrations at various locations within the pupil, a variety of wavefront aberration maps, and photopic and mesopic pupillometry.[6] By computing the corneal wavefront aberration and comparing it with the total wavefront map, it is possible to estimate optical quality due to the internal aberrations of the eye. The internal aberrations represent all aberrations behind the anterior corneal surface. The data provided by the OPD-Scan can be further processed using the OPD-Station software to compute useful metrics of optical quality such as the modulation transfer function (MTF) or to simulate maximum contrast visual acuity charts corresponding to the entire eye, cornea, or internal aberrations. The MTF corresponds to the variation of image contrast with spatial frequency for an object with 100% contrast. The MTF is a quantitative measure of image quality that is far superior to classic resolution criteria, because it describes the ability of the eye to transfer object contrast to the image. The MTF corresponds to the ratio of image contrast to object contrast as a function of the spatial frequency of a sinusoidal grating. The MTF describes the contrast at each spatial frequency, usually normalized to range from zero to one, zero being gray (no contrast) and one being perfect black/white contrast. If an object grating of a given spatial frequency is imaged by the eye, the intensity contrast of adjacent bars in the image at the same spatial frequency will be given by the transfer function. Perfect imagery of black/white motifs corresponds to a transfer function of one. Conversely, when the transfer function is zero, the bars in the image will undergo complete washout and appear as continuous shades of gray. The OPD-Station software allows the determination of the MTF of the entire eye as well as for each of its main optical components (cornea and lens). In addition, the effect of total higher order aberrations, specific aberrations (eg, spherical aberration), and combinations of aberrations[7] on the MTF and visual acuity charts can be determined.

CASE EXAMPLES

PRIMARY CATARACT SURGERY

Case 1. A 55-year-old man presented with unilateral reduced vision. The patient wore spectacles with the

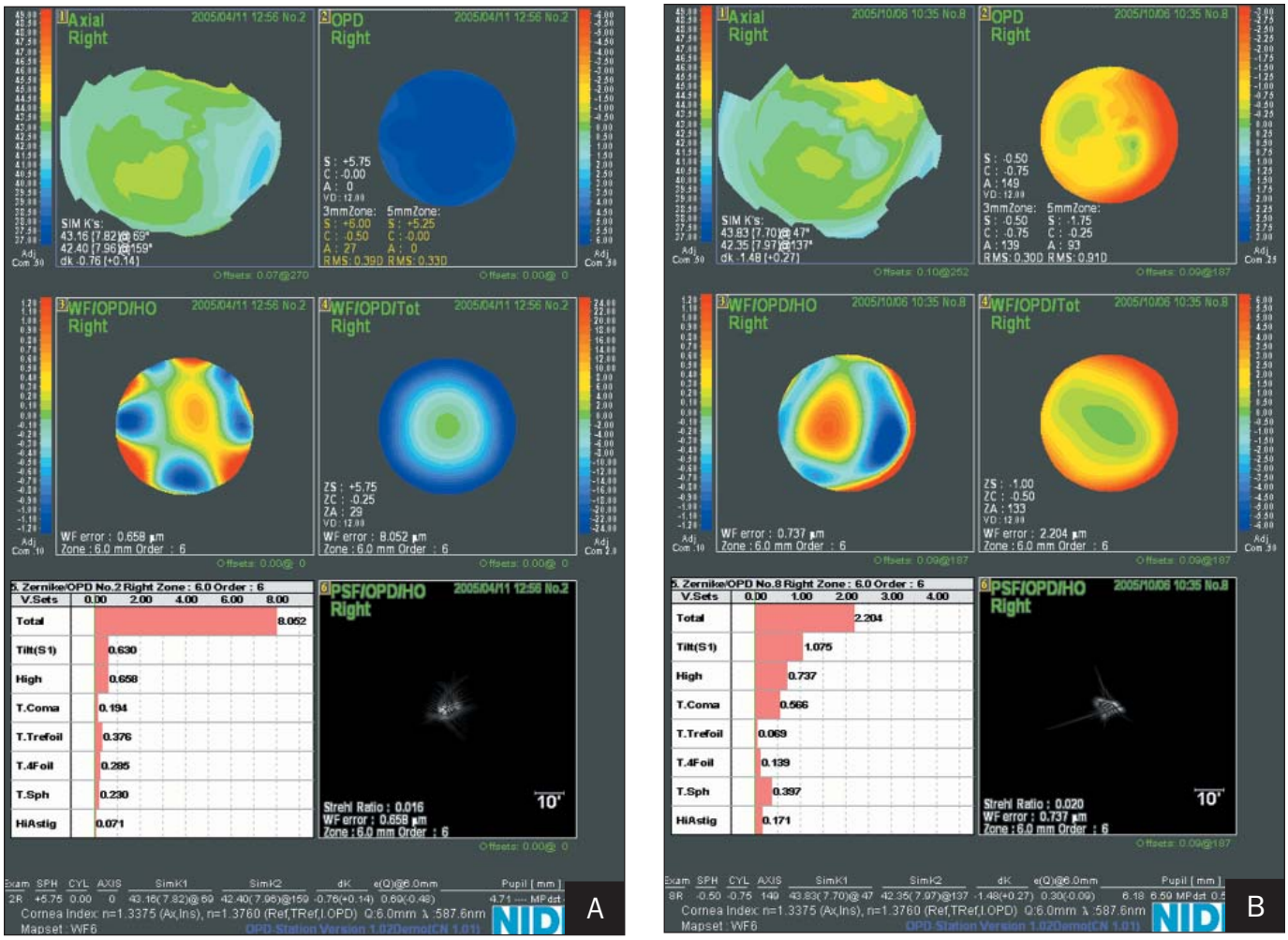

Figure 2. *Case 2.* **A)** Preoperative OPD-Scan analysis of the right eye in a patient with aphakia. **B)** Postoperative OPD-Scan analysis of the right eye after insertion of a spherical IOL.

following prescription: −6.00 +1.25 × 10° (20/20) in the right eye and −9.00 +1.00 × 90° (20/20) in the left eye. Upon further discussion, the patient described reduced vision at night in the right eye, along with the perception of halos at night.

OPD-Scan/OPD-Station analysis of the aberrations of the entire eye showed increased levels of higher order aberrations in the right eye (root-mean-square [RMS] 0.730 µm) compared with the left eye (RMS 0.302 µm) (Figs 1A and 1B). Spherical aberration in the right eye (RMS 0.496 µm) was considerably higher than in the left eye (RMS 0.191 µm) (see Figs 1A and 1B). Corneal spherical aberration was similar in both eyes, measuring 0.119 µm for the right eye and 0.172 µm for the left eye. The difference in spherical aberration must have been due to changes in lens shape and refractive index resulting from the greater nuclear sclerosis in the right eye. A well-developed cataract was seen in the right eye and mild nuclear opalescence in the left eye with slit-lamp microscopy.

Secondary IOL Implantation

Case 2. A 25-year-old man was referred for secondary IOL implantation in the right eye. During his first decade of life, the patient had undergone intracapsular crystalline lens extraction. Spectacle correction was +6.50, yielding 20/20 best spectacle-corrected visual acuity (BSCVA). Preoperative slit-lamp examination revealed a persistent peripheral zonular and capsular rim. The preoperative OPD-Scan map showed an even distribution of hyperopic refractive power across the open pupil (Fig 2A). Comparison of the axial map and higher order map indicate that the aberrations are likely corneal (see Fig 2A).

An AcrySof MA50BM 21.00 diopter (D) spherical IOL (Alcon Laboratories Inc, Ft Worth, Tex) was implanted in the ciliary sulcus through a 3.2-mm incision placed superotemporally, centered on the 150° meridian. The postoperative course was uneventful. Two months postoperatively, uncorrected visual acuity (UCVA) was 20/25, and BSCVA was 20/20 with a man-

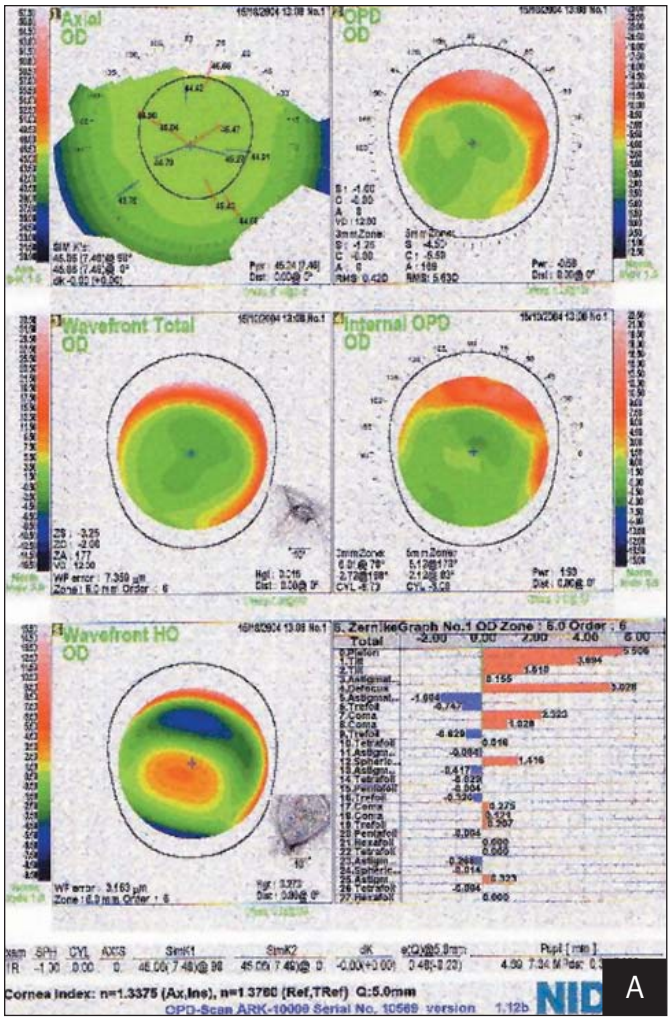

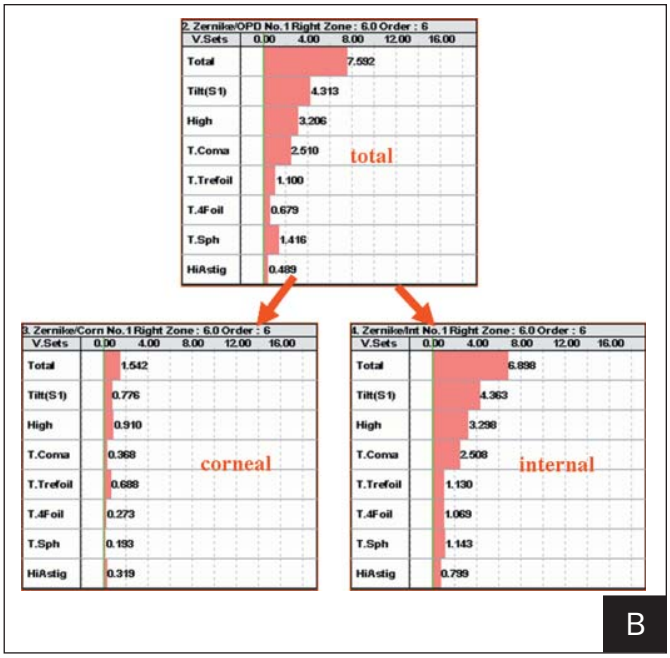

Figure 3. *Case 3.* **A)** OPD-Scan analysis of an eye 3 months after −15.00 D phakic IOL implantation through a 6-mm superior limbal incision. **B)** Zernike analysis of the total, corneal aberrations, and internal aberrations of an eye that underwent phakic IOL implantation out to the sixth order. Root-mean-square values in microns are shown for a 6-mm pupil. Aberrations are tabulated for the total aberrations (Total); tilt; higher order aberration (High); total coma aberration (T. Coma); total trefoil (T. Trefoil); total quadrafoil (T. 4Foil); total spherical aberration (T.Sph); and higher order astigmatism (HiAstig).

ifest refraction of plano −0.50 × 150°. Postoperatively, the OPD-Scan map showed an uneven distribution of refractive power caused by a slight increase in some of the higher order aberrations such as coma-like and spherical aberrations (Fig 2B). The higher order aberrations increased from 0.658 µm preoperatively to 0.737 µm postoperatively. Coma increased from 0.194 µm preoperatively to 0.566 µm postoperatively. Spherical aberrations increased from 0.230 µm preoperatively to 0.397 µm after insertion of the spherical IOL. OPD-Station analysis revealed that corneal higher order aberrations decreased from 1.100 µm preoperatively to 0.909 µm postoperatively. The lower corneal aberrations postoperatively are likely due to the beneficial effects of the 3.2-mm incision on the corneal shape, improving its regularity while reducing both the second order corneal-induced astigmatism and some of the corneal higher order aberrations (see Figs 2A and 2B). Hence, the increase in higher order aberrations seen postoperatively is likely due to the internal optics of the eye. The increase in spherical aberrations due to internal origins is likely due to implantation of a spherical IOL. The increase in coma seen postoperatively is likely due to less than optimal centration of the implanted IOL.

PHAKIC IOL SURGERY

Case 3. A 35-year-old man who had undergone (−15.00 D) Artisan lens implantation 3 months previously was satisfied with his vision during the day; however, he complained about halos and monocular vertical diplopia at night. OPD-Scan analysis showed that higher order aberrations were >3 µm, which is considered very high (Fig 3A). A coma pattern dominates the higher order map, and third order coma has the highest magnitude in the Zernike graphs (Figs 3A and 3B). Slit-lamp examination revealed a slight inferior decentration of the Artisan lens, exposing a crescent of pupil superiorly. The OPD-Scan and internal OPD-Scan maps in Figure 3A show a superior "myopic rim" of persistent myopic power within the pupil corresponding to the crescent of pupil not covered by the phakic IOL. The coma aberrations are highest from

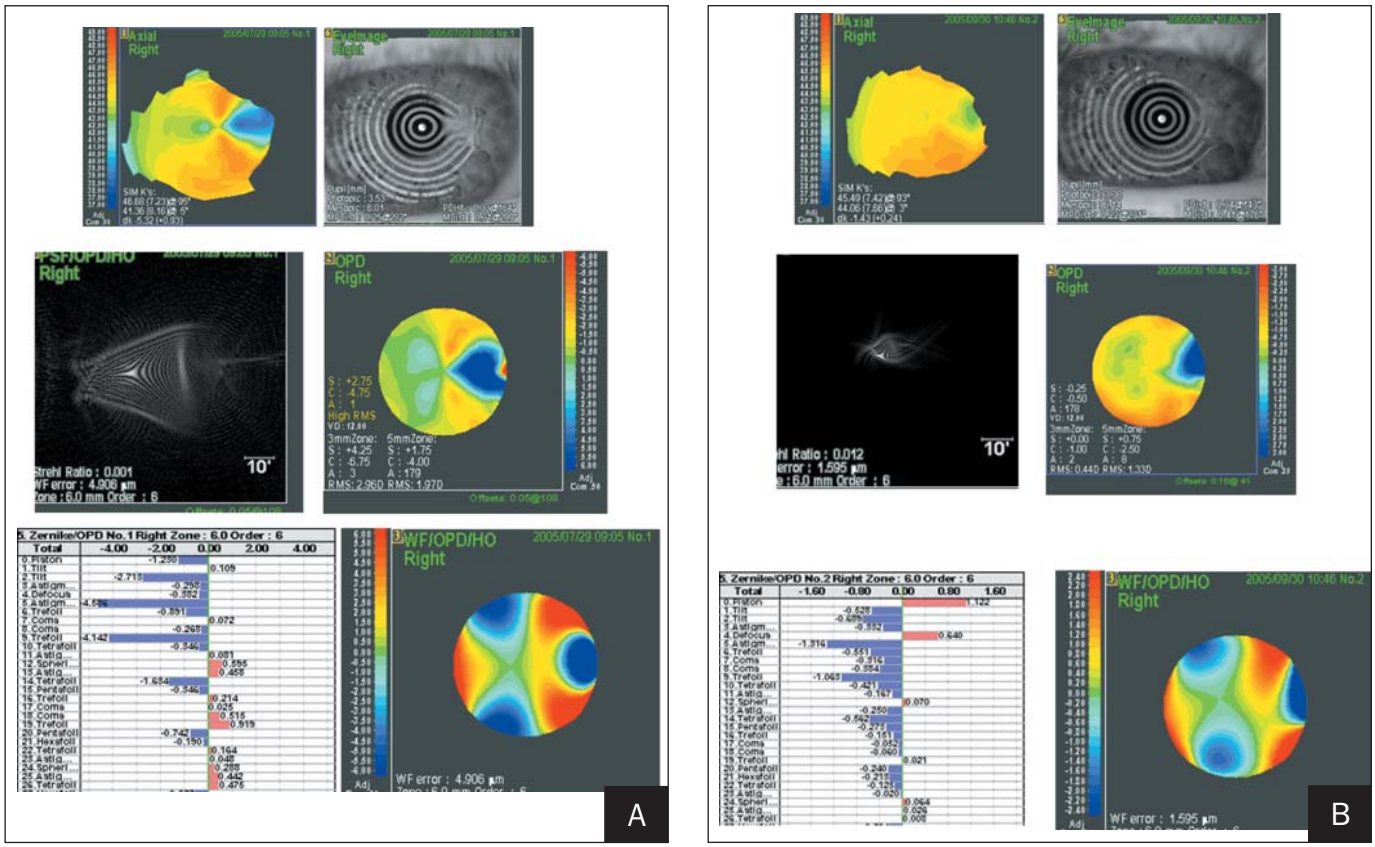

Figure 4. *Case 4.* **A)** OPD-Scan analysis of the right eye of a patient with pterygium invading the nasal quadrant of the cornea. **B)** OPD-Scan analysis after pterygium excision and a limbal autograft.

the internal optics of the eye (see Fig 3B). Hence, the aberrations were arising from the internal optics of the eye due to the decentered IOL. Centration of the IOL relieved the patient's symptoms.

Pterygium Surgery

Case 4. A 38-year-old man was referred for pterygium evaluation in the right eye. Preoperative UCVA was 20/40 and BSCVA was 20/25, with a manifest refraction of +2.00 −4.00 × 180°. The patient complained of glare and permanent horizontal monocular diplopia that increased with spectacle correction. The preoperative OPD-Scan map shows multiple myopic and hyperopic areas within the pupil likely causing the diplopia and degradation of visual quality (Fig 4A). High magnitudes of coma and trefoil were present preoperatively. The preoperative simulations of the optotype images with and without best spectacle correction for a photopic pupil show significant degradation of visual quality. The patient underwent pterygium excision and limbal autograft under local anesthesia, which resulted in immediate improvement of the UCVA and BSCVA with concurrent resolution of the glare and monocular diplopia (Fig 4B). Postoperatively, the magnitude of trefoil and coma were significantly reduced. This reduction was likely due to a combination of mechanisms, including the reduction of tear film pooling beneath the pterygium head and the release of corneal traction by the pterygium.

Contact Lens Fitting After Complicated Refractive Surgery

When further surgical intervention is not possible after excimer laser refractive surgery, rigid contact lenses may be a useful alternative. The OPD-Scan can be used as an aid to contact lens fitting and selection. For example, during the trial lens-fitting procedure, the eye can be measured with the contact lens in place to determine which contact lens provides optimum visual acuity and visual quality. The magnitude of higher order aberrations, the area under the MTF, and the point spread function (PSF) are objective metrics that can be used during contact lens fitting.

Case 5. A 28-year-old woman was referred for the management of a decentered ablation after LASIK in her left eye. Uncorrected visual acuity was 20/30 and BSCVA was 20/25 with a manifest refraction of

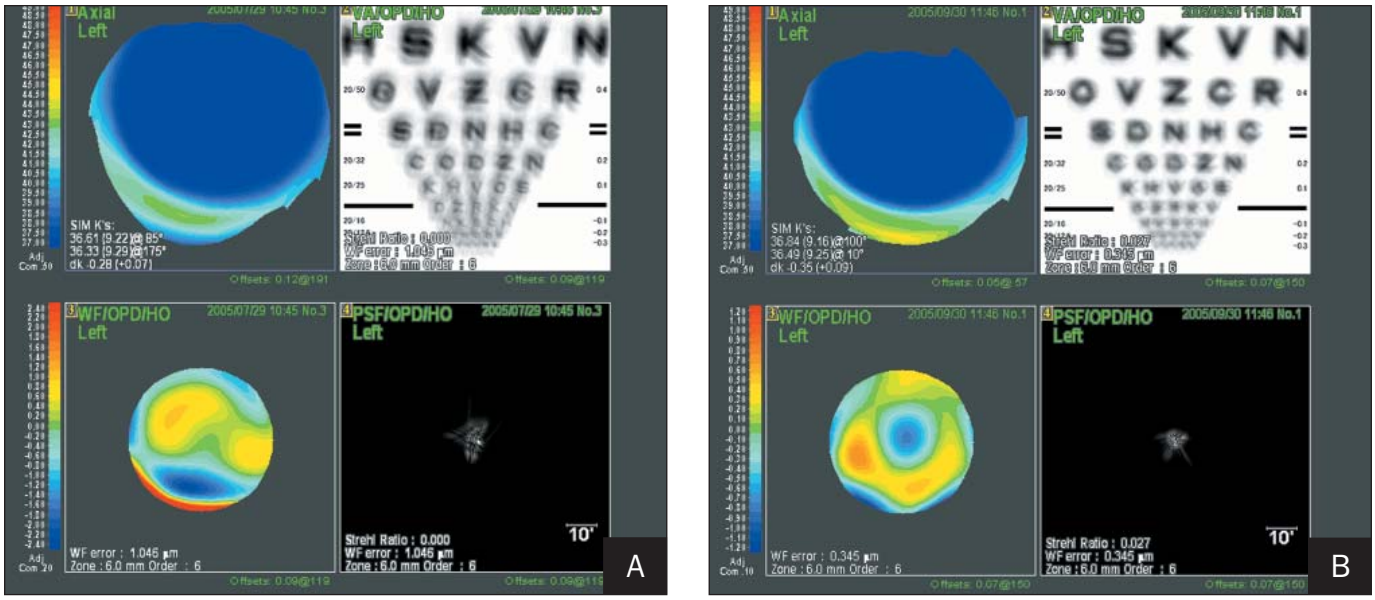

Figure 5. *Case 5.* OPD-Station analysis of an eye with a post-LASIK decentered ablation fitted with **A)** a Menicon Ex RGP contact lens and **B)** a Menicon Ex RGP contact lens with a smaller central radius.

plano −1.50 × 150°. The patient complained about glare, vertical diplopia, and reduced contrast. The decentered ablation was not easily seen on axial corneal topography, but it was clear on the OPD-Scan map. The estimated residual posterior bed thickness was <250 µm and therefore further excimer laser treatment was not performed. Rather, a rigid gas permeable (RGP) contact lens fit was chosen as the appropriate treatment for this patient. Different types of RGP contact lenses were fitted to restore satisfactory UCVA and visual quality. Our selection criteria for the contact lens were based on the standard contact lens fitting parameters and assessing which contact lens yielded a greater reduction in the higher order aberrations, the largest area under the MTF curve, the sharper PSF, and sharper visual acuity simulation. Comparison of Figures 5A and 5B show that a Menicon (Nagoya, Japan) RGP contact lens with reverse geometry and smaller central radius provided a sharper PSF and clearer visual acuity simulation due to reduced levels of high order aberrations. Based on these parameters, we elected to provide the patient with a Menicon RGP contact lens. Upon subjective comparison, the patient preferred the Menicon RGP lens with a smaller central radius curve. An MTF graph showed a larger area under the curve after contact lens insertion, indicating better visual performance. Although contrary to conventional thinking, greater levels of higher order aberrations do not necessarily portend reduced visual quality, because different combinations of higher order aberrations may interact in a manner that is beneficial to visual quality. Therefore, we recommend using a variety of metrics of optical visual quality in combination rather than relying on a single metric to determine the effect of higher order aberrations on vision.

Characterization of Multifocality

The compensation of presbyopia can be achieved by increasing the multifocality of the eye. Multifocality can be achieved by fitting multifocal contact lenses, performing multifocal corneal ablations, or implanting an accommodating IOL. The effect of induced multifocality on the optical quality of the eye is an important factor in patient satisfaction.

Case 6. A 52-year-old woman underwent hyperopic LASIK for a preoperative refractive error of +3.50 +1.00 × 180°. Postoperatively, UCVA was 20/25, and the patient could read J2 at near uncorrected vision. The patient was satisfied with the outcome of the surgery, because it provided her with excellent functional results for both near and far vision. The corneal topography map showed marked steepening and an inferior decentration. However, the OPD-Scan map showed emmetropia centrally and increasing myopia up to −1.50 D inferiorly (Fig 6). The multifocality shown on the OPD-Scan map explains the excellent near and far uncorrected vision. Treatment for this patient demonstrates the importance of measuring the full optical properties of the eye rather than one aspect, such as corneal topography. In this particular patient, corneal topography evaluation alone would lead to the conclusion that this had been an unsuccessful procedure.

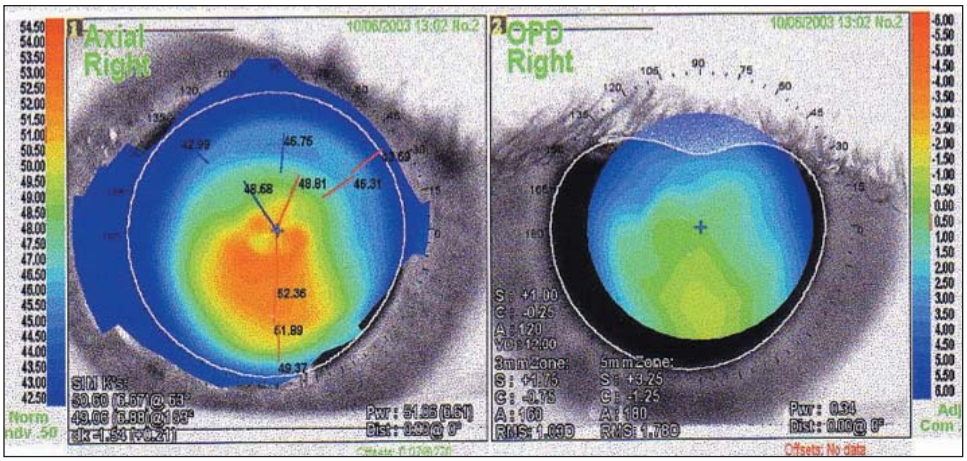

Figure 6. *Case 6.* Postoperative axial corneal topography map and OPD-Scan map of a patient who underwent hyperopic LASIK.

DISCUSSION

The precise qualitative and quantitative assessment of the main components of the eye's optical system (cornea and crystalline lens) facilitates a better understanding of the patient's symptoms in various clinical conditions other than customized laser refractive surgery. Modern cataract surgery and complex contact lens fitting represent a wide range of applications for the use of devices such as the OPD-Scan, which can measure corneal and internal optical quality. We believe that the use of the OPD-Scan will become an indispensable tool in daily ophthalmology practice.

REFERENCES

1. Williams DR, Porter J, Yoon G, Guirao A, Hofer H, Chen L, Cox I, MacRae SM. How far can we extend the limits of human vision? In: Krueger RR, Applegate RA, MacRae SM, eds. *Wavefront Customized Visual Corrections: the Quest for Super Vision II*. Thorofare, NJ: SLACK Inc; 2004:19-38.
2. Applegate RA, Hilmantel G, Thibos LN. Assessment of visual performance. In: Krueger RR, Applegate RA, MacRae SM, eds. *Wavefront Customized Visual Corrections: the Quest for Super Vision II*. Thorofare, NJ: SLACK Inc; 2004:65-75.
3. Artal P, Guirao A, Berrio E, Williams DR. Compensation of corneal aberrations by the internal optics in the human eye. *J Vis*. 2001;1:1-8.
4. Artal P, Guirao A. Contributions of the cornea and lens to the aberrations of the human eye. *Opt Lett*. 1998;23:1713-1715.
5. Yeung IY, Mantry S, Cunliffe IA, Benson MT, Shah S. Correlation of Nidek OPD-Scan objective refraction with subjective refraction. *J Refract Surg*. 2004;20:S734-S736.
6. Pieger S. Pearls, tips, and tricks for use of the Nidek OPD-Scan and FinalFit software. *J Refract Surg*, 2004;20:S741-S746.
7. Applegate RA, Marsack JD, Ramos R, Sarver EJ. Interaction between aberrations to improve or reduce visual performance. *J Cataract Refract Surg*. 2003;29:1487-1495.

Precision of NIDEK OPD-Scan Measurements

Mike P. Holzer, MD; Susanne Goebels; Gerd U. Auffarth, MD

ABSTRACT

PURPOSE: To evaluate the repeatability of wavefront measurements using the NIDEK OPD-Scan.

METHODS: A total of 179 eyes from 90 healthy volunteers (57 women and 33 men) with no corneal or lenticular pathology and normal visual acuity were enrolled in this study. Mean patient age was 39 years (range: 17 to 85 years). All patients underwent four consecutive measurements by one examiner with the NIDEK OPD-Scan. Total, corneal, and internal wavefront errors were measured and calculated with the device, using slit retinoscopy. Repeatability of the measurements was evaluated for spherical aberration, coma, and trefoil.

RESULTS: The repeatability test revealed a good result for all three higher order aberrations evaluated. The best repeatability values were found for total aberrations, followed by internal and corneal aberrations.

CONCLUSIONS: The NIDEK OPD-Scan has good precision in the wavefront measurement of total, corneal, and internal optical aberrations. [*J Refract Surg*. 2006;22: S1021-S1023.]

The innovation of measuring wavefront errors of the eye was an important step in improving treatment plans and surgical outcomes for patients undergoing refractive surgery.[1] Today the examination of wavefront errors of the eye is an important factor in preoperative work-up of candidates for refractive surgery. Customized treatments are becoming more popular, and the success of these treatments relies on a superior excimer laser system as well as on accurate and reliable wavefront measurements.[2,3] Another important treatment for wavefront errors is intraocular lens (IOL) surgery and wavefront-corrected IOLs such as aspheric IOLs.[4] Total wavefront errors of the eye can be evaluated using different systems; however, only a few analyze corneal and internal aberrations. Among these is the NIDEK OPD-Scan (Optical Path Difference Scanning System; NIDEK Co Ltd, Gamagori, Japan).

Most wavefront analyzers are based on Hartmann-Shack aberrometry, whereas the OPD-Scan is based on slit retinoscopy. This provides a total of 1440 measured refractions within a 6-mm pupil.[5]

The purpose of this study was to evaluate the NIDEK OPD-Scan for repeatability of total, corneal, and internal wavefront measurements (Fig).

PATIENTS AND METHODS

A total of 179 eyes from 90 healthy volunteers (57 women and 33 men) with no corneal or lenticular pathology and best spectacle-corrected visual acuity of at least 20/25 were enrolled in this study. Mean patient age was 39 years (range: 17 to 85 years). Prior to enrollment, informed consent was obtained from all patients. All patients underwent four consecutive measurements with the OPD-Scan under dim light conditions by one trained examiner. All patients enrolled

From the International Vision Correction Research Centre (IVCRC), Department of Ophthalmology, Ruprecht-Karls-University of Heidelberg, Germany.

The authors have no financial or proprietary interest in the materials presented herein.

Correspondence: Mike P. Holzer, MD, Dept of Ophthalmology, Ruprecht-Karls-University of Heidelberg, Im Neuenheimer Feld 400, 69120 Heidelberg, Germany. E-mail: mike.holzer@med.uni-heidelberg.de

Figure. OPD-Scan (NIDEK Co Ltd, Gamagori, Japan) used in the repeatability study.

had a pupil size of at least 6 mm. For patients with pupils <6 mm, one dilating drop (neosynephrine 5%) was used to reach a minimal pupil size of 6 mm. Patients were not permitted to use topical drops or ointment prior to the study.

After careful alignment of the pupil, individual measurements were performed. An infrared light source within a rotating drum was projected onto the entrance pupil, producing a scanning slit on the fundus. A special photo diode array detected the timing of the fundus reflex while scanning. To obtain information for each meridian, a chopper wheel was used to change the direction of scanning and the orientation of the photo sensor. The measured refractive errors were then converted into wavefront errors and a wavefront map. In addition, the OPD-Scan evaluated corneal topography and corneal wavefront calculation simultaneously, which minimized alignment errors associated with eye movements that can affect the accuracy of the measurements.

Corneal, internal, and total wavefront errors were calculated as Zernike polynomials for a 6-mm pupil and the data exported to Microsoft Excel (Redwood City, Calif). Repeatability was then tested for coma, spherical aberration, and trefoil higher order aberrations as mean values of the standard deviations for all measurements.

TABLE 1

Repeatability* of the NIDEK OPD-Scan for Spherical Aberration

Aberration	Z12
Total	0.007
Corneal	0.037
Internal	0.012

**Mean value of standard deviations.*

TABLE 2

Repeatability* of the NIDEK OPD-Scan for Coma

Aberration	Z7	Z8
Total	0.011	0.008
Corneal	0.074	0.087
Internal	0.032	0.038

**Mean value of standard deviations.*

TABLE 3

Repeatability* of the NIDEK OPD-Scan for Trefoil

Aberration	Z6	Z9	Z10	Z14
Total	0.038	0.033	0.029	0.033
Corneal	0.245	0.257	0.123	0.142
Internal	0.071	0.068	0.050	0.064

**Mean value of standard deviations.*

RESULTS

The precision tests revealed good repeatability for all aberrations investigated (Tables 1-3). For spherical aberration, the best repeatability was found for total aberration, followed by internal and corneal spherical aberration. A similar distribution was found for coma with best values for total coma, followed by internal and corneal coma. Similarly, trefoil aberrations showed the best values for total aberration, followed by internal and corneal aberration. The lowest repeatability values overall were found for trefoil measurements of the cornea.

DISCUSSION

Wavefront sensors are important devices in the evaluation of refractive surgery and the calculation of cus-

tomized treatment.[1] The OPD-Scan used in this study combines different measurements: wavefront analysis, corneal topography analysis, pupillometry, and autorefraction. When comparisons of the location of higher order aberrations are performed, it is important that the visual axis is well aligned among the different measurements. If a wavefront analyzer and corneal topographer are used separately for the measurements, exact alignment of the eye may be difficult. If one instrument combines these measurements and performs calculations within a short time frame, potential errors can be minimized.

The repeatability test of the OPD-Scan showed a similar distribution for the different aberrations investigated. Total aberrations always revealed the best repeatability values, followed by internal and corneal aberrations. This could be because the wavefront sensor is based on the retinoscopy principle and measures the dioptric changes precisely, whereas the corneal wavefront is based on calculations of topography data.

Rodriguez et al[6] reported good reliability for different wavefront-measuring devices. They compared measurements from five young patients using the Zywave Hartmann-Shack wavefront sensor (Bausch & Lomb, Rochester, NY), laser ray tracing (Tracey Technologies, Houston, Tex), and their own laboratory laser ray tracing prototype. They also emphasized the importance of good pupil alignment, good examiner skills, appropriate accommodation targets, and good subject cooperation. In another study by Cheng et al,[7] the test-retest reliability over time for Hartmann-Shack measurements was evaluated. Four healthy eyes were measured on five consecutive days and on five days on a monthly basis. In this study, variability over a short time was low but increased over time.

The reliability with different corneal topographers has also been reported.[8-10] In general, it seems to be important that the examiner is well trained in the use of the device.[11]

The current study showed good repeatability in consecutive measurements from healthy volunteers for total, corneal, and internal wavefront measurements performed with the NIDEK OPD-Scan.

REFERENCES

1. Mrochen M, Jankov M, Bueeler M, Seiler T. Correlation between corneal and total wavefront aberrations in myopic eyes. *J Refract Surg.* 2003;19:104-112.
2. Pop M, Bains HS. Clinical outcomes of CATz versus OPDCAT. *J Refract Surg.* 2005;21:S636-S639.
3. Canals M, Elies D, Costa-Vila J, Coret A. Comparative study of ablation profiles of six different excimer lasers. *J Refract Surg.* 2004;20:106-109.
4. Mester U, Dillinger P, Anetrist N. Impact of a modified optic design on visual function: clinical comparative study. *J Cataract Refract Surg.* 2003;29:652-660.
5. Rozema JJ, Van Dyck DE, Tassignon MJ. Clinical comparison of 6 aberrometers. Part 1. Technical specifications. *J Cataract Refract Surg.* 2005;31:1114-1127.
6. Rodriguez P, Navarro R, Gonzalez L, Hernandez JL. Accuracy and reproducibility of Zywave, Tracey, and experimental aberrometers. *J Refract Surg.* 2004;20:810-817.
7. Cheng X, Himebaugh NL, Kollbaum PS, Thibos LN, Bradley A. Test-retest reliability of clinical Shack-Hartmann measurements. *Invest Ophthalmol Vis Sci.* 2004;45:351-360.
8. Chui WS, Cho P. A comparative study of the performance of different corneal topographers on children with respect to orthokeratology practice. *Optom Vis Sci.* 2005;82:420-427.
9. Guell JL, Velasco F, Roberts C, Sisquella MT, Mahmoud A. Corneal flap thickness and topography changes induced by flap creation during laser in situ keratomileusis. *J Cataract Refract Surg.* 2005;31:115-119.
10. Rabsilber TM, Becker KA, Auffarth GU. Reliability of Orbscan II measurements in relation to refractive status. *J Cataract Refract Surg.* 2005;31:1607-1613.
11. Rozema JJ, Van Dyck DE, Tassignon MJ. Clinical comparison of 6 aberrometers. Part 2. Statistical comparison in a test group. *J Cataract Refract Surg.* 2006;32:33-44.

Wavefront Analysis in Asian-Brazilians

Eliane Mayumi Nakano, MD; Harkaran Bains, MD; Kozo Nakano, MD; Celso Nakano, MD; Waldir Portellinha, MD; Marivaldo Oliveira, MD; Lenio Alvarenga, MD

ABSTRACT

PURPOSE: To compare the distribution of ocular higher order wavefront aberrations (third to sixth order) in the Brazilian population of Asian and non-Asian refractive surgery patients.

METHODS: Preoperative refractive and wavefront data were reviewed for 648 eyes in 324 patients who underwent custom ablation at the Excimer Laser Santa Cruz refractive surgery center in São Paulo, Brazil, from March 2002 to July 2005. Patients were divided into two groups: Asian patients and non-Asian patients, based on family history. Statistical analysis was performed to assess the differences between the groups with respect to manifest refractive spherical equivalent, astigmatism, pachymetry, OPD-root-square-mean (RMS) for a 6.0-mm pupil, total wavefront aberrations, third- to sixth-order higher order aberrations, and individual aberrations.

RESULTS: The mean spherical equivalent refraction in the Asian group of −4.38 diopters (D) was significantly higher than the spherical equivalent refraction of −3.46 D in the non-Asian group (t=−4.32; *P*=.00001). Comparison of the differences between groups with respect to higher order aberrations, coma, trefoil, quadrafoil, spherical aberration, higher order astigmatism, and pachymetry was not statistically significant.

CONCLUSIONS: Asian patients have a higher prevalence of myopia than non-Asian patients. No differences were noted in higher order aberrations between Asian and non-Asian patients. [*J Refract Surg*. 2006;22:S1024-S1026.]

Taller people are more likely to have longer globes, deeper anterior chambers, thinner lenses, and flatter corneas.[1] Although the many dimensions of various ocular structures may be related to adult height, a correlation does not seem to exist between height and refraction.[1] Nevertheless, it has been documented that some ethnic populations have less myopic progression and axial elongation than others.[2] The higher prevalence of myopia in Japanese patients compared with African and Caucasian patients points to the existence of inherent factors in the Asian population that cause myopia.[3]

Although the factors influencing the prevalence of myopia could be many, the internal optics of the eye may be one possible factor causing the preponderance of myopia in Asian patients. Wavefront aberrometers have been developed recently for ophthalmic applications such as measuring optical aberrations of the eye and determining their correlation to visual symptoms.[4] Aberrometers measure the shape of the wavefront of light that is reflected out of the eye from a point source on the fundus.[5]

Higher order aberrations of the eye are characterized and quantified by Zernike polynomials. Zernike polynomials are mathematical descriptors of optical aberrations. The spherocylindrical terms can be extracted using Zernike analysis, and the remaining terms called higher order aberrations can provide a thorough understanding of the optics of the eye and its effect on visual quality.[5] Thus, wavefront analysis can be used to determine whether optical differences exist among different ethnic populations.

This study compared the distribution of ocular higher order wavefront aberrations (third to sixth order) in the Brazilian population of Asian and non-Asian refractive surgery patients.

From Clínica Oftalmológica Nakano, São Paolo, Brazil (E. Nakano, K. Nakano, C. Nakano, Alvarenga); Excimer Laser Santa Cruz, São Paulo, Brazil (E. Nakano, K. Nakano, Portellinha, Oliveira); and NIDEK Co Ltd, Gamagori, Japan (Bains).

The authors have no financial or proprietary interest in the materials presented herein.

Correspondence: Eliane Mayumi Nakano, MD, Clínica Oftalmológica Nakano, São Paolo, Brazil. Tel: 55 11 5549 2535; E-mail: mayuminakano@uol.com.br

TABLE 1

Mean Wavefront Aberration Values in 384 Asian Eyes

Wavefront Aberration	Mean Wavefront Error (μm)	Standard Deviation (μm)
Total	5.160	2.570
Higher order	0.514	0.711
Coma	0.234	0.304
Trefoil	0.298	0.356
Quadrafoil	0.114	0.234
Spherical	0.172	0.293
Higher order astigmatism	0.114	0.180

TABLE 2

Mean Wavefront Aberration Values in 264 Non-Asian Eyes

Wavefront Aberration	Mean Wavefront Error (μm)	Standard Deviation (μm)
Total	4.470	2.730
Higher order	0.553	0.705
Coma	0.296	0.454
Trefoil	0.302	0.311
Quadrafoil	0.111	0.172
Spherical	0.192	0.341
Higher order astigmatism	0.099	0.161

PATIENTS AND METHODS

STUDY POPULATION

In this retrospective study, preoperative refractive and wavefront data were reviewed for 324 patients who underwent custom ablation at the Excimer Laser Santa Cruz refractive surgery center in São Paulo, Brazil, from March 2002 to July 2005. Patients were divided into two groups: Asian patients and non-Asian patients, based on family history.

Prior to surgery, all patients underwent a comprehensive ophthalmic evaluation that included uncorrected visual acuity, best spectacle-corrected visual acuity, manifest and cycloplegic refractions, topography and wavefront analysis with the OPD-Scan (NIDEK Co Ltd, Gamagori, Japan), pachymetry, and dilated fundus examination. All aberrometry measurements were performed over a 6.0-mm diameter. The patients' gender, race, age, and desired correction were also recorded. Only candidates who underwent refractive surgery were included in this study. Candidates with underlying systemic or ophthalmic disease that would adversely affect corneal wound healing and refractive outcomes were excluded.

DATA COLLECTION AND STATISTICAL ANALYSIS

Preoperative measurements of refraction, wavefront aberrations, pachymetry, and pupil size were recorded and analyzed. Statistical analysis was performed to assess the differences between ethnicity and manifest refractive spherical equivalent (MRSE), astigmatism, OPD-root-mean-square (RMS) for a 6.0-mm pupil, total wavefront aberrations, third to sixth order higher order aberrations, spherical aberration, trefoil, coma, higher order astigmatism, and quadrafoil. Correlations between pachymetry and age, total wavefront aberrations, higher order aberrations, spherical aberration, trefoil, coma, higher order astigmatism, and quadrafoil were analyzed. Correlations between the MRSE and total wavefront aberrations, higher order aberrations, spherical aberration, trefoil, coma, higher order astigmatism, and quadrafoil were also analyzed. In addition, correlations between cylinder power and total wavefront aberrations, higher order aberrations, spherical aberration, trefoil, coma, higher order astigmatism, and quadrafoil were analyzed.

Statistical analysis was performed using Minitab version 12.054 (Minitab Inc, State College, Pa) and Power Analysis and Sample Size (NCSS, Kaysville, Utah) 2000 edition statistical analysis software. The Student *t* test was used for group comparisons. Correlations were analyzed using Pearson correlation coefficient. A P value $<.05$ was considered statistically significant.

RESULTS

Three hundred eighty-four eyes in 192 Asian patients and 264 eyes in 132 non-Asian patients were analyzed. The mean age for Asian and non-Asian patients was 32.78 ± 7.69 years and 30.93 ± 7.98 years, respectively. The difference in age between the two groups was statistically significant (P=.0035). The mean spherical equivalent refraction was −4.38 D in the Asian group and −3.46 D in the non-Asian group. In the Asian group, 69.1% of the patients' eyes had an MRSE between −2.00 and −6.00 D, and 15% were higher than −7.00 D. In the non-Asian group, the mean MRSE was −4.00 D. The increased myopia in Asian patients compared with non-Asian patients was statistically significant (t=−4.32; P=.00001).

Comparison of the differences of the magnitude of total wavefront aberrations between the groups showed statistically significantly higher values in Asian patients compared with non-Asian patients (t=3.26; P=.0012) (Tables 1 and 2). Comparison of the differences between groups with respect to higher order

aberrations, coma, trefoil, quadrafoil, spherical aberration, and higher order astigmatism was not statistically significant (Tables 1 and 2).

The mean pachymetry of 550.3±32.4 µm for the Asian group was nearly identical to the mean pachymetry of 549.9±34.4 µm for the non-Asian group (t=0.13; *P*=.90). Correlation analysis did not yield any significant relationships with the other variables analyzed.

DISCUSSION

This study of the differences in wavefront aberrations of Asian and non-Asian patients from Brazil revealed significantly higher levels of myopia in the Asian group. Total wavefront aberrations were higher in the Asian group. Total wavefront aberrations included the lower order aberrations, such aberrations in sphere and cylinder, in addition to the higher order aberrations. The higher levels of myopia in the Asian group explain the greater magnitude of total wavefront aberration in this group. However, when individual higher order aberrations were analyzed, no difference was noted between the groups. Thus, one must be cognizant of the wavefront analyses being undertaken to determine whether differences exist. For example, in this study, had we reported only the total wavefront aberrations, one would erroneously conclude eyes in Asian patients are more "aberrated."

Additional analyses of each of the individual higher order aberrations such as spherical aberration and coma did not show a difference between groups. This observation leads us to consider a compensatory mechanism of retinal image formation independent of refractive errors. The mechanism is likely attributable to the internal optics of the eye and may somehow modulate the effects of the wavefront aberrations on visual quality.

Although the study population was recruited from a refractive surgery center and may not be indicative of the typical Brazilian population, we believe it provides insight into the population of healthy adults with myopia in Brazil. We found that normal myopic eyes in Asians tend to have greater myopia than eyes in non-Asian patients. In addition, in this large sample of patients, we provide normative values for wavefront error and individual wavefront aberrations in a subset of the population that presents for refractive surgery. These values are especially pertinent for refractive surgery centers, which often screen potential refractive surgery candidates for conventional or wavefront treatment based on the wavefront profile of an eye.

Higher levels of higher order aberrations were found in both groups compared with that reported for a group of refractive surgery candidates from the United States.[6] In the US candidates,[6] the magnitude of wavefront error was approximately 0.313 µm, which is approximately 1.7× lower than the average of both groups of Brazilian candidates reported in the current investigation. In addition, the levels of coma and spherical aberration were at least 1.4× higher in our cohort of Brazilian candidates compared with US refractive surgery candidates.[6] Differing measurement principles could be a cause of the difference between the Brazilian candidates and Caucasian candidates. Hartmann-Shack aberrometers cannot measure highly aberrated eyes and thus there may have been bias in the Wang and Koch[6] study due to technological limitations. However, a recent comparative study found that Hartmann-Shack aberrometers and the OPD-Scan aberrometer provide similar values for wavefront aberrations for normal eyes. Hartmann-Shack aberrometry fails with respect to measurement of highly aberrated eyes.[7] Another explanation for the difference in higher order aberrations shown in studies of US patients and our study population may be related to an increased incidence of lenticular changes induced in the Brazilian cohort due to higher ultraviolet exposure. The differences in wavefront aberrations between the Asian and non-Asian patients from Brazil and those measured in US studies indicate that various ethnic and regional populations may have differing levels of higher order aberrations that must be considered during patient screening and surgical treatment planning.

We believe the results of this study of higher order aberrations in different ethnic groups in Brazil have brought insight to the interaction of wavefront aberrations and refractive error that warrant further investigation.

REFERENCES

1. Wong TY, Foster PJ, Johnson GJ, Klein BE, Seah SK. The relationship between ocular dimensions and refraction with adult stature: the Tanjong Pagar Survey. *Invest Ophthalmol Vis Sci*. 2001;42:1237-1242.
2. Hyman L, Gwiazda J, Hussein M, Norton TT, Wang Y, Marsh-Tootle W, Everett D. Relationship of age, sex, and ethnicity with myopia progression and axial elongation in the correction of myopia evaluation trial. *Arch Ophthalmol*. 2005;123:977-987.
3. Shimizu N, Nomura H, Ando F, Niino N, Miyake Y, Shimokata H. Refractive errors and factors associated with myopia in an adult Japanese population. *Jpn J Ophthalmol*. 2003;47:6-12.
4. Kohnen T, Buhren J, Kuhne C, Mirshani A. Wavefront-guided LASIK with the Zyoptix 3.1 System for the correction of myopia and compound myopic astigmatism with 1-year follow-up. *Ophthalmology*. 2004;111:2175-2185.
5. Moreno-Barriuso E, Navarro R. Laser ray tracing versus Hartmann-Shack sensor for measuring optical aberrations in the human eye. *J Opt Soc Am A Opt Image Sci Vis*. 2000;17:974-985.
6. Wang L, Koch DD. Ocular higher-order aberrations in individuals screened for refractive surgery. *J Cataract Refract Surg*. 2003;29:1896-1903.
7. Rozema JJ, Van Dyck DE, Tassignon MJ. Clinical comparison of 6 aberrometers. Part 2. Statistical comparison in a test group. *J Cataract Refract Surg*. 2006;32:33-44.

Comparison of Measurement of Pupil Sizes Among the Colvard Pupillometer, Procyon Pupillometer, and NIDEK OPD-Scan

Claire McDonnell, MCOptom; Martina Rolincova, MSc; Jan Venter, MD

ABSTRACT

PURPOSE: To compare pupil sizes measured with the Colvard pupillometer, Procyon pupillometer, and NIDEK OPD-Scan.

METHODS: Pupil diameter was measured in 90 consecutive eyes from 55 patients under mesopic and scotopic light conditions with all three instruments.

RESULTS: The mean scotopic pupil diameter was 6.3±0.98 mm with the Colvard pupillometer and 6.45±1.01 mm with the Procyon pupillometer. The mean mesopic pupillometer was 5.58±1.01 mm with the Procyon pupillometer and 6.26±0.99 mm with the NIDEK OPD-Scan.

CONCLUSIONS: The mesopic pupil diameter measured with the NIDEK OPD-Scan is more consistent with the scotopic pupil diameter measured with the Procyon and Colvard pupillometers than the mesopic pupil diameter measured with the Procyon pupillometer. [*J Refract Surg*. 2006;22:S1027-S1030.]

The measurement of pupil diameter has become increasingly important in the field of refractive surgery. Larger scotopic pupil sizes may be partially responsible for the occurrence of postoperative symptoms such as halos, glare, and monocular diplopia.[1,2] Refractive surgeons also need an accurate scotopic pupil measurement to determine appropriate treatment zones for excimer laser, corneal, and intraocular surgery.

Pupil size can be evaluated using various methods. The Colvard hand-held infrared pupillometer (Oasis Medical, Glendora, Calif) has been considered the gold standard for pupil measurement in refractive surgery, and the Procyon pupillometer (Procyon, London, United Kingdom) is considered one of the most accurate pupillometers.[3,4]

The purpose of this study was to compare pupil measurements taken with these two pupillometers, which were designed specifically to perform pupillometry, with pupil measurements taken with the NIDEK OPD-Scan (NIDEK Co Ltd, Gamagori, Japan), which is an autorefractor, topographer wavefront aberrometer that can perform pupil measurements.

MATERIALS AND METHODS

Patients and Pupillometry Measurements

Measurements of pupil sizes were taken for 90 consecutive eyes from 55 patients who presented to the Optimax Laser Eye Treatment Specialists in London, United Kingdom. All patients were candidates undergoing screenings for primary or secondary refractive surgery. None of the patients included in the study had irregular pupils or had received any topical medication that could cause pupil mydriasis or miosis. All three measurements were carried out in the same room within 30 minutes of one another. The ambient room illumination

From the Optimax Laser Eye Treatment Specialists, London, United Kingdom.

The authors have no financial interest in the materials presented herein.

Correspondence: Jan Venter, MD, Optimax Laser Eye Treatment Specialists, 128 Finchley Rd, London NW3 5HT, United Kingdom. Tel: 44 020 7794 2108; Fax: 44 020 7435 5623; E-mail: javenter@onetel.com

TABLE 1

Pupillometry Measurements Using the NIDEK OPD-Scan, Colvard Pupillometer, and Procyon Pupillometer

	Mean Pupil Diameter±Standard Deviation (mm)	
Pupillometer	**Scotopic**	**Mesopic**
Colvard	6.30±0.98	—
Procyon	6.45±1.01	5.58±1.01
NIDEK OPD-Scan	—	6.26±0.99

was <1 lux for each measurement, determined using the Minolta chromameter (Minolta, Glen Cove, NY).

Measurements were performed with the NIDEK OPD-Scan first. Measurements were taken by different operators trained on the use of the OPD-Scan. The OPD-Scan records monocular pupil measurements under binocular conditions.

The OPD-Scan controls accommodation by providing a distance fixation target within the unit. The OPD-Scan does not account for hippus. According to the manufacturer, NIDEK Co Ltd, the OPD-Scan acquires the mesopic pupil measurement when aberrometry is being performed. To standardize nomenclature, we refer to the pupil size measurement generated by the OPD-Scan as mesopic pupil size; however, the manufacturer's designation of mesopic may not be correct for this particular instrument. The luminance emitted by the OPD-Scan at this point is 10 to 12 cd/m^2. Aberrometry measurements and mesopic pupillometry measurements are taken using infrared light, which does not affect pupil size. Ambient room illumination was <1 lux while the mesopic pupil measurements were obtained with the OPD-Scan. Subsequently, the OPD-Scan calculates one photopic pupil measurement, while the corneal topography measurements are being obtained. The luminance emitted by the OPD-Scan at this point is 100 to 150 cd/m^2. OPD-Scan measurements are recorded to ±0.01 mm.

Measurements obtained with the Procyon pupillometer were calculated next. Measurements obtained with the Procyon pupillometer were taken by the same operator for all patients. For all Procyon measurements, the scotopic pupil size was measured first, followed by low mesopic pupil size. The Procyon is a digital infrared pupillometer that can measure pupil size monocularly or binocularly at three different illumination levels: scotopic (0.04 lux), low mesopic (0.4 lux), and high mesopic (4 lux).[5] In this study, only binocular measurements were obtained with the Procyon pupillometer. Infrared light-emitting diodes illuminate the eyes with long-wave light that does not affect pupil size but is recognized by the charge-coupled device camera in the system.

Measurements are not affected by ambient illumination, because rubber cups encompass the patient's orbit, preventing stray light from entering the eye. The Procyon pupillometer takes hippus into account. At each illuminance level, a sequence of 10 images is acquired within 2 seconds. Mean values are then reported as the pupil diameter. Measurements are recorded to ±0.01 mm.

The final measurement was performed using the Colvard hand-held infrared pupillometer. Measurements obtained with the Colvard pupillometer were taken by the same operator for all patients. This device calculates monocular measurements. Ambient light does not enter the eye being measured because of a rubber cup that encompasses the orbit to prevent stray light entry. The opposite eye is occluded during measurements. The Colvard pupillometer does not account for hippus. This device uses light amplification technology and is subjective. The examiner has to focus on the iris and pupil while the patient fixates on an infrared light-emitting diode, which emits a red light at very low levels. A millimeter ruler is superimposed as a reticule in the device. The reticule is calibrated in 1-mm increments. In this study, Colvard measurements were taken to the nearest 0.25 mm. Other studies have attempted to measure to the nearest 0.1 mm.[4] The Colvard pupillometer performs only scotopic measurements.

Data Analysis

The data were analyzed using the Bland-Altman technique,[6] which compares two methods of measurements by plotting their mean against their differences. Bland-Altman plots were also used for the comparison of agreement in pupil size between different pupillometers. Using the Bland-Altman method, the average pupil size measured with the two instruments is plotted on the x axis, and the difference between the two measurements is plotted on the y axis. The closer the mean difference is to zero, the better the agreement. The limits of agreement are the mean±2 standard deviations (SD).

RESULTS

Ninety eyes in 55 patients (23 men and 32 women) who presented at a refractive surgery center were evaluated for this study. Mean patient age for the entire cohort was 38±12.6 years (range: 19 to 63 years). The mean pupil diameter obtained with each instrument is shown in Table 1. The mean scotopic pupil size with

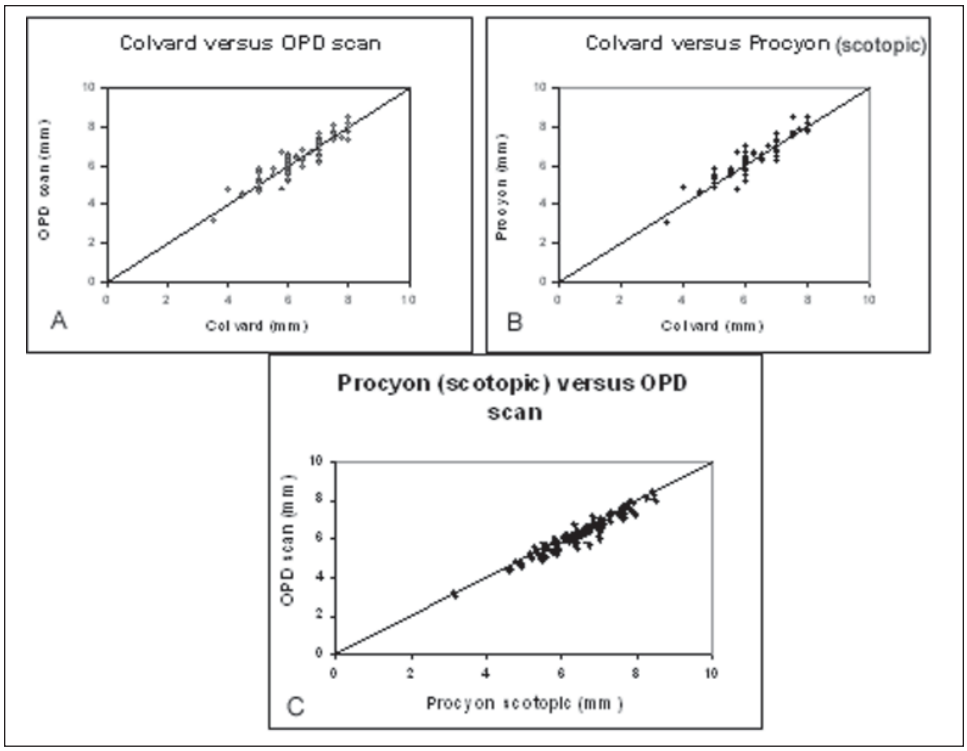

Figure 1. A) Measurement of scotopic pupil size using the Colvard pupillometer versus the mesopic pupil size using the NIDEK OPD-Scan. **B)** Measurement of scotopic pupil size using the Colvard pupillometer versus the scotopic pupil size using the Procyon pupillometer. **C)** Measurement of scotopic pupil size using the Procyon pupillometer versus the mesopic pupil size using the NIDEK OPD-Scan.

the Colvard pupillometer showed better agreement with the mean mesopic pupil size as measured with the OPD-Scan than it did with the mean mesopic pupil size as measured with the Procyon (Table 1). Comparison of measurements of pupil size with each instrument plotted against each other show the tightest group of points between the Procyon scotopic pupil sizes and the OPD-Scan mesopic pupil size (Fig 1). Values comparing the scotopic pupil size with the Colvard pupillometer with the scotopic pupil size with the Procyon pupillometer and the scotopic pupil size with Colvard pupillometer with the mesopic pupil size with the OPD-Scan were also similar.

With the exception of the Procyon pupillometer on low mesopic setting versus the OPD-Scan, all of the mean differences were near zero, and all of the limits of agreement were within ±1 mm (Table 2). Almost all of the points on all of the graphs were within the limits of agreement (Fig 2). The best agreement was between the mesopic pupil size with the OPD-Scan and the Procyon pupillometer on a scotopic setting and the worst agreement was between the mesopic pupil size on the OPD-Scan and the Procyon pupillometer on a low mesopic setting.

TABLE 2

Mean Difference in Pupillometry Measurements Using the NIDEK OPD-Scan, Colvard Pupillometer, and Procyon Pupillometer

	Mean Difference (mm)	Limits of Agreement (mm)
Colvard (scotopic) vs OPD-Scan (mesopic)	−0.14	0.70; −0.98
Colvard (scotopic) vs Procyon (scotopic)	0.01	0.80; −0.79
Procyon (mesopic) vs OPD-Scan (mesopic)	−0.71	0.30; −1.72
Procyon (scotopic) vs OPD-Scan (mesopic)	0.14	0.65; −0.37

DISCUSSION

Measurement of pupil size is important in corneal refractive surgery, cataract surgery, and implantable corrective lens surgery. Pupil size must be considered by refractive surgeons in planning their treatment. It is likely that binocular measurement of pupil diameter under low mesopic conditions approaches the realistic situation of daily night driving more than monocular measurement.[7]

Currently one of the most widely used instruments to measure pupil size in refractive surgery centers is the Colvard pupillometer. The popularity of the Colvard pupillometer is likely due to its cost-effectiveness, portability, and ease of use. However, it has a number of inherent flaws, including 1) it does not take into account hippus during measurement, 2) the measure-

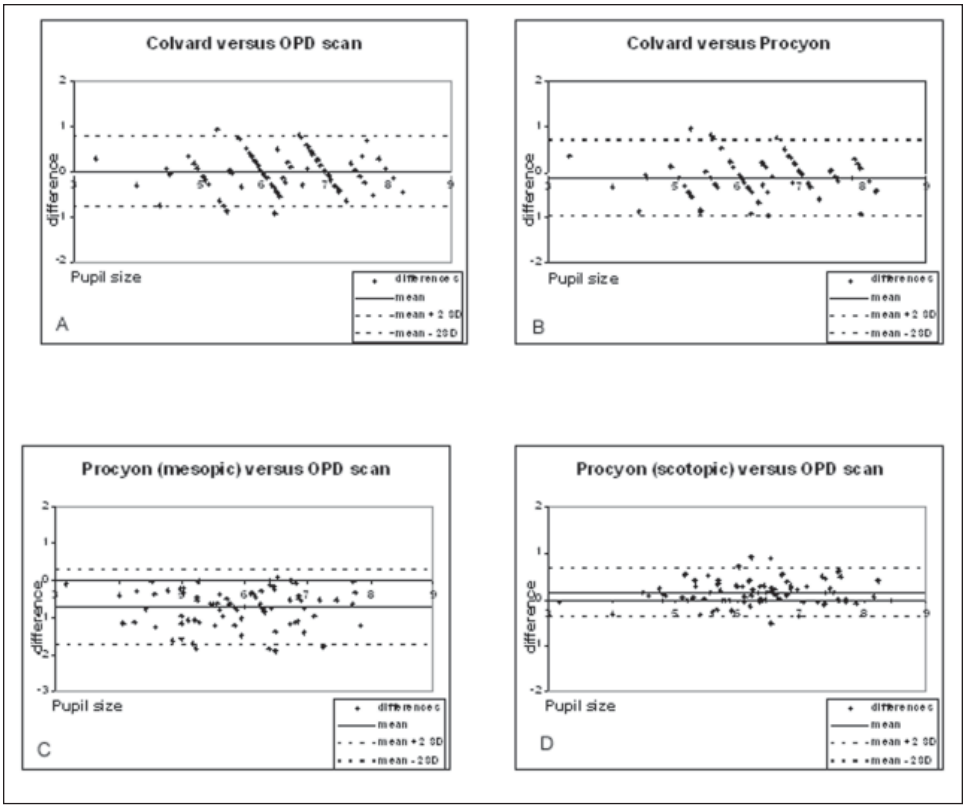

Figure 2. A) Agreement of the scotopic pupil size using the Colvard pupillometer and the mesopic pupil size using the NIDEK OPD-Scan. **B)** Agreement of the scotopic pupil size using the Colvard pupillometer and the scotopic pupil size of the Procyon pupillometer. **C)** Agreement of the mesopic pupil size using the Procyon pupillometer on low mesopic setting and the mesopic pupil size using the NIDEK OPD-Scan. **D)** Agreement of the scotopic pupil size using the Procyon pupillometer on scotopic setting and the mesopic pupil size using the NIDEK OPD-Scan.

ment is subjective and monocular, and 3) it can only measure pupil size under scotopic conditions.

The Procyon pupillometer may be much more accurate than the Colvard pupillometer, because it addresses a number of the disadvantages inherent to the Colvard pupillometer. For example, the Procyon pupillometer accounts for hippus, is objective, and takes binocular measurements. Moreover, measurements can be taken at three different illumination levels. The disadvantages of the Procyon pupillometer are that it is expensive and, similar to the Colvard, has no function other than pupillometry.

The OPD-Scan is a multifunction instrument used by refractive surgeons for a variety of applications, including wavefront measurement, corneal topography, and autorefraction, in addition to pupil measurement. Although the manufacturer, NIDEK Co Ltd, claims the machine measures mesopic pupil size, in this study the OPD-Scan "mesopic" pupil was, in fact, closer to the Procyon pupillometer and Colvard pupillometer scotopic pupil size. From the results obtained in this study, we believe that the OPD-Scan is actually measuring a scotopic pupil and not a mesopic pupil. If corneal topography and aberrometry are already being performed with the OPD-Scan, then the surgeon could use the pupil size data from the OPD-Scan rather than carry out this measurement on a different instrument.

REFERENCES

1. Haw WW, Manche EE. Effect of preoperative pupil measurements on glare, halos and visual function after photoastigmatic refractive keratectomy. *J Cataract Refract Surg.* 2001;27:907-916.
2. Martinez CE, Applegate RA, Klyce SD, McDonald MB, Medina JP, Howland HC. Effect of pupillary dilation on corneal optical aberrations after photorefractive keratectomy. *Arch Ophthalmol.* 1998;116:1053-1062.
3. Probst LE. The problem with pupils. *J Cataract Refract Surg.* 2004;30:2-4.
4. Kohnen T, Terzi E, Bühren J, Kohnen EM. Comparison of a digital and a handheld infrared pupillometer for determining scotopic pupil diameter. *J Cataract Refract Surg.* 2003;29:112-117.
5. Procyon P2000SA [technical specifications]. London, UK: Procyon Instruments Ltd; 2000.
6. Bland JM, Altman DG. Statistical methods for assessing agreement between two methods of clinical measurement. *Lancet.* 1986;i:307-310.
7. Kurz S, Krummenauer F, Pfeiffer N, Dick HB. Monocular versus binocular pupillometry. *J Cataract Refract Surg.* 2004;30:2551-2556.

Optical Quality Analysis After Surface Excimer Laser Ablation: The Relationship Between Wavefront Aberration and Subepithelial Haze

Yan Wang, MD; Jichang He, PhD; Kanxing Zhao, MD, PhD; Ying Jin, MD; Tong Zuo, OD; Wei Wang, PhD

ABSTRACT

PURPOSE: To investigate the relationship between mild and moderate corneal haze and the distribution of higher order wavefront aberrations after photorefractive keratectomy (PRK).

METHODS: Thirty-six eyes from 18 patients who underwent PRK were divided into two groups: 10 eyes with corneal haze and 26 eyes without corneal haze (control). All eyes were evaluated up to 6 months after PRK. Wavefront aberrations were measured using a psychophysical wavefront sensor and the NIDEK OPD-Scan. Topography, point spread function, and modulation transfer function maps were obtained from the OPD-Scan.

RESULTS: The mean total higher order aberration was slightly higher in the corneal haze group than in the control group. This difference was not statistically significant. The mean third order coma aberrations were higher and mean fourth order spherical aberrations were lower in the haze group compared with the control group, although neither difference attained statistical significance. The *t* test values were 1.05, −0.38, −1.10, −0.08, and −0.23, when comparing the mean third, fourth, fifth, sixth, and seventh order aberrations, respectively. None of these differences attained statistical significance. In terms of Zernike coefficients, Z_3^{-1} and Z_3^1 showed greater mean root-mean-square (RMS) in the haze group (0.33 and 0.35 μm, respectively) than those for the control group (0.26 and 0.23 μm, respectively) (t=0.71 and P=.49; t=0.84 and P=.43, respectively). However, Z_4^0 had lower RMS in the haze group (0.18 μm) than in the control group (0.28 μm). This difference also was not statistically significant.

CONCLUSIONS: In this study comparing the optical aberrations of eyes with and without corneal haze after PRK, corneal haze did not affect the magnitude and distribution of higher order aberrations in a predictable manner. [*J Refract Surg*. 2006;22:S1031-S1036.]

Renewed interest has arisen in surface excimer laser ablation procedures such as photorefractive keratectomy (PRK) for the correction of myopia, hyperopia, and astigmatism. Long-term visual performance for PRK and LASIK is similar for low to moderate ametropia.[1] Furthermore, surgical complications due to keratectomy during LASIK, such as buttonhole and partial flaps, can be avoided in PRK. Other postoperative complications associated with LASIK such as dry eye, diffuse lamellar keratitis, and rarely iatrogenic keratectasia also do not occur in PRK.[2,3] For custom ablation, better optical quality has been reported after PRK compared with LASIK.[4]

However, corneal haze is one major complication of surface excimer laser corneal ablation. Corneal haze has been extensively investigated at biochemical and histological levels and has been attributed to epithelial hyperplasia, newly synthesized collagens, and proteoglycans synthesized during the wound-healing process.[5-9] Corneal haze decreases corneal transparency and correlates significantly with regression of the refractive effect postoperatively.[10-12] Corneal haze after PRK has been implicated in impaired contrast sensitivity after PRK.[13-15] The aim of refractive surgery is not only to improve uncorrected visual acuity (UCVA) without losing best spectacle-corrected visual acuity (BSCVA), but to maintain or enhance visual function. Thus, it would be clinically beneficial to identify the effect of haze on the optical quality of the eye and the interaction of haze and visual performance.

Wavefront aberrations induced by refractive surgery have been recently demonstrated using a variety of aberrometric techniques.[16,17] The primary effect of the induced aberrations on visual performance is decreased low contrast acuity.[16,18] We hypothesize that subepithelial haze may be a cause of sur-

From the Refractive Surgery Center, Tianjin Eye Institute and Hospital, Teaching Hospital of Tianjin Medical University, Tianjin, China (Y. Wang, Zhao, Jin, Zuo, W. Wang); and New England College of Optometry, Boston, Mass (He).

The authors have no proprietary interest in the materials presented herein.

Correspondence: Yan Wang, MD, Refractive Surgery Center, Tianjin Eye Hospital, No. 4, Gansu Rd, Heping District Tianjin, 300020, China. Tel: 86 22 27305083; Fax: 86 22 27313336 82068; E-mail: wangyan7143@vip.sina.com.cn

gically induced aberrations. In this study, higher order aberrations were measured in both eyes with and without clinically significant corneal haze after PRK, and the difference in postoperative wavefront aberrations was compared between groups. As a secondary goal, we attempted to investigate the relationship between corneal haze and the distribution of higher order wavefront aberrations.

PATIENTS AND METHODS

Patient Population and Examinations

Thirty-six eyes from 18 myopic patients were selected from a group of 3000 eyes that underwent PRK with the NIDEK EC-5000 excimer laser (NIDEK Co Ltd, Gamagori, Japan). The selected patients were divided into two groups: those with clinically significant haze (haze group) and those without clinically significant haze (control group). Ten eyes from 5 patients had clinically significant haze. Twenty-six eyes from 13 patients of similar age and with similar refractions were selected as the control group.

The mean preoperative sphere for the haze group was −4.97 diopters (D) (range: −4.50 to −5.50 D), and the mean astigmatism was −0.17 D (range: 0.00 to −0.50 D). The mean preoperative sphere for the control group was −5.23 D (range: −4.50 to −5.75 D), and the mean preoperative astigmatism was −0.45 D (range: 0.00 to −1.25 D). All patients underwent preoperative examination, including UCVA, BSCVA, slit-lamp examination, wavefront aberrometry using the NIDEK OPD-Scan, corneal topography (Orbscan, version 3.0; Bausch & Lomb, Rochester, NY), and dilated fundus examination. Patients with ocular disease were excluded from surgery.

Surgical Procedure

Myopic PRK was performed using the NIDEK EC-5000 excimer laser at the Tianjin Eye Hospital, Teaching Hospital of Tianjin Medical University. The laser operates at a wavelength of 193 nm, a fixed pulse repletion rate of 30 Hz, and a radiant exposure of 100 to 140 mJ/cm^2 on the treatment plane. An optical zone of 6 mm with a 7-mm transition zone was used in all cases. Two drops of topical anesthetic were instilled, and a lid speculum was inserted in the operative eye. Photorefractive keratectomy was performed by mechanical debridement of epithelium to a diameter that encompassed the transition zone, followed by laser ablation. Immediately after surgery, topical tobramycin 0.3% combined with fluorometholone 0.1% was instilled in the eye. The patient was instructed to instill topical tobramycin 0.3% and fluorometholone 0.1% four times daily for 1 month followed by a tapered schedule of fluorometholone 0.1% over the subsequent 3 months.

Assessment of Corneal Haze

Corneal haze was categorized from grade 0 to grade 4 according to the United States Food and Drug Administration haze scale. Grade 0 indicated a clear cornea; grade 1 indicated trace haze; grade 2 indicated mild haze; grade 3 indicated haze; and grade 4 indicated marked haze.

Assessment of Aberrations

The wavefront aberrations were measured using the Suzhou BriteEye Model Wavefront Analyzer 1000 (Suzhou Medical Co Ltd, Suzhou, China), which uses a psychophysical ray-tracing technique described in previous studies.[19-21] The NIDEK OPD-Scan aberrometer was also used to measure aberration and simulate the point spread function (PSF) and modulation transfer function (MTF) for optical image analysis in relation to pupil size. Both aberrometers performed similarly for the patient population under study.

Wavefront aberrations were measured from 3 to 6 months after PRK. All aberrometry measurements were performed on a physiologically dilated pupil after the eye adapted to the dark for 10 minutes. The retinal illumination performing aberrometry in a dark room was less than 2 log trolands. All aberrometry data presented in this study are for a 6-mm pupil diameter.

Statistical Analysis

Analyses were performed using SPSS 11.0 for Windows (SPSS, Chicago, Ill). The comparison between the haze and control groups was evaluated using the independent *t* test. Statistical tests for Zernike aberrations were corrected for multiple comparisons using Bonferroni correction. A P value $<.05$ was considered statistically significant.

RESULTS

In the haze group, seven eyes had haze ranging from grade 1 to grade 2; the remaining three eyes developed grade 2 haze. Mean patient age was 24.2 years (range: 20 to 28 years) for the haze group versus 24.3 years (range: 18 to 33 years) for the control group. No statistically significant difference was noted between age and preoperative refraction between the two groups in this study.

Postoperative wavefront aberrations for all 36 eyes are plotted in Figure 1. Substantial individual variation in the magnitude of the wavefront aberrations is seen for the haze group and control group. For the haze group, the total wavefront root-mean-square (RMS) values varied from 0.63 to 1.99 µm, and the higher order

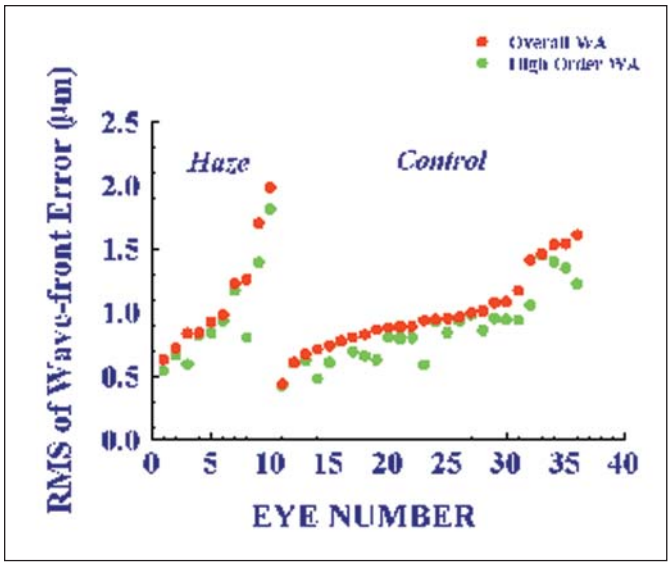

Figure 1. Magnitude of the wavefront aberrations for the haze group (n=10) and control group (n=26) after PRK. The root-mean-square (RMS) values (μm) of total wavefront aberrations (red solid circles) and high order wavefront aberrations (green solid circles) were plotted against the eye number. The values are plotted in ascending order based on the magnitude of the RMS value (μm).

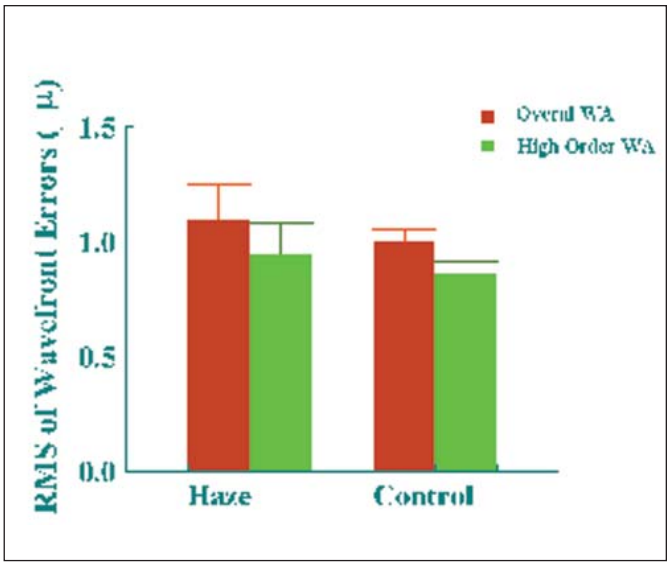

Figure 2. Mean root-mean-square (RMS) values (μm) of wavefront aberrations for the haze group and control group. The mean RMS values for overall wavefront aberrations are shown by the red bar and mean higher order wavefront aberrations are shown by the green bar. The error bar represents ±1 standard deviation.

aberrations varied from 0.55 to 1.82 μm (see Fig 1). For the control group, the total wavefront RMS values varied from 0.44 to 1.62 μm and the higher order aberrations varied from 0.43 to 1.23 μm (see Fig 1). The RMS value for the total wavefront aberrations was 1.10 μm for the haze group and 1.00 μm for the control group (Fig 2). The mean RMS for higher order aberrations was 0.95 μm for the haze group and 0.86 μm for the control group (see Fig 2). The total wavefront aberrations were larger than the higher order wavefront aberrations in both groups; however, the difference was not statistically significant (t=0.75, P>.05 for the haze group and t=1.66, P>.05 for the control group). No statistically significant differences were found between the two groups for total wavefront aberrations (t=0.65, P>.05) or for high order aberrations (t=0.62, P>.05).

The haze group was found to have greater mean RMS than the control group in third order aberrations but smaller mean values from the fourth to seventh Zernike orders (Fig 3). However, none of the differences between the two groups was statistically significant. The t values were 1.05, −0.38, −1.10, −0.08, and −0.23 for third, fourth, fifth, sixth, and seventh order aberrations, respectively.

Comparisons of individual Zernike coefficients for the third and fourth order (using the absolute coefficient value) between the haze group and the control group are summarized in Table 1. Results of t tests for differences in the mean coefficients between the two

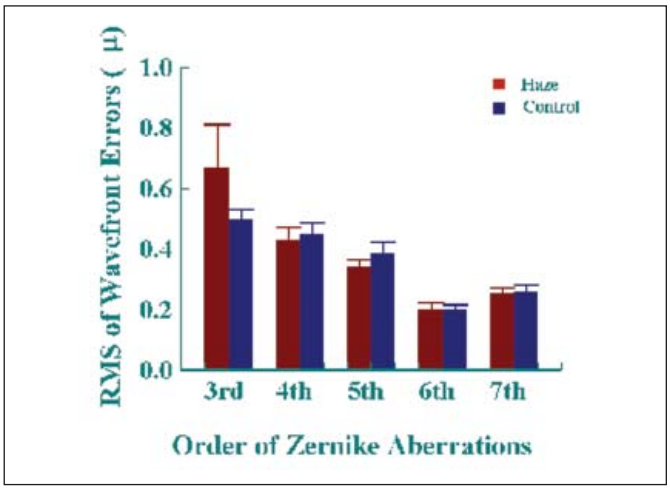

Figure 3. Mean root-mean-square (RMS) values (μm) of higher order wavefront aberrations (y-axis) separated by each order from the third to seventh order (x-axis) for the haze group (red bar) and the control group (blue bar). The error bar represents ±1 standard deviation.

groups are also presented in Table 1. No statistically significant difference was noted for the individual Zernike aberrations between the two groups.

Comparisons of individual Zernike coefficients for the third and fourth order (respecting the sign of each coefficient) between the haze group and the control group are summarized in Table 2. No statistically significant difference was noted for the individual Zernike aberrations between the two groups.

TABLE 1

Mean Absolute Values of the Root-Mean-Square (RMS) of the Individual Zernike Coefficients for the Third and Fourth Order Aberrations of the Haze and Control Groups

Zernike Coefficient	RMS (μm) Haze (n=10)	RMS (μm) Control (n=26)	*t*	*P* Value
Third order				
Z_3^{-3}	0.24	0.16	1.13	.29
Z_3^{-1}	0.33	0.26	0.71	.49
Z_3^{1}	0.35	0.23	0.84	.43
Z_3^{3}	0.18	0.17	0.17	.87
Fourth order				
Z_4^{-4}	0.10	0.09	0.51	.62
Z_4^{-2}	0.13	0.10	0.65	.53
Z_4^{0}	0.18	0.28	−1.75	.11
Z_4^{2}	0.19	0.13	1.10	.30
Z_4^{4}	0.13	0.18	−1.15	.28

TABLE 2

Mean Values of the Root-Mean-Square (RMS) of the Individual Zernike Coefficients for the Third and Fourth Order Aberrations of the Haze and Control Groups

Zernike Coefficient	RMS (μm) Haze (n=10)	RMS (μm) Control (n=26)	*t*	*P* Value
Third order				
Z_3^{-3}	−0.16	−0.13	−0.35	.74
Z_3^{-1}	−0.24	−0.02	−1.59	.15
Z_3^{1}	−0.17	−0.05	−0.69	.51
Z_3^{3}	−0.09	−0.03	−0.67	.52
Fourth order				
Z_4^{-4}	−0.03	0.03	−1.31	.22
Z_4^{-2}	−0.12	0.03	−3.04	.14
Z_4^{0}	0.11	0.26	−1.86	.10
Z_4^{2}	0.09	0.07	0.32	.76
Z_4^{4}	−0.002	0.02	−0.34	.74

CASE REPORT

A 25-year-old woman presented to Tianjan Eye Institute complaining of poor visual acuity in both eyes. Best spectacle-corrected visual acuity was 20/40 in the right eye with a manifest refraction of $-1.75\ -1.50 \times 180$ and 20/40 in the left eye with a manifest refraction of $-1.00\ -1.50 \times 15$.

Slit-lamp examination revealed grade 2 corneal haze in both eyes; other examination results were unremarkable. Evaluation of the corneal topography showed no topographic abnormalities that might be contributing to the decreased vision. Evaluation of the wavefront aberrations showed third order coma-like aberrations were higher than average values at 0.74 μm in the right eye. In the right eye, Z_3^{-1} was 0.58 μm and Z_3^{1} was 1.44 μm, both of which were appreciably higher than the mean values in the control group (Table 2). Point spread function and MTF evaluation demonstrated readily visible horizontal coma pattern in the right eye. The remaining higher order wavefront aberrations were within normal levels compared with the control group.

DISCUSSION

This is the first study that measures wavefront aberrations in eyes with corneal haze after PRK. In general, haze occurs in two phases. The first phase occurs early, within 2 weeks of surgery. The second phase occurs between 2 and 6 months and generally presents with a whitish appearance on slit-lamp examination. It is this second type of opacity that is commonly referred to as haze.

Although various studies have investigated corneal haze and visual function, few have considered the quality of the optical system of the eye.[22,23] The quality of the optical system can be determined using different methods. One method describes the detailed shape of the image for a simple geometrical object such as a point of light or a line. The distribution of light in the image plane is a PSF. Another method assesses underlying optical aberrations, rather than the secondary effect of these aberrations, on image quality. The results of this assessment can be presented in terms of the deviation of light rays from perfect reference rays (ray aberrations) or the deviation of optical wavefronts from the ideal reference wavefront (wavefront aberration). By measuring the optical aberrations of the eye, the image quality and visual performance can be directly correlated.

The hypothesis of this study was that subepithelial haze was more likely to induce wavefront aberrations after PRK. The magnitude of higher order aberrations of the eyes with corneal haze was slightly higher than that of the eyes without postoperative haze. However, this difference was not statistically significant ($P>.05$),

which indicates that there is little to no effect of mild to moderate corneal haze on optical aberrations.

Some studies report that visual performance is inversely related to the amount of haze and that haze did not appear to be an important contributing factor in the presence of persistent visual disturbances.[23,24] Monochromatic wavefront aberrations are primarily caused by surface irregularity of the cornea and the lens, misalignment of the optical axis between the cornea and the lens, and decoupling of aberrations between the cornea and the lens. Laser ablation on the corneal surface may disrupt the compensation of aberrations between the cornea and lens. The amount of wavefront aberrations induced by laser surgery could depend on many factors such as the level of preoperative aberrations, volume of tissue removal, excimer laser system used for performing surgery, experience of the surgeon, and perhaps corneal haze.[25-27]

The normal cornea is visible to an observer both by way of light reflected from its surface and light scattered toward the observer. Based on previous findings in rabbit eye models, one theory of corneal haze development after PRK proposed that haze dramatically enhances backscattering of light from highly reflective wound-healing keratocytes within the ablated region.[26,27] A confocal microscopic study on human eyes showed that enhanced cellular reflections from high numbers of wound-healing keratocytes are an important contributor to haze.[26] The appearance of corneal haze, therefore, is determined by combination of reflected and backscattered light.[25-27] Visual performance, particularly mesopic contrast sensitivity, is affected by wavefront aberrations, because wavefront aberrations cause the PSF to be widely distributed and thus reduce the image contrast on the retinal plane.[16,18]

In this study, fourth order spherical aberration was lower in the eyes with corneal haze compared with eyes in the control group. Although not a statistically significant difference, this observation is still noteworthy because it indicates that there may be lower amounts of spherical aberration with corneal haze than without corneal haze after PRK. Some studies have shown that mean spherical aberration increases after PRK and that the majority of corneas exhibit positive central asphericity, changing from a more prolate (negative asphericity) to an oblate shape.[17] In this study, observation of decreased spherical aberration in the haze group corresponds with histologic studies on human corneal tissue. Histologic studies have shown that corneal haze arises from epithelial hyperplasia, newly synthesized collagens, and proteoglycans.[26-28] Stromal wound healing and remodeling gradually lead to stromal thickening, especially within the central optical zone. The normal cornea is aspheric, with less curvature peripherally than centrally, which partially compensates for spherical aberration. After PRK for myopia, the peripheral cornea is steeper than the central cornea.[29,30] The newly synthesized tissue associated with corneal haze, however, results in thickening of the central cornea, mitigating the effect of the oblate corneal contour postoperatively by decreasing the induced spherical aberration.

Although not statistically significant, coma aberrations were slightly higher in the haze group compared with the control group. We believe that coma may be caused by slight distortion of the cornea induced by the haze. The three-dimensional representation of coma consists of a bulge above the reference plane or a bulge laterally with an adjacent opposite deformation within the pupil. Although the corneal haze appeared to be uniformly distributed within the ablation zones, there is a tendency for it to distribute heterogeneously over time.[30] The subjective clinical impression was that in the eyes with more severe corneal haze (see the Case Report), the different regions of pupil appeared deformed in patterns that corresponded somewhat to pattern and magnitude of the aberration map. This was also observed as an irregular reflection during corneal topography acquired with the Orbscan.

In the present study of the optical aberrations of eyes with corneal haze after PRK, haze was found to affect the magnitude and distribution of higher order aberrations in an unpredictable manner.

REFERENCES

1. Hersh PS, Brint SF, Maloney RK, Durrie DS, Gordon M, Michelson MA, Thompson VM, Berkeley RB, Schein OD, Steinert RF. Photorefractive keratectomy versus laser in situ keratomileusis for moderate and high myopia. A randomized prospective study. *Ophthalmology*. 1998;105:1512-1522.
2. Perez Santonja JJ, Ayala MJ, Sakla HF, Ruiz Moreno JM, Alio JL. Retreatment after laser in situ keratomileusis. *Ophthalmology*. 1999;106:21-28.
3. Stulting RD, Carr JD, Thompson KP, Waring GO III, Wiley WM, Walker JG. Complications of laser in situ keratomileusis for the correction of myopia. *Ophthalmology*. 1999;106:13-20.
4. Panagopoulou SI, Pallikaris IG. Wavefront customized ablations with the WASCA Asclepion workstation. *J Refract Surg*. 2001;17:S608-S612.
5. Hanna KD, Pouliquen YM, Waring GO III, Savoldelli M, Cotter J, Morton K, Menasche M. Corneal stromal wound healing in rabbits after 193-nm excimer laser surface ablation. *Arch Ophthalmol*. 1989;107:895-901.
6. Tuft SJ, Zabel RW, Marshall J. Corneal repair following keratectomy. A comparison between conventional surgery and laser photoablation. *Invest Ophthalmol Vis Sci*. 1989;30:1769-1777.
7. Malley DS, Steinert RF, Puliafito CA, Dobi ET. Immunofluorescence study of corneal wound healing after excimer laser anterior keratectomy in the monkey eye. *Arch Ophthalmol*. 1990;108:1316-1322.

8. Latvala T, Tervo K, Mustonen R, Tervo T. Expression of cellular fibronectin and tenascin in the rabbit cornea after excimer laser photorefractive keratectomy: a 12 month study. *Br J Ophthalmol.* 1995;79:65-69.
9. Amm M, Wetzel W, Winter M, Uthoff D, Duncker GI. Histopathological comparison of photorefractive keratectomy and laser in situ keratomileusis in rabbits. *J Refract Surg.* 1996;12:758-766.
10. Gartry DS, Kerr Muir MG, Marshall J. The effect of topical corticosteroids on refraction and corneal haze following excimer laser treatment for myopia: an update. A prospective, randomized, double masked study. *Eye.* 1993;7:584-590.
11. Epstein D, Tengroth B, Fagerholm P, Hamberg-Nystrom H. Excimer retreatment of regression after photorefractive keratectomy. *Am J Ophthalmol.* 1994;117:456-461.
12. Siganos DS, Katsanevaki VJ, Pallikaris IG. Correlation of subepithelial haze and refractive regression 1 month after photorefractive keratectomy for myopia. *J Refract Surg.* 1999;15:338-342.
13. Lohmann CP, Gartry D, Kerr Muir M, Timberlake G, Fitzke F, Marshall J. Haze in photorefractive keratectomy: its origins and consequences. *Laser and Light in Ophthalmology.* 1991;4:15-34.
14. McCarty CA, Aldred GF, Taylor HR. Comparison of results of excimer laser correction of all degrees of myopia at 12 months postoperatively. The Melbourne Excimer Laser Group. *Am J Ophthalmol.* 1996;121:372-383.
15. Shah S, Chatterjee A, Smith RJ. Predictability of spherical photorefractive keratectomy for myopia. *Ophthalmology.* 1998;105:2178-2184.
16. Seiler T, Kaemmerer M, Mierdel P, Krinke HE. Ocular optical aberrations after photorefractive keratectomy for myopia and myopic astigmatism. *Arch Ophthalmol.* 2000;118:17-21.
17. Moreno-Barriuso E, Lloves JM, Marcos S, Navarro R, Llorente L, Barbero S. Ocular aberrations before and after myopic corneal refractive surgery: LASIK-induced changes measured with laser ray tracing. *Invest Ophthalmol Vis Sci.* 2001;42:1396-1403.
18. Applegate RA, Hilmantel G, Howland HC, Tu EY, Starck T, Zayac EJ. Corneal first surface optical aberrations and visual performance. *J Refract Surg.* 2000;16:507-514.
19. He JC, Marcos S, Webb RH, Burns SA. Measurement of the wavefront aberration of the eye by a fast psychophysical procedure. *J Opt Soc Am A.* 1998;15:2449-2456.
20. He JC, Burns SA, Marcos S. Monochromatic aberrations in the accommodated human eye. *Vision Res.* 2000;40:41-48.
21. He JC, Sun P, Held R, Thorn F, Sun X. Gwiazda J. Wavefront aberrations in eyes of emmetropic and moderately myopic school children and young adults. *Vision Res.* 2002;42:1063-1070.
22. Tomidokoro A, Soya K, Miyata K, Armin B, Tanaka S, Amano S, Oshika T. Corneal irregular astigmatism and contrast sensitivity after photorefractive keratectomy. *Ophthalmology.* 2001;108:2209-2212.
23. Corbett MC, Prydal JI, Oliver KM, Pande M, Marshall J. An in vivo investigation of the structures responsible for corneal haze after photorefractive keratectomy and their effect on visual function. *Ophthalmology.* 1996;103:1366-1380.
24. Shimizu K, Amano S, Tanaka S. Photorefractive keratectomy for myopia: one-year follow-up in 97 eyes. *J Refract Corneal Surg.* 1994;10:S178-S187.
25. Lohmann CP, Timberlake GT, Fitzke FW, Gartry DS, Muir MK, Marshall J. Corneal light scattering after excimer laser photorefractive keratectomy: the objective measurements of haze. *J Refract Corneal Surg.* 1992;8:114-121.
26. Moller-Pedersen T, Cavanagh D, Petroll M, Jester JV. Stromal wound healing explains refractive instability and haze development after photorefractive keratectomy: a 1-year confocal microscopic study. *Ophthalmology.* 2000;107:1235-1245.
27. Moller-Pedersen T, Cavanagh D, Petroll M, Jester JV. Corneal haze development after PRK is regulated by the volume of stromal tissue removal. *Cornea.* 1998;17:627-639.
28. Wang Y, Zhao KX, Su LY, Wang LJ, Geng WL, Jin Y. The expression of TGF-ß1 and bFGF after LASEK and the effects of 20% ethanol exposure on corneal wound healing [Chinese]. *Zhonghua Yan Ke Za Zhi.* 2005;41:498-504.
29. Martinez C, Applegate R, Klyce S. Effects of pupillary dilation on corneal optical aberrations after photorefractive keratectomy. *Arch Ophthalmol.* 1998;116:1053-1062.
30. Maldonado MJ, Arnau V, Navea A, Martinez-Costa R, Mico FM, Cisneros AL, Menezo JL. Direct objective quantification of corneal haze after excimer laser photorefractive keratectomy for high myopia. *Ophthalmology.* 1996;103:1970-1978.

Precision of Higher Order Aberration Repeatability With NIDEK OPD-Scan Retinoscopic Aberrometry

Jackson Barreto, Jr, MD; Marcelo V. Netto, MD; Alberto Cigna, MD; Samir Bechara, MD; Newton Kara-José, MD

ABSTRACT

PURPOSE: To evaluate repeatability of the total high order aberrations with a retinoscopic wavefront sensor.

METHODS: This prospective case series analyzed 12 eyes from 6 patients who underwent wavefront measurement using retinoscopic aberrometry with the NIDEK Optical Path Difference Scan (OPD-Scan). Four consecutive wavefront measurements of each eye were taken by two trained examiners for 5.8±0.8-mm and 8.2±0.6-mm pupils (P=.002, Wilcoxon test). Total high order aberrations out to the eighth order were assessed including third order coma, third order trefoil, fourth order quadrafoil, fourth order secondary astigmatism, and fourth order spherical aberrations. Differences between measurements of all of the variables were analyzed. A P value $<$.05 was considered statistically significant.

RESULTS: Repeatability analysis of the root-mean-square of total higher order aberrations, coma, trefoil, quadrafoil, secondary astigmatism, and spherical aberrations for both dilated and nondilated pupils did not show a statistically significant difference among all repeated measurements, except for trefoil and secondary astigmatism (analysis of variance and the Friedman test). The repeatability of total higher order aberrations was 0.15 μm for nondilated pupils and 0.18 μm for dilated pupils. Except for trefoil measurements, all high order aberrations showed reproducibility $>$0.15 μm when Zernike coefficients were analyzed individually.

CONCLUSIONS: The NIDEK OPD-Scan aberrometer measures total higher order astigmatism and most individual aberrations with acceptable repeatability. However, measurement of trefoil with this instrument is less repeatable. [*J Refract Surg*. 2006;22:S1037-S1040.]

In the past few decades, multiple keratorefractive surgical procedures have been proposed to correct spherocylindrical errors and improve final uncorrected visual acuity. Despite the safety, predictability, and efficacy of current laser surgery techniques, issues involving postoperative visual function remain a challenge in the field. Previous studies have reported a consistent decrease in visual performance after laser surgery. Contrast sensitivity reduction, especially decreased low-contrast visual acuity, and night vision problems after LASIK and photorefractive keratectomy have been frequently reported.[1-9]

Motivated by the desire to monitor and optimize visual quality after refractive surgery, the development of wavefront sensing technology has enabled the quantification of ocular aberrations.[10] Wavefront maps generated by such devices represent deviation from the ideal diffraction-limited optical systems and help the ophthalmologist understand debilitating visual complaints after conventional refractive surgery.[11-13]

The ability to measure optical wavefront errors also offers the potential to surgically control them, launching a concerted effort toward individually customized wavefront treatments. However, before relying on measurements by any device to diagnose or treat a wavefront abnormality, it is necessary to ensure that the device provide consistent information. This study aims to assess the total high order aberrations measurement repeatability with a retinoscopic wavefront sensor.

PATIENTS AND METHODS

Twelve eyes from six patients (two women and four men) with a mean age of 31±6.8 years (range: 23 to 43 years) were prospectively evaluated. All patients were healthy with no previous ocular history or abnormalities other than the current refractive error. Patients with ocular pathology, previous corneal or refractive surgery, surface irregularities, signs

From the Department of Ophthalmology, University of São Paulo, Brazil.

The authors have no proprietary or financial interest in the materials presented herein.

Correspondence: Marcelo V. Netto, MD, Alameda Lorena 1360/114 - Jardim Paulista 01424-001 - São Paulo, SP - Brazil. Tel/Fax: 55 11 3085 8714; E-mail: mvnetto@gmail.com

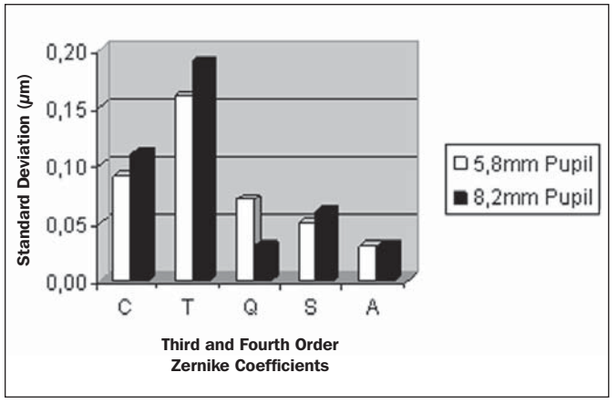

Figure 1. Reproducibility (standard deviation in microns) of the third and fourth order Zernike coefficients at 5.8-mm and 8.2-mm pupils. C = coma, T = trefoil, Q = quadrafoil, S = spherical aberration, A = secondary astigmatism

and symptoms of dry eye, and corneal opacities were excluded from the study. The research followed the tenets of the Declaration of Helsinki, and informed consent was obtained after explanation of the nature and possible consequences of the study.

All patients underwent retinoscopic aberrometry using the NIDEK Optical Path Difference Scan system (OPD-Scan; NIDEK Co Ltd, Gamagori, Japan) for both 5.8±0.8-mm and 8.2±0.6-mm pupils. Four consecutive OPD-Scan measurements were performed without pupil dilation or cycloplegia by two different examiners under standardized light conditions. Successive measurements were taken 1 minute apart. After instillation of one drop each of tropicamide 1% and phenylephrine 2.5%, measurements were repeated as described above. Head positioning and eye alignment were carefully checked before every measurement.

The OPD-Scan uses dynamic retinoscopy that is somewhat similar to standard autorefraction technology. Four sensors at different diameters of the cornea capture 1440 points in 0.4 seconds. As a result, there is a total refractive power aberration map (OPD map) that shows the total refractive power of the entire eye (cornea, vitreous, and lens) in diopters. The baseline wavefront plane is calculated using the information derived from the OPD measurements, and the deviations from a wavefront reference plane are expressed in micrometers of light. The normalized Zernike polynomial expansion was used to decompose the wavefront error into individual error modes. The magnitudes of the coefficients of the Zernike polynomials were represented as the root-mean-square (RMS, in micrometers) and are used to show the wavefront aberrations. The following data were evaluated: total higher order aberration RMS from the third to the eighth radial orders, third order coma (Z_3^1, Z_3^{-1}), third order trefoil (Z_3^3, Z_3^{-3}), fourth order quadrafoil (Z_4^4, Z_4^{-4}), fourth order secondary astigmatism (Z_4^2, Z_4^{-2}), and fourth order spherical aberration (Z_4^0).

All measurements were analyzed together using the discriminant function analysis. Differences among all measures of each variable (higher order aberration, coma, trefoil, quadrafoil, astigmatism, and spherical aberration) were examined separately with both the Friedman test and analysis of variance (ANOVA) with repeated measures. The Wilcoxon matched pairs test was used to analyze the difference in the mean values of all possible combinations of measurements for each variable. All statistical tests were conducted at an alpha level of 0.05. The following four types of statistical software were used: Statistica for Windows 5.0A (StatSoft Inc, Tulsa, Okla); Minitab 14.2 (Minitab Inc, State College, Pa); SPSS for Windows 10.0.1 (SPSS Inc, Chicago, Ill); and NCSS 2000 (NCSS Inc, Kaysville, Utah).

RESULTS

Twelve eyes from six patients with a mean OPD spherical equivalent refraction of −5.50±3.40 diopters (D) were analyzed. The mean nondilated pupil diameter was 5.8±0.8 mm, and the mean pharmacologically dilated pupil diameter was 8.2±0.6 mm (P=.002, Wilcoxon test). All pupil diameters were measured with the Colvard pupillometer (Oasis Medical, Glendora, Calif). Higher order aberration repeatability in the same eye varied according to pupil size (Fig 1). When measurements were taken with larger pupils (dilated pupils), a higher standard deviation was found for coma, trefoil, and secondary astigmatism, whereas a lower standard deviation was found for quadrafoil.

Repeatability analysis of the RMS of total higher order aberrations, coma, trefoil, quadrafoil, secondary astigmatism, and spherical aberration for both dilated and nondilated pupils did not show a statistically significant difference among all repeated measurements, except for trefoil and secondary astigmatism (Tables 1 and 2) (ANOVA and the Friedman test).

Repeatability of total higher order aberrations for nondilated pupils was 0.15 µm and 0.18 µm for dilated pupils. Except for trefoil measurements, all higher order aberrations showed reproducibility <0.15 µm when Zernike coefficients were analyzed individually (see Fig 1). Figures 2 and 3 show the mean and confidence intervals (95% CI) for spherical aberration and coma, respectively. All possible combinations of measurements, taken from two examiners (J and A) for dilated and nondilated pupils, for each variable (J1×J2; A1×A2; J1×A1; J2×A2; J1×A2; J2×A1) were tested using the Wilcoxon matched pairs test. The P value was >.05 for all coma, trefoil, and spherical aberration

TABLE 1

Repeatability Analysis of Total High Order Aberration, Coma, Trefoil, Quadrafoil, Astigmatism, and Spherical Aberration Root-Mean-Square Using ANOVA and the Friedman Test for Non-dilated Pupils

	Mean±Standard Deviation (μm)				*P* Level	
Variable	**1st**	**2nd**	**3rd**	**4th**	**Friedman**	**ANOVA**
Total high order aberration	0.456±0.15	0.375±0.15	0.409±0.14	0.396±0.17	0.512	0.167
Coma	0.190±0.08	0.161±0.10	0.225±0.11	0.188±0.10	0.341	0.133
Trefoil	0.342±0.19	0.273±0.14	0.268±0.15	0.270±0.18	0.051	0.036*
Quadrafoil	0.086±0.04	0.093±0.06	0.091±0.10	0.088±0.06	0.809	0.995
Astigmatism	0.086±0.03	0.058±0.02	0.086±0.04	0.076±0.04	0.024*	0.072
Spherical aberration	0.061±0.04	0.060±0.04	0.061±0.06	0.068±0.06	0.736	0.950

**Significant difference.*

TABLE 2

Repeatability Analysis of Total High Order Aberration, Coma, Trefoil, Quadrafoil, Astigmatism, and Spherical Aberration Root-Mean-Square Using ANOVA and the Friedman Test for Dilated Pupils

	Mean±Standard Deviation (μm)				*P* Level	
Variable	**1st**	**2nd**	**3rd**	**4th**	**Friedman**	**ANOVA**
Total high order aberration	0.455±0.15	0.478±0.16	0.461±0.17	0.517±0.23	0.328	0.056
Coma	0.229±0.11	0.235±0.11	0.248±0.10	0.261±0.13	0.202	0.368
Trefoil	0.331±0.18	0.357±0.17	0.317±0.20	0.384±0.24	0.088	0.034*
Quadrafoil	0.060±0.03	0.069±0.04	0.070±0.04	0.071±0.03	0.658	0.673
Astigmatism	0.076±0.03	0.071±0.03	0.074±0.03	0.079±0.03	0.453	0.590
Spherical aberration	0.077±0.07	0.069±0.06	0.077±0.06	0.088±0.07	0.097	0.090

**Significant difference.*

combinations for both pupil diameters. Statistically significant differences were found for astigmatism measurements at the 5.8-mm pupil diameter and for trefoil measurements at both pupil diameters.

DISCUSSION

In this study, retinoscopic aberrometry measurements for two different pupil sizes were acquired by two different examiners to assess measurement repeatability with the NIDEK OPD-Scan. According to previous findings,[14-18] the ocular wavefront aberrations differed from patient to patient, with a mean standard deviation of approximately 0.25 μm for total higher order aberrations. However, we found better values for total higher order aberration reproducibility when analyzing the total third to eighth radial orders (0.15 and 0.18 μm for nondilated and dilated pupils, respectively). Using a Hartmann-Shack wavefront sensor, Carkeet et al[19] reported similar findings (0.15 μm) for higher order aberration (third to fifth order) test-retest measurement repeatability.

Overall reproducibility was good in this study. When Zernike coefficients were analyzed individually, repeatability of trefoil was not satisfactory, with the highest variability among all coefficients (Tables 1 and 2). Analysis of secondary astigmatism revealed low reproducibility for a 5.2-mm pupil (Table 1). Coma, quadrafoil, and spherical aberration measurements showed better agreement when ANOVA for repeated measurements and the Friedman test were used (Tables 1 and 2). Focusing on the repeatability of coma and spherical aberration, Zadok et al[18] reported a higher standard deviation with the OPD-Scan than described in the present

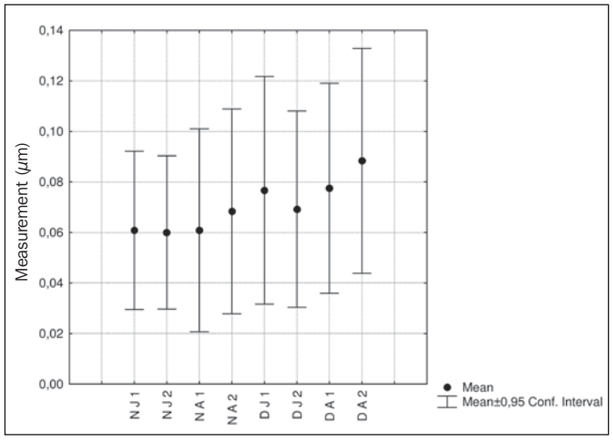

Figure 2. The mean and 95% confidence interval for all measurements of spherical aberration. Two examiners [(J), (A)] performed two measurements each (1) and (2) for both dilated (D) and nondilated (N) pupils.

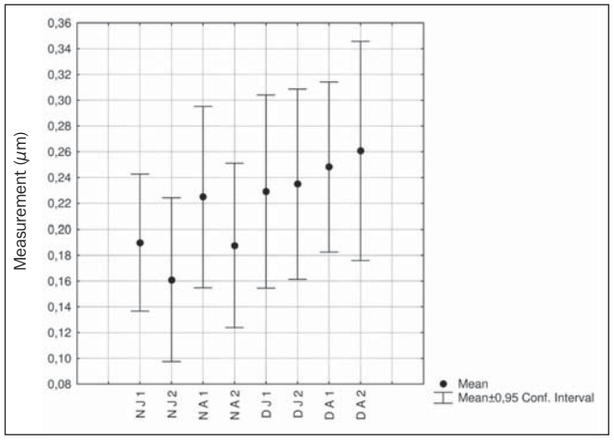

Figure 3. The mean and 95% confidence interval for all measurements of coma. Two examiners [(J), (A)] performed two measurements each (1) and (2) for both dilated (D) and nondilated (N) pupils.

study. This may be explained by the different z-axis adjustments in the device, which are operator dependent. We believe that variability can be minimized by acquiring three or more consecutive manual autorefractions prior to topographic captures rather than using the automatic measuring mode.

This study also evaluated all variables in two different zones of the entrance aperture (pupil sizes) and found higher standard deviation values for dilated pupils, with the exception of standard deviation values for quadrafoil (see Fig 1). Although not statistically different, there was a higher variation of the mean for coma measurements in nondilated pupils (see Fig 3). In addition, there was a higher CI value for coma measurements in nondilated pupils (see Fig 1). Conversely, nondilated pupils showed a more uniform pattern in spherical aberration measurements (see Fig 2).

The NIDEK OPD-Scan aberrometer measures total higher order aberration and most individual aberrations with acceptable repeatability, although measurement of trefoil with this instrument is less repeatable.

REFERENCES

1. Mutyala S, McDonald MB, Scheinblum KA, Ostrick MD, Brint SF, Thompson H. Contrast sensitivity evaluation after laser in situ keratomileusis. *Ophthalmology*. 2000;107:1864-1867.
2. Chan JW, Edwards MH, Woo GC, Woo VC. Contrast sensitivity after laser in situ keratomileusis: one-year follow-up. *J Cataract Refract Surg*. 2002;28:1774-1779.
3. Sano Y, Carr JD, Takei K, Thompson KP, Stulting RD, Waring GO III. Videokeratography after excimer laser in situ keratomileusis for myopia. *Ophthalmology*. 2000;107:674-684.
4. Perez-Santonja JJ, Sakla HF, Alio JL. Contrast sensitivity after laser in situ keratomileusis. *J Cataract Refract Surg*. 1998;24:183-189.
5. Holladay JT, Dudeja DR, Chang J. Functional vision and corneal changes after laser in situ keratomileusis determined by contrast sensitivity, glare testing, and corneal topography. *J Cataract Refract Surg*. 1999;25:663-669.
6. Nakamura K, Bissen-Miyajima H, Toda I, Hori Y, Tsubota K. Effect of laser in situ keratomileusis correction on contrast visual acuity. *J Cataract Refract Surg*. 2001;27:357-361.
7. Ghaith AA, Daniel J, Stulting RD, Thompson KP, Lynn M. Contrast sensitivity and glare disability after radial keratotomy and photorefractive keratectomy. *Arch Ophthalmol*. 1998;116:12-18.
8. Bullimore MA, Olson MD, Maloney RK. Visual performance after photorefractive keratectomy with a 6-mm ablation zone. *Am J Ophthalmol*. 1999;128:1-7.
9. Niesen U, Businger U, Hartmann P, Senn P, Schipper I. Glare sensitivity and visual acuity after excimer laser photorefractive keratectomy for myopia. *Br J Ophthalmol*. 1997;81:136-140.
10. Liang J, Grimm B, Goelz S, Bille JF. Objective measurement of wave aberrations of the human eye with the use of a Hartmann-Shack wave-front sensor. *J Opt Soc Am A*. 1994;11:1949-1957.
11. Chalita MR, Chavala S, Xu M, Krueger RR. Wavefront analysis in post-LASIK eyes and its correlation with visual symptoms, refraction, and topography. *Ophthalmology*. 2004;111:447-453.
12. Tuan KA, Chernyak D, Feldman ST. Predicting patients' night vision complaints with wavefront technology. *Am J Ophthalmol*. 2006;141:1-6.
13. Chalita MR, Xu M, Krueger RR. Correlation of aberrations with visual symptoms using wavefront analysis in eyes after laser in situ keratomileusis. *J Refract Surg*. 2003;19:S682-S686.
14. MacRae S, Fujieda M. Slit skiascopic-guided ablation using the Nidek laser. *J Refract Surg*. 2000;16:S576-S580.
15. Porter J, Guirao A, Cox IG, Williams DR. Monochromatic aberrations of the human eye in a large population. *J Opt Soc Am A Opt Image Sci Vis*. 2001;18:1793-1803.
16. Castejón-Mochon JF, López-Gil N, Benito A, Artal P. Ocular wave-front aberration statistics in a normal young population. *Vision Res*. 2002;42:1611-1617.
17. Wang L, Koch DD. Ocular higher-order aberrations in individuals screened for refractive surgery. *J Cataract Refract Surg*. 2003;29:1896-1903.
18. Zadok D, Levy Y, Segal O, Barkana Y, Morad Y, Avni I. Ocular higher-order aberrations in myopia and skiascopic wavefront repeatability. *J Cataract Refract Surg*. 2005;31:1128-1132.
19. Carkeet A, Velaedan S, Tan YK, Lee DY, Tan DT. Higher order ocular aberrations after cycloplegic and non-cycloplegic pupil dilation. *J Refract Surg*. 2003;19:316-322.

Clinical Use of In Vivo Confocal Microscopy Through Focusing in Corneal Refractive Surgery

Li Ying, MD, PhD; Zhang Xiao; Zhong Liuxueying; Jin Yumei

ABSTRACT

PURPOSE: To illustrate the use of in vivo confocal microscopy through focusing to observe normal cornea and corneal wound healing after excimer laser refractive surgery.

METHODS: A total of 197 eyes, including both unoperated eyes and eyes that had undergone LASIK, photorefractive keratectomy (PRK), or laser epithelial keratomileusis (LASEK), were examined using in vivo confocal microscopy through focusing. Images of the various corneal layers resolved by confocal microscopy through focusing were recorded and analyzed. Pachymetry of the cornea, epithelium, and stroma was also recorded for all eyes. The *t* test was used to evaluate the differences between unoperated eyes and postoperative eyes and the change in corneal pachymetry preoperatively to postoperatively with each type of surgery. A *P* value $<.05$ was considered statistically significant.

RESULTS: Each layer of the cornea could be resolved in unoperated eyes and eyes that had undergone refractive surgery. Wound healing could be followed over time using confocal microscopy through focusing. In eyes that underwent PRK, at 1 month postoperatively, the entire cornea and stroma were thinner than preoperatively, whereas the epithelial layer was statistically significantly thicker ($P<.05$). Haze after PRK is seen as reflectivity of subepithelial anterior stroma. No clinically significant haze was observed in eyes that underwent LASEK or LASIK. The features of the eyes that underwent LASIK were the same as those of unoperated eyes.

CONCLUSIONS: Confocal microscopy through focusing was useful in documenting cellular morphology in unoperated corneas and corneas that had undergone refractive surgery. Wound-healing characteristics of eyes that had undergone refractive surgery were also documented using confocal microscopy. [*J Refract Surg*. 2006;22: S1041-S1046.]

In vivo confocal microscopy through focusing is a relatively new, noninvasive technique that allows direct visualization of the cornea in vivo. Through continuous confocal scanning and focus analysis, a repeatable and real-time display of each of the corneal layers can be performed. Each layer of the cornea can be visualized separately using varying light intensities. The ability to visualize the cornea structures in vivo enables the determination of normal or pathologic processes occurring within each layer and allows accurate diagnoses of various corneal conditions.

Clinically, confocal microscopy can be used to identify pathogens in the cornea and to investigate the cornea after corneal refractive surgery. This study illustrates the use of in vivo confocal microscopy through focusing examination before and after LASIK, photorefractive keratectomy (PRK), and laser epithelial keratomileusis (LASEK) in a Chinese population. In this study, the investigators attempted to provide normative values for normal and postsurgical corneas.

PATIENTS AND METHODS

Patient Population

In vivo confocal microscopy through focusing using the ConfoScan 2.0 (NIDEK Co Ltd, Gamagori, Japan) was used to evaluate 197 healthy corneas from 100 patients (43 men and 57 women). Mean patient age was 25.3 years (range: 18 to 45 years). Twenty-five patients (50 eyes) were healthy volunteers consisting of students, physicians, and nurses from the Department of Ophthalmology, Peking Union Medical College Hospital, Chinese Academy of Medical Sciences, Beijing, China. Forty patients (77 eyes) underwent PRK, 20 patients (40 eyes) underwent LASIK, and 15 patients (30 eyes) underwent LASEK. Confocal microscopy through focusing was performed at 10 days and 1 month, 3 months, and 6 months postoperatively.

From the Department of Ophthalmology, Peking Union Medical College Hospital, Chinese Academy of Medical Sciences, Beijing, China.

The authors have no financial interest in the materials presented herein.

Correspondence: Li Ying, MD, PhD, Dept of Ophthalmology, Peking Union Medical College Hospital, Chinese Academy of Medical Sciences, Beijing, China, 100730. Tel: 86 10 65296114; E-mail: liyingpumch@sohu.com

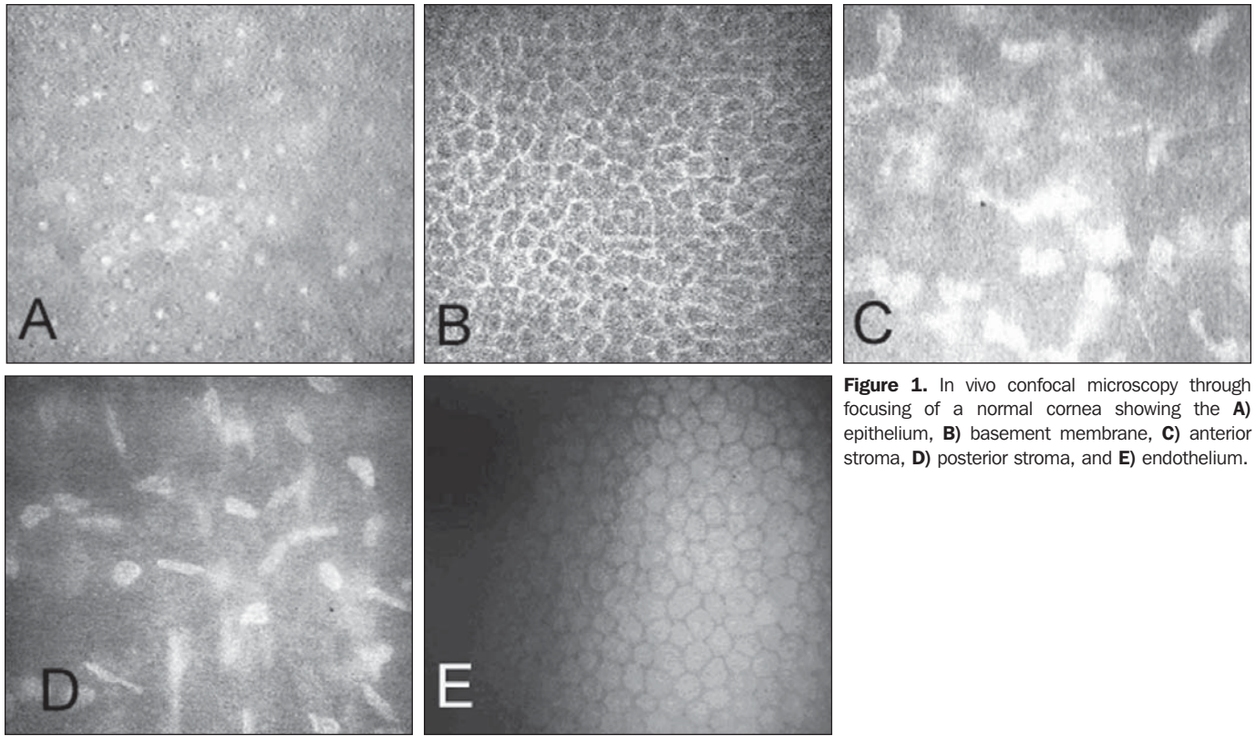

Figure 1. In vivo confocal microscopy through focusing of a normal cornea showing the **A)** epithelium, **B)** basement membrane, **C)** anterior stroma, **D)** posterior stroma, and **E)** endothelium.

Examination, Data Collection, and Analysis

All patients underwent slit-lamp microscopy to rule out corneal dystrophies and diseases. The ConfoScan 2.0 probe was properly positioned by manual adjustment. All images were viewed on a digital video monitor. A digital videorecorder was used to record all images. Topical anesthetic was instilled in the cornea followed by instillation of 2.5% carboxymethylcellulose as a coupling gel between the objective lens and the cornea. Examination of the corneal epithelium, stroma, and endothelium was performed at 200× magnification. Confocal microscopy through focusing was used to observe every position of the central cornea, consisting of an area 400×400 μm^2 along the x- and y-axes. Recording of every layer began at the surface epithelium and ended posteriorly at the endothelium. All images were acquired from the central cornea, recorded, and then analyzed by an experienced clinician for consistency. A Z-scan was used to measure the thickness of the corneal epithelium and stroma. The cellular density (mm^2) and thickness (µm) of every corneal layer were recorded as mean±standard deviation. The *t* test was used to evaluate the differences between unoperated and postoperative eyes. A *P* value <.05 was considered statistically significant.

RESULTS

Normal Corneal Structure in Unoperated Eyes

Each of the corneal layers was recorded anteriorly to posteriorly (Fig 1). Table 1 shows the distribution of cells and the characteristics of each corneal layer. The epithelial cells were relatively large, irregular, and round or oval. The cell nucleus was bright, with a diameter of 2 to 4 µm. The basement cells were relatively small and regular and polygonal, and the cytoplasm was dark and the nuclei were not resolved. The nuclei of anterior stromal cells were irregular. Stromal cells were more numerous anteriorly than posteriorly. The nuclei of posterior stromal cells were oval, long oval, and stick-like. In most patients, Bowman's membrane and Descemet's membrane could not be visualized. In Bowman's membrane, only the nerve fibers were visible. The endothelial cells were bright, uniform, and hexagonal. The nucleus was not resolved, and the adhesion between cells was dark.

The tear film, including its components such as the lipid layer, was easily observed. The nerve plexus appeared as fine bead-like structures, and the primary nerve fibers could be visualized within the corneal stroma, along the three-dimensional space.

The mean corneal thickness was 543.0±67.9 µm (range: 508.4 to 681.2 µm), the mean stromal thickness

TABLE 1

Characteristics of the Layers of a Normal Unoperated Cornea Using In Vivo Confocal Microscopy Through Focusing

Layer	Cell size (μm)	Configuration	Cell Nucleus	Density (mm^2) (range)
Epithelium				
Epithelial	19 to 21	Irregular round/oval, dark cytoplasm	Round, bright, 2 to 4 μm uniform	1297±265 (987 to 1933)
Epithelial basement	10 to 16	Polygon, regular size, dark cytoplasm, bright joints of cells	Unobvious	3875±491 (3312 to 4021)
Stroma*				
Anterior		Slightly irregular, background among nucleus	Large amount, weak glisten, regular	982±113 (720 to 1072)
Posterior		Oval/long oval/stick-like	Diameter 10 to 30 μm	731±73.7 (540 to 782)
Endothelium				
Endothelial	16 to 19	Uniform, regular hexagon, bright cells, dark joints of cells	Unobvious	2570±162 (2278 to 2824)

**Cell adhesion can only been seen in pathologic conditions, when the cellular activity increase or tissues are edematous.*

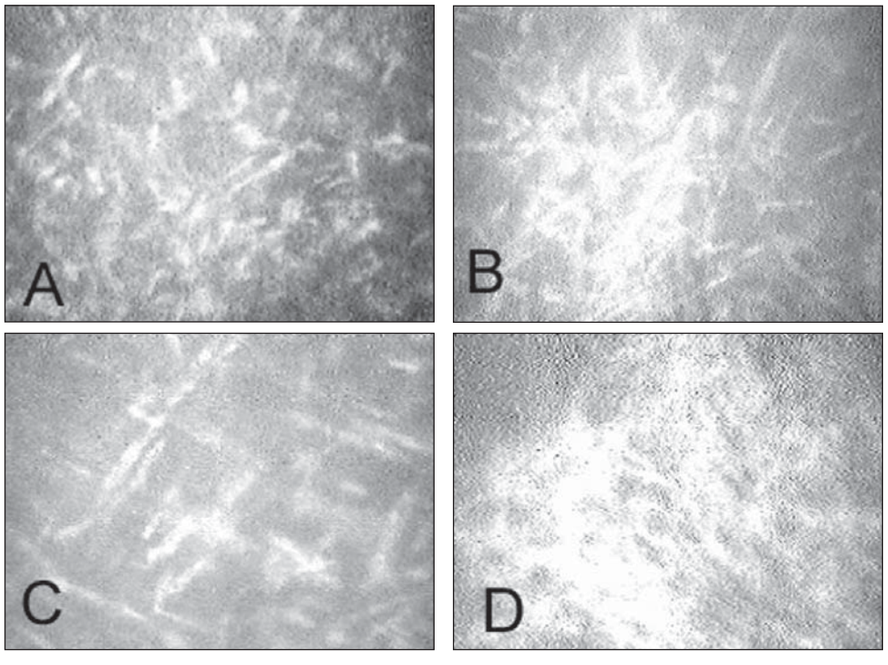

Figure 2. Changes of anterior stroma layer after PRK **A)** 10 days postoperatively, **B)** 1 month postoperatively, **C)** 3 months postoperatively, and **D)** showing haze.

was 317.0±114.8 μm (range: 270.2 to 432.6 μm), and the mean thickness of the epithelial layer was 71.0±6.7 μm (range: 63 to 81 μm).

Corneal Structure of Eyes That Underwent PRK

Forty patients (11 men and 29 women) with a mean age of 25.1±4.3 years (range: 19 to 40 years) underwent PRK. The mean preoperative refractive error was −3.45 diopters (D). The number of keratocytes changed primarily in the anterior stromal layer after PRK. The number of cells increased at 10 days and 1 month postoperatively. At 3 months postoperatively, the number had begun to decrease and within 6 months returned to normal levels.

Corneal nerves and effects of wound healing after PRK were primarily visible at 10 days postoperatively (Fig 2A). Immature superficial epithelium, fine nerves, activated stromal cells, extracellular matrix remodel-

TABLE 2

Corneal Thickness Before and After PRK in 77 Eyes of 40 Patients*

	Mean±Standard Deviation (Range) (μm)		
Layer	Preop	1 Month Postop	6 Months Postop
Whole cornea	543±67 (508 to 681)	534±65† (468 to 683)	559±73 (508 to 640)
Epithelium	71±6 (63 to 81)	129±22† (91 to 154)	89±21 (56 to 119)
Stroma	317±114 (200 to 432)	160±26† (130 to 187)	215±78† (148 to 365)

*Mean refractive error −3.45±1.71 D.
†P<.05 (t test).

TABLE 3

Corneal Thickness Before and After LASEK in 30 Eyes of 15 Patients*

	Mean±Standard Deviation (Range) (μm)		
Layer	Preop	1 Month Postop	6 Months Postop
Whole cornea	523±56 (487 to 563)	501±45† (422 to 601)	504±65 (482 to 569)
Epithelium	67±8 (50 to 76)	167±43† (112 to 135)	71±23 (51 to 101)
Stroma	259±131 (204 to 454)	156±29† (127 to 169)	201±86 (201 to 354)

*Mean refractive error −8.35±2.54 D.
†P<.05 (t test).

ing, and deposits in scar tissue were noted at 10 days postoperatively (see Fig 2A). One month postoperatively, the epithelium appeared healthy, and active star-shaped anterior stromal cells were visible (Fig 2B). At 1 month, the anterior stomal cells appeared less fusiform or spindle-shaped and were similar to myofibroblasts, with a round reflectivity nucleus. The cell density of the anterior stroma increased significantly. Between 3 and 6 months, cell density and light intensity decreased gradually, indicating that the activated stromal cells were gradually being replaced by less active cells (Fig 2C). In some patients, there were extracellular scar tissues visible from 3 to 6 months postoperatively. From 3 to 6 months postoperatively, regenerative subepithelial nerves became more prominent. The reflectivity from the activated stromal cells diminished starting at the sixth to seventh month postoperatively. The morphology of subepithelial nerves was normal after 6 months postoperatively. Haze after PRK was seen as reflectivity of subepithelial anterior stroma using confocal microscopy through focusing. Estimation of haze by confocal microscopy through focusing corresponded to the clinical grade of haze (Fig 2D). The junction of epithelium and stroma was a reticular structure of high reflectivity, with a cellular area of low reflectivity just below it.

Scarring after PRK appeared as reflectivity of the extracellular matrix along with numerous activated keratocytes (similar to fibroblasts). The scars were characterized by an irregular array, with multiple projections and an elongated nucleus. Scar thickness could be measured using the Z-scan.

Corneal thickness pre- and postoperatively at 1 and 6 months is shown in Table 2. At 1 month postoperatively, the entire cornea and stroma were thinner than preoperatively, whereas the epithelial layer was statistically significantly thicker ($P<.05$) (Table 2). The epithelial and corneal thickness returned to preoperative levels at 6 months postoperatively; however, the stromal layers remained statistically significantly thinner (Table 2). No statistical correlation was noted between stromal thinning and estimation of haze using confocal microscopy through focusing or grade of haze.

Corneal Structure of Eyes That Underwent LASEK

Fifteen patients (seven men and eight women) with a mean age of 28.6±5.1 years (range: 18 to 45 years) underwent LASEK. The mean preoperative spherical error was −8.35 D. At all points recorded, the changes in cell numbers and morphology of eyes that underwent LASEK were similar to those that underwent PRK.

The thickness of cornea layers preoperatively and at 1 month and 6 months postoperatively is shown in Table 3. A statistically significant increase was noted in the corneal epithelium at 1 month postoperatively. There was a statistically significant decrease in the corneal stroma at 1 month postoperatively.

Corneal Structure of Eyes That Underwent LASIK

Twenty patients (10 men and 10 women) with a mean age of 25.6±4.1 years (range: 18 to 37 years) underwent LASIK. The mean refractive error was −5.65 D. Confocal microscopy through focusing examination found negligible differences in appearance of keratocytes at all postoperative visits. On days 1 and 10 postoperatively, there were some small (<10 μm) focal areas of dense deposits, with strong reflectivity at the interface. One month postoperatively, these deposits were not visible. On days 1 and 10 postoperatively, anterior stromal cells were smaller and slightly more numerous than those in an unoperated cornea. From 1 to 6 months postoperatively, the cells of every layer ap-

peared healthy. On postoperative day 1, the mean cell count was 996±73 (range: 732 to 1087) for the anterior stroma, 743±57 (range: 548 to 789) for the posterior stroma, and 2610±113 (range: 2430 to 2748) for the endothelium. The mean 1-day postoperative cell counts for the anterior stroma, posterior stroma, and endothelium were not significantly different from preoperative levels ($P>.05$). There were no premature superficial epithelial cells, fine nerve fibers, activated anterior stromal cells and extracellular reflectivity, or deposits or scar tissue as seen in eyes that underwent PRK.

The mean corneal thickness preoperatively was 556.0±65.3 µm (range: 509.7 to 684.1 µm). One month postoperatively, the mean thickness was 558.3±71.4 µm (range: 512.7 to 697.2 µm), and at 6 months postoperatively, it was 549.8±66.7 µm (range: 503.9 to 685.6 µm). No statistically significant differences were noted in corneal thickness pre- to postoperatively ($P>.05$) (Table 4).

TABLE 4

Corneal Thickness Before and After LASIK in 40 Eyes of 20 Patients*

	Mean±Standard Deviation (µm)		
Layer	Preop	1 Month Postop	6 Months Postop
Whole cornea	556±65.3 (509 to 684.1)	558.3±71.4 (512.7 to 697.2)	549.8±66.7 (503.9 to 685.6)
Epithelium	73±6.2 (64 to 81)	88±10.2 (69 to 91)	78±8.2 (66 to 89)
Stroma	321±108 (234 to 411)	296±31 (231 to 404)	295±54 (219 to 305)

*Mean refractive error −7.85±2.71 D.
†P>.05 (t test).

DISCUSSION

Cornea wound healing involves complex cellular and molecular interactions that directly affect the stability and predictability of corneal refractive surgery. Corneal wound healing consists of a series of phases, characterized by histologic, histochemical, and biochemical changes, including activation, proliferation, and differentiation of cells; release of cytokines; and formation and remodeling of extracellular matrix.[1]

Confocal microscopy through focusing is a relatively new, accurate, and repeatable technique that analyzes the cornea in vivo. With the help of confocal microscopy through focusing, the morphology of the epithelium and stroma can be visualized and corneal thickness directly measured. By scanning from epithelium to endothelium, confocal microscopy through focusing can display corneal nerves, wound-healing processes, and changes in the configuration and density of anterior stromal cells after corneal refractive surgery. Confocal microscopy through focusing allows the clinician to observe the structure of the cornea at the cellular level, which provides first-hand, objective measurements and data to evaluate corneal function. This provides important supplementary information for determining treatment or assessing the effects of surgery.[2,3]

In this investigation of healthy corneas in vivo from Chinese patients, the epithelial layer was found to include the superficial epithelium and the inner layer of epithelial basement membrane. The stroma layer was divided into anterior stroma and posterior stroma, with the cells arranged in a regular pattern. The stromal cell nuclei were easily resolved and were seen to have dark cytoplasm. Normally, the amount of endothelia is approximately 2500/mm^2. The mean corneal thickness for unoperated, healthy eyes was 543 µm, with a 71-µm-thick mean epithelial layer and a 317-µm-thick mean stromal layer.

Observation of the changes of the corneal structure after PRK, LASEK, and LASIK can provide early histologic data of postoperative wound healing. This can provide important information to analyze the dynamic changes in corneal structure and diagnose abnormalities over time. Confocal microscopy through focusing demonstrated that in the early phase after PRK and LASEK (4 hours to 1 week), the morphology of the superficial epithelium was immature, with fine nerves and stroma cells decreased markedly in number, indicating the death of anterior stroma cells.[4] At 10 days postoperatively, the stroma cells showed increased cellular activity and increases in number and deposits of extracellular scar tissues.[5] Previous studies indicate that the high reflectivity seen after PRK and LASEK represents activated stromal fibroblasts and excessive disorganized collagen, primarily collagen VII, secreted by the fibroblasts.[3,6] Observations obtained from the ConfoScan 2.0 in this study confirm that the high reflectivity represents activated stroma cells. Refractive regression corresponds to an overproliferation of the activated anterior stroma cells, the cellular framework, cell-adhesion molecules, and cellular connections synthesized by stromal cells.[7]

During the late stage after PRK and LASEK (3 months or later), there is a decrease in the anterior stromal cells primarily due to apoptosis. By 6 months postoperatively, stromal cells return to normal levels. The high reflectivity of the activated stroma cells disappears and the subepithelial nerves increase between 6 and 7 months postoperatively. If continuous hyperplasia of the anterior stroma cells occurs, a hyperplastic scar characteristic of polycellular components would form,

which represents clinical haze.[7] This in vivo study confirms earlier finding of apoptosis and wounding of stromal cells in PRK and LASEK.[8-10] In this study, tissue necrosis and wound healing were found to cause a thinning of the stroma after PRK and LASEK. Although the stroma becomes thinner, there is no correlation between stroma thinning and estimation of haze by confocal microscopy through focusing or clinical grading. Balance between cellular activation and apoptosis during corneal wound healing is important to maintain a stable refraction.

In our experience, the corneal reaction is mild, and haze is not evident after LASEK; however, we did not find any differences between LASEK and PRK using confocal microscopy through focusing in vivo. The eyes that underwent PRK had a lower preoperative refractive error and thicker corneas compared with the eyes that underwent LASEK; thus, the refraction cannot explain the incidence of greater haze in PRK eyes. Additional research is needed to determine the factors that may diminish the occurrence of haze in LASEK.

In the eyes that underwent LASIK, confocal microscopy through focusing examination found no significant differences in keratocyte activity and corneal thickness at all postoperative visits, compared with preoperatively. During the early phase, anterior stromal cells were smaller in LASIK eyes than unoperated eyes. By the late phase, the cells and cytoplasm of every layer were normal in appearance and number. There were no immature superficial epithelial cell or fine nerve fibers as seen in PRK and LASEK. The activated anterior stromal cells, extracellular high reflectivity, and deposits in scar tissue seen in PRK and LASEK were not seen in LASIK. Stromal cell apoptosis is rare after LASIK, and the activation, proliferation, migration, and synthesis of extracellular matrix is mild to rebuild the integrity of cornea.

In this study, we have shown that in vivo confocal microscopy through focusing allows the observation of changes in the various corneal layers of the corneal wound-healing process.[11,12] With the development of confocal microscopy through focusing, the cornea can be observed in four dimensions (along the x, y, and z axes and in time). Confocal microscopy through focusing may provide various avenues of research into corneal wound healing after excimer laser ablation.[13-15] Confocal microscopy through focusing was useful in documenting cellular morphology and wound-healing characteristics in unoperated corneas and corneas that had undergone refractive surgery.

REFERENCES

1. Sappino AP, Schurch W, Gabbiani G. Differentiation repertoire of fibroblastic cells: expression of cytoskeletal proteins as marker of phenotypic modulations. *Lab Invest.* 1990;63:144-161.
2. Mathers WD, Goldberg MA, Sutphin JE, Ditkoff JW, Folberg R. Coexistent Acanthamoeba keratitis and herpetic keratitis. *Arch Ophthalmol.* 1997;115:714-718.
3. Moller-Pedersen T, Vogel M, Li HF, Petroll WM. Cavanagh D, Jester JV. Quantification of stromal thinning, epithelial thickness, and corneal haze after photorefractive keratectomy using in vivo confocal microscopy. *Ophthalmology.* 1997;104:360-368.
4. Li HF, Petroll WM, Moller-Pedersen T, Maurer JK, Cavanagh D, Jester JV. Epithelial and corneal thickness measurements by in vivo confocal microscopy through focusing (CMTF). *Curr Eye Res.* 1997;16:214-221.
5. Li Y, Pang G, Zhan S, Jin Y, Sun Y, Li Y, Li W. The apoptosis and proliferation after photorefractive keratectomy [Chinese]. *Zhonghua Yan Ke Za Zhi.* 1999;35:29-32.
6. Linna T, Tervo T. Real-time confocal microscopic observations on human corneal nerves and wound healing after excimer laser photorefractive keratectomy. *Curr Eye Res.* 1997;16:640-649.
7. Moller-Pedersen T, Li HF, Petroll WM, Cavanagh D, Jester JV. Confocal microscopic characterization of wound repair after photorefractive keratectomy. *Invest Ophthalmol Vis Sci.* 1998;9:487-501.
8. Del Pero RA, Gigstad JE, Roberts AD, Klintworth GK, Martin CA, L'Esperance FA Jr, Taylor DM. A refractive and histopathologic study of excimer laser keratectomy in primates. *Am J Ophthalmol.* 1990;109:419-429.
9. Desmouliere A, Badid C, Bochaton-Piallat M, Gabbiani G. Apoptosis during wound healing, fibrocontractive diseases and vascular wall injury. *Int J Biochem Cell Biol.* 1997;29:19-30.
10. Fantes FE, Hanna KD, Waring GO III, Pouliquen Y, Thompson KP, Savoldelli M. Wound healing after excimer laser keratomileusis (photorefractive keratectomy) in monkeys. *Arch Ophthalmol.* 1990;108:665-675.
11. Wu WC, Stark WJ, Green WR. Corneal wound healing after 193-nm excimer laser keratectomy. *Arch Ophthalmol.* 1991;109:1426-1432.
12. Cavanagh HD, Petroll WM, Alizadeh H, He YG, McCulley JP, Jester JV. Clinical and diagnostic use of in vivo confocal microscopy in patients with corneal diseases. *Ophthalmology.* 1993;100:1444-1454.
13. Buhren J, Kohnen T. Stromal haze after laser in situ keratomileusis: clinical and confocal microscopy findings. *J Cataract Refract Surg.* 2003;29:1718-1726.
14. Vinciguerra P, Torres I, Camesasca FI. Applications of confocal microscopy in refractive surgery. *J Refract Surg.* 2002;18:S378-S381.
15. Nakano E, Oliveira M, Portellinha W, de Freitas D, Nakano K. Confocal microscopy in early diagnosis of Acanthamoeba keratitis. *J Refract Surg.* 2004;20:S737-S740.

Corneal Diabetic Neuropathy: A Confocal Microscopy Study

Edoardo Midena, MD; Erica Brugin, MD; Alessandra Ghirlando, MD; Marco Sommavilla, MD; Angelo Avogaro, MD

ABSTRACT

PURPOSE: To evaluate the role of corneal confocal microscopy in the diagnosis of morphologic damage of the corneal sub-basal nerve plexus in diabetic patients and to correlate corneal confocal microscopy findings with peripheral diabetic neuropathy.

METHODS: Corneal sub-basal nerve plexus parameters were quantified by corneal confocal microscopy in 42 diabetic patients and 27 age-matched controls. The parameters quantified were the number of fibers, the tortuosity of fibers, the number of beadings, and the branching pattern of the fibers. Peripheral neuropathy was also quantified using the Michigan Neuropathy Screening Instrument.

RESULTS: The number of fibers, number of beadings, and branching pattern of fibers significantly decreases in diabetic patients versus control subjects ($P<.0001$; $P<.0001$; $P=.0006$, respectively), whereas nerve tortuosity significantly increases ($P<.0001$). The same corneal sub-basal nerve plexus parameters show a statistical trend, suggesting progression of corneal neuropathy with peripheral diabetic neuropathy.

CONCLUSIONS: Corneal confocal microscopy represents a new tool in the diagnosis, clinical evaluation, and follow-up of peripheral diabetic neuropathy. This study found that diabetes damages corneal nerves, particularly the corneal sub-basal nerve plexus. This damage may be easily and accurately documented using corneal confocal microscopy. [*J Refract Surg*. 2006;22: S1047-S1052.]

The prevalence of diabetes mellitus is dramatically increasing worldwide and consequently, the prevalence of chronic complications due to diabetes will increase in the near future.[1] The most common cause of chronic disability in diabetic patients is diabetic neuropathy, particularly peripheral diabetic neuropathy. Peripheral diabetic neuropathy affects 50% of diabetic patients within 25 years of diagnosis.[2] Long-term effects of undetected and untreated peripheral diabetic neuropathy can lead to foot infections that do not heal, as well as foot ulcers. Patients may require subsequent amputation of the foot or digits, which can lead to a decreased quality of life and increased mortality.[3]

The early and accurate diagnosis and quantification of peripheral diabetic neuropathy are important in defining at-risk patients, decreasing patient morbidity, and assessing new therapies.[4] The clinical diagnosis of peripheral diabetic neuropathy is often missed or diagnosed only in later stages, likely because a simple, noninvasive method for the early detection of peripheral diabetic neuropathy is not yet available,[5,6] and clinical diagnosis is made only when patients with peripheral diabetic neuropathy become symptomatic. Early diagnosis is currently based on electrophysiological tests,[7] or more recently, on skin biopsy.[8-10] Electrophysiological tests cannot detect the minute nerve fiber damage that is the most relevant component of nerve damage in patients with diabetes. Although skin biopsy can detect this minute damage, the disadvantage of this technique is its invasiveness.

The cornea is the most innervated tissue of the human body.[11-13] Corneal epitheliopathy is clinically well known in diabetic patients and is likely multifactorial in origin.[14-17] The cornea may be examined with noninvasive procedures, such as in vivo corneal confocal microscopy, which allows

From the Departments of Ophthalmology (Midena, Brugin, Ghirlando) and Clinical and Experimental Medicine, Division of Metabolic Disease (Sommavilla, Avogaro), University of Padova, Italy; and Fondazione GB Bietti per l'Oftalmologia, IRCSS, Roma, Italy (Midena).

The authors have no financial interest in the materials presented herein.

Correspondence: Edoardo Midena, MD, Dept of Ophthalmology, University of Padova, Via Giustiniani 2, 35128 Padova, Italy. Tel: 390498212110; Fax: 390498212129; E-mail: edoardo.midena@unipd.it

the visualization and recording of each corneal layer, including corneal nerves. Qualitative and quantitative analysis of the corneal nerves, particularly the corneal sub-basal nerve plexus, within images taken by corneal confocal microscopy may be an ideal method to evaluate nerve fiber pathology in patients with diabetes mellitus.

The goal of this study was to evaluate the role of corneal confocal microscopy in the diagnosis of morphologic damage of the corneal sub-basal nerve plexus in diabetic patients and to correlate corneal confocal microscopy findings with peripheral diabetic neuropathy.

PATIENTS AND METHODS

PATIENTS AND CLINICAL EXAMINATION

Forty-two consecutive patients with diabetes mellitus (type I and type II) were evaluated using corneal confocal microscopy. Twenty-seven healthy subjects served as controls. Informed consent was obtained from all subjects, and all subjects underwent a complete ophthalmologic examination including anterior segment slit-lamp microscopy, fundus biomicroscopy, and intraocular pressure measurement. Patients with central neuropathy, peripheral neuropathy, or ocular diseases not related to diabetes were excluded.

Peripheral diabetic neuropathy was documented using the Michigan Neuropathy Screening Instrument (MNSI), which is a simple, reproducible, and noninvasive peripheral diabetic neuropathy screening test.[18,19] An MNSI score >2 suggests the presence of peripheral diabetic neuropathy.[20] Patients were classified into groups according to MNSI score based on the clinical examination of feet as proposed by Rosenberg et al.[21] Subjects without diabetic neuropathy had an MNSI score $\leqslant 2$; patients with mild to moderate diabetic neuropathy had an MNSI score >2 and $\leqslant 4.5$; patients with moderate to severe diabetic neuropathy had an MNSI score of $\geqslant 4.6$ to $\leqslant 4.9$; and patients with severe diabetic neuropathy had an MNSI score $\geqslant 5$.[21]

CONFOCAL MICROSCOPY

Corneal confocal microscopy was performed using the NIDEK Confoscan 4.0 (CS4; NIDEK Co Ltd, Gamagori, Japan) scanning slit confocal microscope fitted with a z-ring adapter and an Achroplan (Carl Zeiss-Meditec, Jena, Germany) nonapplanating 40× immersion objective lens designed for full-thickness examination of the cornea. The working distance was 1.98 mm, and a motorized focusing device was used to image the area of interest properly. The z-ring adapter system uses an optomagnetic sensor, which aligns the eye with the tip of the confocal microscope during examination. Thus, with the z-ring sensor, the confocal microscope tip position is fixed with regard to the examined cornea, compensating for eye movements along the z-axis.

The center of the cornea was examined. Prior to examination, a drop of topical anesthetic 0.4% oxybuprocaine chlorohydrate (Novartis AG, Basel, Switzerland) was instilled in the lower conjunctival fornix of the eye to reduce blinking. The patient was seated in front of the microscope while fixating the examined eye on a bright blue target on the instrument. One drop of 0.2% polyacrylic gel (Viscotears; Ciba Vision, Atlanta, Ga) was applied to the tip of the objective lens as an immersion fluid. Coarse alignment with the corneal apex was carried out manually by the operator by moving the z-ring adapter to the apex of the cornea. Fine adjustment was completed automatically by a motor-driven system within the CS4. Subsequently, the focal plane was automatically adjusted to recognize the anterior chamber, and corneal scanning and recording began. Images were always taken from the endothelium to the corneal epithelium. Image intensity depth profiles were generated from confocal microscope videorecordings by averaging the pixel intensity in the center of each consecutive video frame image and plotting data as a function of z-depth in the z-scan curve. Due to the z-ring adapter, all points on the z-scan curve directly correlate to high-resolution images, and the exact z-axis position of specific tissue landmarks (eg, surface epithelium, sub-basal nerve plexus, endothelium, etc) can be used to calculate the distance between individual corneal layers. Each examination lasted approximately 14 seconds. The highest quality image of the corneal sub-basal nerve plexus was identified by an experienced clinician. Four corneal sub-basal nerve plexus parameters were evaluated, including the number of fibers, the number of fiber beadings, the degree of fiber branching, and the degree of fiber tortuosity.

The number of fibers was defined as the sum of the nerve fibers seen in the selected frame of the corneal sub-basal nerve plexus. The number of beadings was defined as the number of hyper-reflective points per unit of length (100 µm) in a single nerve fiber, randomly selected from all the nerve fibers seen in the corneal sub-basal nerve plexus image.

Grading systems were used to classify fiber branches and fiber tortuosity. For fiber tortuosity, the grading system proposed by Oliveira-Soto and Efron,[22] based on frequency and amplitude of changes in nerve fiber direction, was used. Values ranged from 0 to 4, whereby grade 0 nerve fibers appear almost straight; grade 1 nerve fibers appear slightly tortuous; grade 2 nerve fibers appear moderately tortuous, with frequent, small amplitude changes in the direction of fibers; grade 3

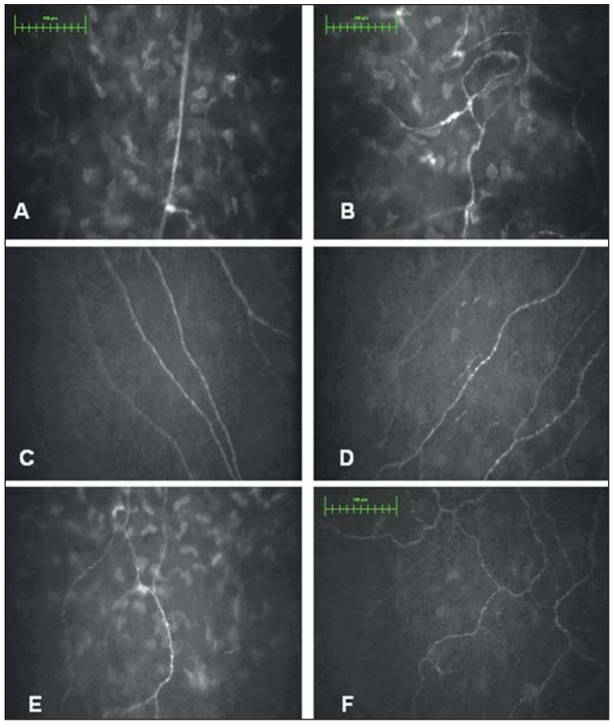

Figure 1. Images of stromal and corneal sub-basal nerve plexus fibers analyzed using corneal confocal microscopy. Parameter: fiber tortuosity degree. **A)** Stromal nerve fiber in a control subject, tortuosity degree 0; **B)** stromal tortuous nerve fiber in a diabetic patient; **C)** tortuosity degree 1 in the corneal sub-basal nerve plexus of a control subject; **D)** tortuosity degree 2 in the corneal sub-basal nerve plexus of a control subject; **E)** tortuosity degree 3 in the corneal sub-basal nerve plexus of a diabetic patient; and **F)** tortuosity degree 4 in the corneal sub-basal nerve plexus of a diabetic patient.

nerve fibers appear tortuous, with the amplitude of changes in fiber direction quite severe; and grade 4 nerve fibers appear very tortuous, showing abrupt and frequent changes in direction (Fig 1).

For fiber branching, the grading system values ranged from 0 to 3, whereby grade 0 shows no corneal sub-basal nerve plexus fibers branching; grade 1 shows one fiber presenting one or more direct branchings from the major nerve trunk; grade 2 shows one fiber presenting one branching originating from a principal nerve trunk branching; and grade 3 shows one fiber presenting one branching originating from a grade 2 fiber branching (Fig 2).

Statistical Analysis

All statistics were calculated using SAS Software (SAS Institute Inc, Cary, NC). Pearson index correlation, Spearman index correlation, Fisher test, analysis of covariance, multiple linear regression model, analysis of variance, post hoc test for multiple comparisons

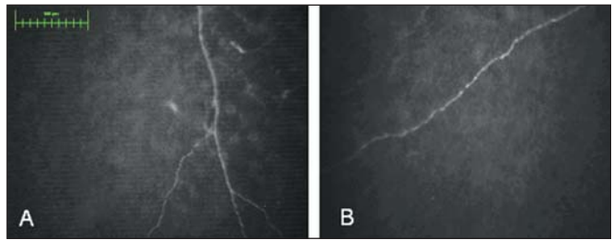

Figure 2. Images of the corneal sub-basal nerve plexus analyzed using corneal confocal microscopy. Parameter: branching pattern degree. **A)** Branching pattern degree 2 in a control subject; and **B)** branching pattern degree 0 in a diabetic patient.

Sheffé test, and Student *t* test were all used for analysis. Results with $P<.05$ were considered statistically significant.

RESULTS

Forty-two patients with diabetes (18 women and 24 men) were evaluated. Mean age was 55.4±13 years (range: 30 to 73 years). Twenty-nine patients (7 women and 22 men) had type II diabetes, and 13 patients (11 women and 2 men) had type I diabetes. Twenty-seven healthy subjects (18 women and 9 men) with a mean age of 49.3±19.9 years (range: 24 to 85 years) acted as controls. No statistical correlation between corneal sub-basal nerve plexus parameters and age was found when glycemic control and duration of disease were considered. No statistical difference between type I and type II diabetic patients was found when corneal sub-basal nerve plexus parameters and glycemic control and duration of diabetes were considered. No statistical difference was found in average MNSI score between type I and type II diabetic patients. Given these findings, results are classified as a single pathologic group.

Corneal sub-basal nerve plexus parameters were statistically significantly different between diabetic patients and control subjects. The mean number of fibers was 2.2±0.3 in diabetic patients versus 4.4±0.3 in control subjects ($P<.0001$). The number of beadings was 5.6±0.4 for diabetic patients versus 12.3±0.4 for control subjects ($P<.0001$). The degree of fiber branching was 0.8±0.1 for diabetic patients and 1.3±0.1 for control subjects ($P=.0006$). The tortuosity grading was −2.6±0.2 for diabetic patients compared with 1.3±0.1 for control subjects ($P<.0001$) (Fig 3).

Using the MNSI clinical examination score, 12 patients were classified as group A (absence of diabetic neuropathy), 12 patients as group M (mild to moderate diabetic neuropathy), and 18 patients as group S (severe diabetic neuropathy). Corneal sub-basal nerve plexus parameters were not statistically different among the three different peripheral diabetic

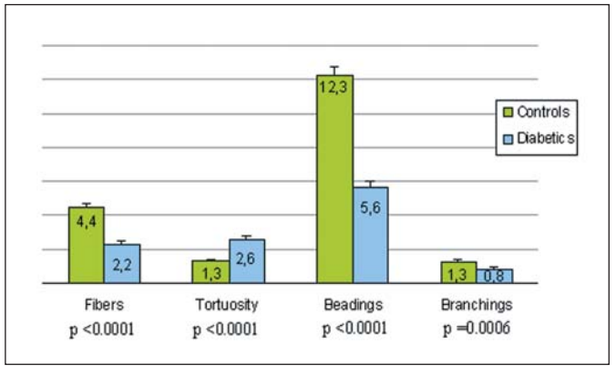

Figure 3. Corneal sub-basal nerve plexus parameters: diabetic patients versus control subjects. (Fibers = number of fibers within the frame; beadings = number of beadings for 100 μm of nerve fiber; tortuosity = nerve fiber tortuosity grade; branchings = nerve fiber branching grade.)

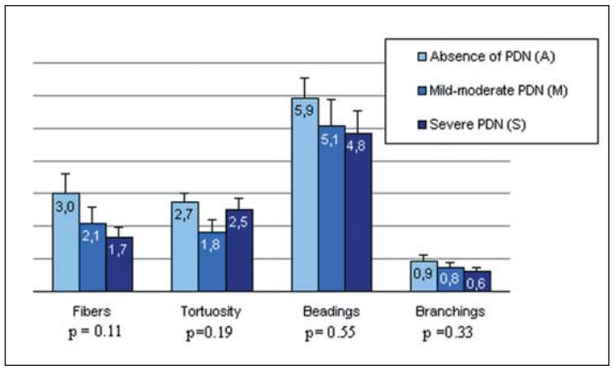

Figure 4. Corneal sub-basal nerve plexus parameters: three groups of diabetic patients classified according to peripheral diabetic neuropathy assessed by MNSI examination. (Fibers = number of fibers within the frame; beadings = number of beadings for 100 μm of nerve fiber; tortuosity = nerve fiber tortuosity grade; branchings = nerve fiber branching grade.)

neuropathy groups (number of fibers, P=.11; number of beadings P=.55; branching degree, P=.33; tortuosity degree, P=.19). However, three parameters (number of fibers, number of beadings, and branching grade) showed a decreasing trend among A, M, and S groups (Fig 4).

Further analysis revealed that the number of fibers was statistically significantly lower in the M and S groups compared with the control group (P<.0001) (Fig 5). The number of beadings was statistically higher in subjects in the control group compared with patients in all peripheral diabetic neuropathy groups (P<.0001). The degree of branching was statistically different between control subjects and diabetic patients, with the S group having the least branching compared with the control group (P=.004). Nerve fiber tortuosity was significantly lower in the control group compared with the A and S groups (P=.0002).

DISCUSSION

Peripheral diabetic neuropathy is a major cause of disability among diabetic patients and can lead to chronic foot ulceration and amputation.[1-4] Clinical evaluation of peripheral diabetic neuropathy is performed using screening tests such as the MNSI or more invasive techniques such as electrophysiological tests or skin biopsy. More invasive techniques are limited to selected patients or populations and cannot be used as standardized follow-up tests.[5-10] The major limitations are related to the strict follow-up that is necessary when using an invasive test in diabetic patients whose healing problems and high rate of infection are well known. Therefore, peripheral diabetic neuropathy is more frequently screened using a simple, reliable test such as the MNSI, which does not indicate fine changes of small nerve fiber morphology or function.[18-20] These observations emphasize the importance of developing new tests to quantify peripheral diabetic neuropathy.

Corneal confocal microscopy enables the clinician to examine corneal nerves, and specifically the corneal sub-basal nerve plexus in vivo with high repeatability. The corneal sub-basal nerve plexus is a monolayer of unmyelinated nerve fibers with a diameter of 4 µm. The corneal sub-basal nerve plexus may be easily documented using confocal microscopy, as previously reported.[22-27] Morphology of the corneal sub-basal nerve plexus is not influenced by age, as reported by Erie et al.[24] This allows the exclusion of a relevant biologic parameter when evaluating changes in the corneal sub-basal nerve plexus. Corneal confocal microscopy has been previously reported in the evaluation of the corneal sub-basal nerve plexus in diabetics.[21,25-27] Rosenberg et al[21] found that the number of nerve fibers of the corneal sub-basal nerve plexus is significantly lower in diabetic patients with mild to moderate and severe peripheral neuropathy versus control subjects, suggesting enhanced nerve degeneration. In addition, the decrease in nerve fiber numbers preceded impairment of corneal sensitivity assessed with a mechanical esthesiometer.[21] Malik et al[25] also found a statistically significantly reduced number of fibers in the corneal sub-basal nerve plexus of diabetic patients compared with control subjects, with a tendency for greater reduction in fiber number with increasing severity of peripheral diabetic neuropathy. They also reported a significant reduction of fiber branch density in the corneal sub-basal nerve plexus of diabetic patients, which suggests a reduction in regenerative capacity with progression of neuropathy severity.[25] Popper et al[26] demonstrated that the number of fibers in the corneal sub-basal nerve plexus of diabetic patients, even with short diabetes duration, was significantly lower than that in

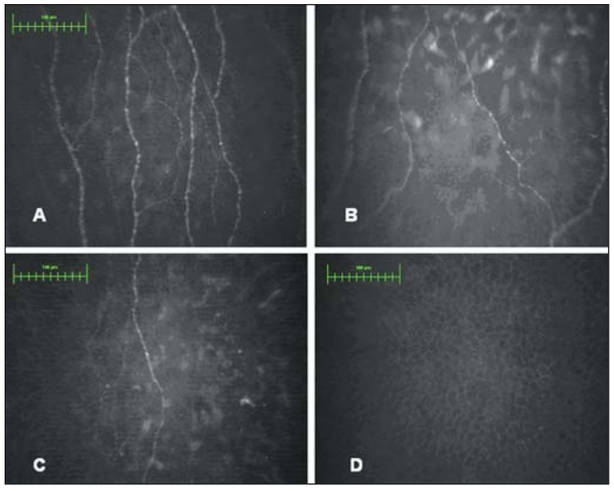

Figure 5. Images of corneal sub-basal nerve plexus evaluated in this study. Parameter: number of nerve fibers. **A)** High number of nerve fibers in the corneal sub-basal nerve plexus of a control subject; **B)** corneal sub-basal nerve plexus of a diabetic patient: decrease of nerve fibers number; **C)** severe reduction of the corneal sub-basal nerve plexus fibers number in a diabetic patient; and D) absence of the corneal sub-basal nerve plexus in a diabetic patient.

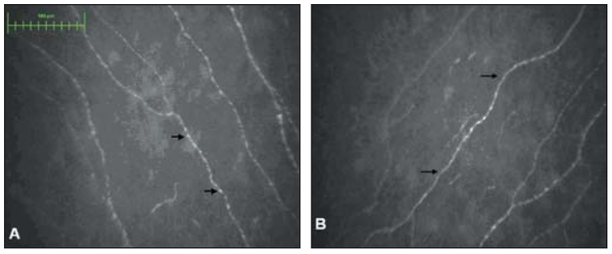

Figure 6. Images of the corneal sub-basal nerve plexus examined in this study. Parameter: number of beadings. **A)** Beadings in the corneal sub-basal nerve plexus of a control subject (arrows); **B)** beadings in the corneal sub-basal nerve plexus of a diabetic patient (arrows show two parts of fibers without beadings).

healthy control subjects.[26] Kallinikos et al[27] used corneal confocal microscopy to quantify corneal sub-basal nerve plexus tortuosity in diabetic and healthy subjects. They demonstrated increased corneal sub-basal nerve plexus fiber tortuosity (which was independent of age, duration of diabetes, and glycemic control) in diabetic patients with increasing severity of peripheral diabetic neuropathy. They hypothesized that the increased tortuosity may represent a morphologic marker of nerve regeneration.[27]

Previous studies have not considered all corneal sub-basal nerve plexus parameters in the same group of diabetic patients versus control subjects. Data from the current researchers show that diabetic patients have significant corneal sub-basal nerve plexus parameter changes compared with control subjects. Corneal sub-basal nerve plexus alterations do not depend on glycemic control, age, or duration of diabetes. In diabetic eyes, the number of corneal sub-basal nerve plexus fibers was significantly reduced, and the remaining fibers were altered. The increase of tortuosity of visible fibers is a sign of degeneration and an attempt at fiber repair. Even lower corneal sub-basal nerve plexus branching may signal reduced nerve regeneration. The metabolic activity of the corneal sub-basal nerve plexus is documented by nerve beadings, which represent accumulation of mitochondria along the nerve.[12] The significant decrease of nerve beadings represents pathologic metabolic activity of diabetic small nerve fibers (Fig 6). Peripheral diabetic neuropathy "classified" with the MNSI shows contrasting results when compared with confocal microscopy corneal sub-basal nerve plexus data. Data from the current researchers showed that not all corneal sub-basal nerve plexus parameters were significantly different between controls and all MNSI score groups. However, this probably reflects the "screening" value of the MNSI, which cannot be used as a specific grading score of peripheral diabetic neuropathy.

These clinical findings may also be useful when interpreting refractive surgery results, particularly in diabetic patients. In eyes treated with photorefractive keratectomy (PRK), the recovery of subepithelial corneal nerves starts from the borders of the ablated zone in a centripetal way.[28] Corneal nerve regeneration is considered complete in 12 months, although the original nerve structure is not fully restored, and corneal sub-basal nerve plexus is similar (abnormal branching and increased nerve tortuosity) to that observed in the diabetic patients we examined. After LASIK, corneal nerve regeneration is slower, approximately 2 years, because larger nerve trunks have been severed by the microkeratome.[28] The relationship between corneal nerves and keratocytes is disrupted after refractive surgery.[29,30] Mueller et al[29] have shown that there is a direct innervation of individual keratocytes, whereas Vesaluoma et al[30] suggested that corneal denervation may play a role in reducing the density of keratocytes in central ablated cornea. The long-term consequences of corneal denervation and regeneration after refractive surgery are relatively unknown, and the impact of diabetes on this process is poorly documented.[14] Future controlled trials evaluating the efficacy and safety of refractive surgery (LASIK and PRK) in diabetic patients should consider baseline corneal nerve status as a relevant parameter to stratify tested groups. Even dry eye syndrome before and after refractive surgery should be reconsidered according to the status of corneal nerves, particularly in diabetic patients.

The present investigators are confident that corneal sub-basal nerve plexus morphologic parameters directly documented using in vivo corneal confocal microscopy is the clinical tool of choice for evaluating small nerve fiber damage in diabetic patients. The correlation observed between corneal nerve alterations and peripheral diabetic neuropathy, even using a screening test, confirms that the in vivo evaluation of sub-basal corneal nerve plexus allows an improved diagnosis of peripheral diabetic neuropathy. The investigators aim to compare corneal sub-basal nerve plexus corneal confocal microscopy results with peripheral diabetic neuropathy classification using skin biopsy, which is an invasive morphologic test.[8-10]

Corneal confocal microscopy in vivo is a noninvasive test for peripheral diabetic neuropathy, which causes decreased corneal sensitivity and neurotrophic damage to the ocular surface.[14-16] In the future, corneal diabetic neuropathy should be routinely documented with corneal confocal microscopy using a specific, universal grading system.

REFERENCES

1. Mokdad A, Ford ES, Bowman BA, Nelson DE, Engelgau MM, Vinicor F, Marks JS. Diabetes trends in the US: 1990-1998. *Diabetes Care.* 2000;23:1278-1283.
2. Gooch C, Podwall D. The diabetic neuropathies. *The Neurologist.* 2004;10:311-322.
3. Partanen J, Niskanen L, Lehtinen J, Mervaala E, Siitonen O, Uusitupa M. Natural history of peripheral neuropathy in patients with non-insulin-dependent diabetes mellitus. *N Engl J Med.* 1995;333:89-94.
4. Park TS, Park JH, Baek HS. Can diabetic neuropathy be prevented? *Diabetes Res Clin Pract.* 2004;66:S53-S56.
5. Nasseri K, Strijers RL, Dekhuijzen LS, Buster M, Bertelsmann FW. Reproducibility of different methods for diagnosing and monitoring diabetic neuropathy. *Electromyogr Clin Neurophysiol.* 1998;38:295-299.
6. Rahman M, Griffin SJ, Rathmann W, Wareham NJ. How should peripheral neuropathy be assessed in people with diabetes in primary care? A population-based comparison of four measures. *Diabet Med.* 2003;20:368-374.
7. Daube JR. Electrophysiologic testing in diabetic neuropathy. In: Dyck P, Thomas P, eds. *Diabetic Neuropathy*. Philadelphia, Pa: WB Saunders; 1999:213-215.
8. Aprile I, Stalberg E, Caliandro P, Pazzaglia C, Tonali P, Padua L. Skin denervation in type 2 diabetes: correlations with diabetic duration and functional impairments. *Brain.* 2004;127:20.
9. Lauria G, McArthur JC, Hauer PE, Griffin JW, Cornblath DR. Neuropathological alterations in diabetic truncal neuropathy: evaluation by skin biopsy. *J Neurol Neurosurg Psychiatr.* 1998;65:762-766.
10. Pittenger GL, Ray M, Burcus NI, McNulty P, Basta B, Vinik AI. Intraepidermal nerve fibers are indicators of small-fiber neuropathy in both diabetic and nondiabetic patients. *Diabetes Care.* 2004;27:1974-1979.
11. Muller LJ, Pels L,Vrensen GFJM. Ultrastructural organization of human corneal nerves. *Invest Ophthalmol Vis Sci.* 1996;37:476-488.
12. Muller LJ, Marfurt CF, Kruse F, Tervo TMT. Corneal nerves: structure, contents and function. *Exp Eye Res.* 2003;76:521-542.
13. Guthoff RF, Wienss H, Hahnel C, Wree A. Epithelial innervation of human cornea. A three-dimensional study using confocal laser scanning fluorescence microscopy. *Cornea.* 2005;24:608-613.
14. Fraunfelder FW, Rich LF. Laser-assisted in situ keratomileusis complications in diabetes mellitus. *Cornea.* 2002;21:246-248.
15. Kaji Y. Prevention of diabetic keratopathy. *Br J Ophthalmol.* 2005;89:254-255.
16. Murphy PJ, Patel S, Kong N, Ryder REJ, Marshall J. Noninvasive assessment of corneal sensitivity in young and elderly diabetic and non diabetic subjects. *Invest Ophthalmol Vis Sci.* 2004;45:1737-1742.
17. Verrotti A, Giuva T, Morgese G, Morgese G, Chiarelli F. New trends in the etiopathogenesis of diabetic peripheral neuropathy. *J Child Neurol.* 2001;6:389-394.
18. Bax G, Fagherazzi C, Piarulli F, Nicolucci A, Fedele D. Reproducibility of Michigan Neuropathy Screening Instrument (MNSI). *Diabetes Care.* 1996;19:89-90.
19. Lunetta M, Le Moli R, Grasso G, Sangiorgio L. A simplified diagnostic test for ambulatory screening of peripheral diabetic neuropathy. *Diabetes Res Clin Pract.* 1998;39:165-172.
20. Feldman EL, Stevens MJ, Thomas PK, Brown MB, Canal N, Greene DA. A practical two-step quantitative clinical and electrophysiological assessment for the diagnosis and staging of diabetic neuropathy. *Diabetes Care.* 1994;17:1281-1289.
21. Rosenberg ME, Tervo TMT, Immonen IJ, Muller LJ, Gronhagen-Riska C, Vesaluoma H. Corneal structure and sensitivity in type 1 diabetes mellitus. *Invest Ophthalmol Vis Sci.* 2000;41:2915-2921.
22. Oliveira-Soto L, Efron N. Morphology of corneal nerves using confocal microscopy. *Cornea.* 2001;20:374-384.
23. Grupcheva CN, Wong T, Riley AF, McGhee CN. Assessing the subbasal nerve plexus in living healthy human corneas by in vivo confocal microscopy. *Clin Exp Ophthalmol.* 2002;30:187-190.
24. Erie JC, McLaren JW, Hodge DO, Bourne WM. The effect of age on the corneal subbasal nerve plexus. *Cornea.* 2005;6:705-709.
25. Malik RA, Kallinikos P, Abbott CA, van Schie CH, Morgan P, Efron N, Boulton AJM. Corneal confocal microscopy: a non-invasive surrogate of nerve fibre damage and repair in diabetic patients. *Diabetologia.* 2003;46:683-688.
26. Popper M, Quadrado MJ, Morgado AM, Murta JN, van Best JA, Muller LJ. Subbasal nerves and highly reflective cells in corneas of diabetic patients: in vivo evaluation by confocal microscopy [program/poster: 879/B853]. Presented at: Association for Research in Vision and Ophthalmology Annual Meeting; May 1-5, 2005; Ft Lauderdale, Fla.
27. Kallinikos P, Berhanu M, O'Donnell C, Boulton AJ, Efron N, Malik RA. Corneal nerve tortuosity in diabetic patients with neuropathy. *Invest Ophthalmol Vis Sci.* 2004;45:418-422.
28. Cavillo MP, McLaren JW, Hodge DO, Bourne WM. Corneal reinnervation after LASIK. Prospective 3-year longitudinal study. *Invest Ophthalmol Vis Sci.* 2004;45:3991-3996.
29. Mueller I, Pels L, Vrensen GF. Ultrastructural organization of human corneal nerves. *Invest Ophthalmol Vis Sci.* 1996;37:476-488.
30. Vesaluoma M, Perez-Santonja J, Petroli WM, Linna T, Alio J, Tervo T. Corneal stromal changes induced by myopic LASIK. *Invest Ophthalmol Vis Sci.* 2000;41:369-376.

Improvement of Best Spectacle-corrected Visual Acuity After LASIK in Highly Myopic Eyes With Reduced Preoperative Best Spectacle-corrected Visual Acuity

Rui He, MB; Min Qu, MM; Yi Fen, MM; Shun Yu, MB

ABSTRACT

PURPOSE: To evaluate the visual acuity after LASIK in patients with high myopia and in patients with preoperative best spectacle-corrected visual acuity (BSCVA) <0.6.

METHODS: This retrospective study comprised 97 consecutive eyes in 57 patients who underwent LASIK. Preoperative spherical refractive error ranged from −1.75 to −22.00 diopters (D) (mean: −11.77±3.61 D) with mean astigmatism of −1.54±10.6 (range: 0 to −4.00 D). Pre- and postoperative BSCVA and uncorrected visual acuity (UCVA) were measured and analyzed.

RESULTS: The mean preoperative BSCVA was 0.54±0.07 (range: 0.3 to 0.6). The mean postoperative BSCVA was 0.75±0.16 (range: 0.5 to 1.2). The mean postoperative UCVA was 0.60±0.25 (range: 0.5 to 1.2). A statistically significant improvement was noted in the mean postoperative BSCVA compared with the mean preoperative BSCVA (t=12.78; P<.001) and mean postoperative UCVA compared with preoperative mean BSCVA (t=2.866; P<.01). The safety index was 1.38, which was statistically significant (P<.001). The efficacy index was 1.11, which was statistically significant (P<.01).

CONCLUSIONS: LASIK improved the mean postoperative BSCVA and UCVA compared with preoperative BSCVA in highly myopic eyes with reduced BSCVA. [*J Refract Surg*. 2006;22:S1053-S1055.]

Laser in situ keratomileusis (LASIK) has been extensively used to treat myopia, hyperopia, and astigmatism.[1-3] Most candidates who undergo LASIK surgery have best spectacle-corrected visual acuity (BSCVA) close to 1.0 before and after surgery. However, there are a number of candidates who present with BSCVA significantly lower than 1.0 preoperatively. In many cases, surgeons elect not to perform surgery in these patients. Many of these patients have high refractive errors and have never attained 1.0 BSCVA. These eyes are considered to have refractive amblyopia. The authors' experience with LASIK for correcting high myopia and astigmatism in adult patients with BSCVA <0.6 had previously shown encouraging results. In the present study, the authors present results using LASIK for the treatment of myopia with astigmatism for a subset of patients with reduced BSCVA.

PATIENTS AND METHODS

Patient Population and Surgery

This retrospective study evaluated 97 consecutive eyes in 57 patients (31 women and 26 men) who underwent LASIK for myopia with or without astigmatism from December 2003 to August 2005. To be included in the study, patients had to have a preoperative BSCVA of ≤0.6 and have undergone previous myopic LASIK surgery. Patients with underlying ophthalmic disease other than refractive amblyopia that could affect vision were excluded.

Pre- and postoperative ophthalmic examinations included slit-lamp microscopy, OPD-Scan (NIDEK Co Ltd, Gamagori, Japan), corneal topography and aberrometry, uncorrected visual acuity (UCVA), BSCVA, tonometry, pachymetry, manifest and cycloplegic refractions, and fundus examination. Patients underwent examination postoperatively at 1 day, 1 week, 1 month, and 3 months.

From the Shanxi Eye Hospital, Taiyuan, China.

The authors have no financial or proprietary interest in the materials presented herein.

Correspondence: Rui He, MB, Shanxi Eye Hospital, 030002, Taiyuan, Shanxi, China. Tel: 86 0351 3085268; Fax: 86 0351 4167043; E-mail: he.r@163.com

Laser in situ keratomileusis was performed using the NIDEK Advanced Vision Excimer Laser platform (NAVEX), which comprises the NIDEK MK-2000 microkeratome, the OPD-Scan, and the CXII excimer laser. Flap sizes and laser ablation zones were chosen for each eye based on a variety of factors including corneal diameter, preoperative keratometry, and pupil diameter. All surgeries were performed using the same technique. Patients were administered topical anesthesia before the placement of a sterile drape and a lid speculum. A corneal flap with a nasal hinge was created. The laser delivery was properly centered using a 60-Hz eye-tracking system and cooperative patient fixation. Following the ablation, the flap was floated back into position and irrigated with balanced salt solution and allowed to adhere. Patients were discharged with instructions to administer topical antibiotic and lubricating drops four times a day for 1 week.

Data and Statistical Analyses

The safety index was determined by mean postoperative BSCVA/mean preoperative BSCVA. The efficacy index was determined by mean postoperative UCVA/mean preoperative BSCVA.

Statistical analysis of the data was performed using Statistica Version 5.5 software program (StatSoft Inc, Tulsa, Okla). A *t* test was used to analyze visual acuity. A *P* value $<.05$ was considered statistically significant.

RESULTS

Preoperative Refractive Error and Visual Acuity

Mean patient age was 28.40±6.88 years (range: 18 to 42 years). Mean follow-up was 6.74±6 months (range: 1 to 21 months). The mean preoperative spherical refractive error was −11.77±3.61 diopters (D) (range: −1.75 to −22.00 D), mean astigmatism was −1.54±1.06 D (range: 0 to −4.00 D), and mean spherical equivalent was −13.33±3.39 D (range: −4.50 to −22.00 D). The mean preoperative UCVA was 0.11±0.05 D (range: 0.01 to 0.30 D), and the mean preoperative BSCVA was 0.54±0.07 (range: 0.30 to 0.60 D).

Postoperative Refractive Error and Visual Acuity

The mean spherical refractive error was −1.42±1.69 D (range: 0 to −6.00 D), and the mean astigmatism was −0.10±0.30 D (range: 0 to −1.75 D). None of the eyes developed irregular astigmatism postoperatively.

The mean postoperative BSCVA was 0.75±0.16 D (range: 0.50 to 1.20 D) and mean postoperative UCVA was 0.60±0.25 D (range: 0.10 to 1.20 D). Statistically significant improvements were noted in the mean postoperative BSCVA compared with the mean preoperative BSCVA (t=12.78; $P<.001$) and the mean postoperative UCVA compared with mean preoperative BSCVA (t=2.866; $P<.01$).

The postoperative BSCVA and preoperative BSCVA were the same in 19 (19.6%) eyes, and 78 (80.4%) eyes exceeded preoperative BSCVA (safety index). Postoperative BSCVA was >1.0 in 14 (14.4%) eyes. No eyes experienced a loss of BSCVA.

In 45 (46.4%) eyes, the postoperative UCVA exceeded the preoperative BSCVA. Postoperative UCVA and preoperative BSCVA were the same in 18 (18.6%) eyes. The postoperative UCVA did not exceed the preoperative BSCVA in 34 (35.1%) eyes. The postoperative UCVA exceeded the preoperative UCVA in all cases.

The safety index was 0.75/0.54 = 1.38, which was statistically significant ($P<.001$). The efficacy index was 0.60/0.54 = 1.11, which was a statistically significant ($P<.01$).

DISCUSSION

Laser in situ keratomileusis for the treatment of myopia has been widely accepted by ophthalmologists and the general public, especially in cases of optimal preoperative BSCVA. In this investigation of high myopia with refractive amblyopia, a statistically significant improvement in BSCVA after LASIK was found.

The preoperative BSCVA ranged from 0.3 to 0.6, with a mean of 0.54. Based on the standard clinical classifications, all patients were diagnosed as amblyopic preoperatively.[4,5] It must be noted that this was a study of adults aged 18 to 42 years who presumably would have lost retinal or neurosensorial potential for increasing vision after any form of amblyopia therapy.[6] Based on our understanding of amblyopia, these patients should have had no improvement in UCVA and BSCVA after LASIK. Yet, surprisingly, the present study found that the UCVA postoperatively exceeded the preoperative BSCVA in almost half the eyes (46.4%). The study also found the postoperative BSCVA of the majority of eyes (80.4%) exceeded the preoperative BSCVA. Based on our results, we suspect that the clinical diagnosis of amblyopia may not have been accurate for this subpopulation of patients. Although the preoperative spherical equivalent refraction was −13.33 D in this study population of patients with up to 22.00 D of myopia, we postulate that these patients had mild to moderate myopia during the critical period of visual development and amblyopia may not have actually occurred. With increasing age, the myopia and astigmatism increased, and the patients began to wear stronger spectacles, resulting in reduced visual function from image magnification. Following LASIK, object minifi-

cation was significantly decreased, resulting in the reported improvement in UCVA and BSCVA.

Regression resulting in undercorrection after LASIK is common in high myopia.[7] Despite this possibility of regression, the current investigators believe that highly myopic patients will likely appreciate the quality of life associated with less dependence on spectacles or contact lenses.

Laser in situ keratomileusis for highly myopic patients with reduced preoperative BSCVA results in a statistically significant improvement in mean postoperative BSCVA and UCVA compared with preoperative assessment.

REFERENCES

1. Pop M, Bains HS. Clinical outcomes of CATz versus OPDCAT. *J Refract Surg.* 2005;21:S636-S639.
2. Kermani O, Schmeidt K, Oberheide U, Gerten G. Hyperopic laser in situ keratomileusis with 5.5-, 6.5-, and 7.0-mm optical zones. *J Refract Surg.* 2005;21:52-58.
3. Chayet AS, Montes M, Gomez L, Rodriguez X, Robledo N, MacRae S. Bitoric laser in situ keratomileusis for the correction of simple myopic and mixed astigmatism. *Ophthalmology.* 2001;108:303-308.
4. Von Noorden GK. Examination of the patient. In: *Binocular Vision and Ocular Motility.* 5th ed. St Louis, Mo: Mosby; 1996:206-279.
5. Chinese Ophthalmological Society of the Chinese Medical Association. Definition, classification and therapeutic effectiveness criteria of amblyopia. *Chinese Journal of Strabismus and Pediatric Ophthalmology.* 1996;4:97.
6. Epelbaum M, Milleret C, Buisseret P, Dufier JL. The sensitive period for strabismic amblyopia in humans. *Ophthalmology.* 1993;100:323-327.
7. Magallanes R, Shah S, Zadok D, Chayet AS, Assil KK, Montes M, Robledo N. Stability after laser in situ keratomileusis in moderately and extremely myopic eyes. *J Cataract Refract Surg.* 2001;27:1007-1012.

Optical Factors in Increased Best Spectacle-corrected Visual Acuity After LASIK

Uzeyir Erdem, MD; Orkun Muftuoglu, MD

ABSTRACT

PURPOSE: To study the factors that correlate with improved best spectacle-corrected visual acuity (BSCVA) after LASIK.

METHODS: This was a nonrandomized, prospective clinical trial of 850 eyes from 480 patients undergoing LASIK for myopia, hyperopia, and mixed astigmatism. The mean preoperative spherical equivalent refraction was −3.75±4.82 diopters (D) (range: −13.88 to 6.00 D). From this population, 72 eyes (including 22 amblyopic eyes) from 43 patients were found to have improved BSCVA 6 months after LASIK. All patients underwent LASIK with the NAVEX platform. These eyes were analyzed to evaluate factors that correlated with improved BSCVA. Pre- and postoperative BSCVA, refraction, pupil diameter, corneal topography, asphericity (Q value), total aberrations, and higher order wavefront aberrations were analyzed. All wavefront aberrations were measured using the NIDEK Optical Path Difference Scan aberrometer (OPD-Scan) preoperatively and at 6 months postoperatively.

RESULTS: Postoperatively, the mean sphere was −0.44±1.30 D (range: −4.50 to +2.50 D). The mean increase in BSCVA was 0.15±0.09 logMAR. A statistically significant negative correlation was observed between the increase in BSCVA and the preoperative BSCVA ($P<.01$). Mixed astigmatic and highly myopic eyes are more likely to gain BSCVA after LASIK than moderately myopic ($P<.05$) and hyperopic eyes ($P<.001$). In patients with myopia, the amount of BSCVA improvement correlated with the magnitude of the correction ($P<.05$). The induction of spherical aberration negatively correlated with the increase in BSCVA ($P<.05$). There were no significant differences between normal eyes and amblyopic eyes with respect to postoperative improvement in BSCVA ($P>.05$).

CONCLUSIONS: Decreased preoperative BSCVA, lower total spherical aberration induction, and preoperative mixed astigmatism and high myopia correlate with an increase in BSCVA after LASIK. [*J Refract Surg*. 2006;22: S1056-S1068.]

Laser in situ keratomileusis (LASIK) is the most popular laser refractive surgery technique for the correction of refractive errors.[1] The primary goal of laser refractive surgery is to increase uncorrected visual acuity (UCVA) by correcting the refractive error. Although best spectacle-corrected visual acuity (BSCVA) usually does not change significantly, sometimes an increase in BSCVA can be observed after laser refractive surgery.[2-9]

Amblyopia is defined as BSCVA <20/30 in one eye or a two-line difference between eyes in the absence of other visible signs of eye disease.[10] Recently, a number of studies have reported statistically significant improvement in postoperative BSCVA in amblyopic eyes after excimer laser refractive surgery.[11-15] The reasons for this increase in BSCVA postoperatively are not clear. Improvement in the precision of the refractive correction and improvement in neurosensory function are possible contributing factors to this improvement in BSCVA.[6] Changes in pupil size, corneal asphericity, and higher order aberrations may also affect the optical quality of the eye and consequently the quality of the retinal image.[16-18] Understanding these factors and their differences with regard to the presence of amblyopia and different ablation patterns (myopic, hyperopic, astigmatic, and bitoric) is important for improving the optical quality of future corneal excimer laser surgery.

The primary goal of this study was to assess the relationship between any changes in BSCVA and the refractive error, corneal asphericity, and wavefront aberrations after LASIK. A secondary goal was to compare the outcomes between eyes with and without amblyopia with respect to improvement in BSCVA.

PATIENTS AND METHODS

Patient Population

This prospective study evaluated 72 eyes from 43 patients (18 men and 25 women) who demonstrated a BSCVA in-

From Gulhane Military Medical Faculty, Ankara, Turkey.

The authors have no financial or proprietary interest in the materials presented herein.

Correspondence: Uzeyir Erdem, MD, Gulhane Military Medical Faculty Ankara, Turkey. Tel: 090 312 304 5874; E-mail: erdemuzeyir@hotmail.com

crease of a total population of 850 eyes from 480 patients who underwent LASIK. Criteria for inclusion in the study were age ⩾18 years, documented stability of refraction for 6 months before surgery, availability of preoperative and 6-month postoperative Optical Path Difference Scan (OPD-Scan; NIDEK Co Ltd, Gamagori, Japan) maps within the central 6.0-mm zone, no intra- or postoperative complications, and patients who did not require retreatments. Exclusion criteria were previous refractive surgery, evidence or suspicion of keratoconus as shown by corneal topography, active ocular or systemic disease likely to affect corneal wound healing, pregnant and nursing women, inability to comply with postoperative follow-up regimen, eyes with any intraoperative difficulties such as flap irregularities, and postoperative complications such as recurrent epithelial defects. All patients signed an informed consent before the surgery. Institutional review board approval was obtained for the study.

Surgical Procedure

All procedures were performed by one surgeon (U.E.), using the same surgical technique. The NIDEK Advanced Vision Excimer Laser (NAVEX) platform was used for all treatments. NAVEX consists of the NIDEK CXII excimer laser system, Final Fit ablation planning software, OPD-Scan, and the MK-2000 microkeratome. A 9.50-mm–diameter suction ring and 130-µm blade holder were used to create nasal hinges in all patients. All laser refractive surgeries were performed under stringently controlled conditions using the NIDEK CXII excimer laser equipped with a 200-Hz infrared eye tracker. The mean optical zone was 5.83±0.69 mm and the mean transition zone was 8.72±0.45 mm for all treatments. The optimized aspheric treatment zone (OATz) or the customized aspheric treatment zone (CATz) software was used for the treatment of myopic eyes. The NAVEX system consists of seven profiles for the transition zone to maintain a prolate corneal shape postoperatively. Profile 4 was used for high myopic treatments, and profiles 4 to 6 were used for the other myopic ablations. The Chayet bitoric ablation nomogram originally developed for the NIDEK excimer laser was used for the correction of all cases of mixed astigmatism.[3] The excimer laser repetition rate was 40 Hz, and the laser energy per pulse was between 105 and 135 mJ. Before every treatment, fluence and calibration were checked using calibration plates provided by the manufacturer. The postoperative eye drop regimen included topical ofloxacin 0.3%, prednisolone acetate 1%, and artificial tears. Patients were seen at 1 day, 1 week, and 1, 2, and 6 months postoperatively.

Patient Examination

All patients underwent a baseline examination that included UCVA and BSCVA evaluation, manifest and cycloplegic refractometry, slit-lamp evaluation, ultrasound pachymetry and corneal topography, and wavefront measurement using the OPD-Scan. Measurements of mesopic and photopic pupil diameter; average central keratometry (K) and the difference between the major corneal meridians K2 and K1 (dK); asphericity (Q) derived for the 6.0-mm corneal region; and OPD wavefront refraction root-mean-square (RMS) values at 3 mm (RMS-3) and 5 mm (RMS-5) were recorded, and wavefront aberrations were recorded from the OPD-Scan preoperatively and at their last visit. The OPD RMS values represent the distribution of refractive power caused by all aberrations of the eye. The higher this value, the more likely that there is irregular astigmatism or high levels of wavefront aberration within the optical system that could reduce visual quality. Normal levels of RMS-3 and RMS-5 are ⩽0.5 D. The pre- and postoperative UCVA and BSCVA were recorded in logMAR units, which were calculated by taking the negative log value of the decimal Snellen visual acuity.

Data and Statistical Analysis

Vector Analysis. Vectorial analysis proposed by Thibos and Horner was used to convert spherocylindrical refractive errors (S [sphere], C [cylinder] × φ [axis]) into a set of three dioptric powers: M, J_0, J_{45}, by the following formulas[19]:

$$M = S + C/2;\ J_0 = (-C/2)\cos(2\varphi); \quad (1)$$

$$J_{45} = (-C/2)\sin(2\varphi) \quad (2)$$

$$B = (M^{2} + J_0^{2} + J_{45}^{2})^{1/2}, \quad (3)$$

where M denotes the spherical equivalent refraction, B denotes the overall blur strength of the refractive error, C denotes mean cylinder, J_{45} denotes the power of the Jackson Cross Cylinder at axis 45°, and J_0 denotes the power of the Jackson Cross Cylinder at axis 180°. This mathematical approach has the advantage that astigmatism is represented in rectangular vector form, allowing statistical analysis to be applied to each component separately (orthogonality) and test hypotheses.[2,19]

Analysis of Wavefront Aberrations. Three successive measurements were taken with the OPD-Scan wavefront analyzer. The analyzed parameters included:

1) RMS of higher order aberrations from the third to eighth orders;
2) RMS of the total spherical aberration (square root

TABLE 1

Classification of Eyes With and Without Amblyopia Based on Preoperative Refractive Status

	No. Eyes				
	High Myopia	Moderate Myopia	Hyperopia	Mixed Astigmatism	Total
Amblyopia	7	4	3	8	22
No amblyopia	9	26	6	9	50
Total	16	30	9	17	72

of the sum of the squared coefficients of C_4^0, C_6^0, and C_8^0);

3) RMS of total coma (square root of the sum of the squared coefficients of C_3^{-1}, C_3^1, C_5^{-1}, C_5^1, C_7^{-1}, and C_7^1);
4) RMS of total trefoil (square root of the sum of the squared coefficients of C_3^{-3}, C_3^3, C_5^{-3}, C_5^3, C_7^{-3}, and C_7^3);
5) RMS of total tetrafoil (square root of the sum of the squared coefficients of C_4^{-4}, C_4^4, C_6^{-4}, C_6^4, C_8^{-4}, and C_8^4); and
6) RMS of total high order astigmatism (square root of the sum of the squared coefficients of C_4^{-2}, C_4^2, C_6^{-2}, C_6^2, C_8^{-2}, and C_8^2).

The difference between pre- and postoperative value of each parameter was defined as:

$$\Delta\text{data} = \text{data}_{\text{postoperative}} - \text{data}_{\text{preoperative}}$$

(Negative values of Δdata represent an increase in value for each parameter.)

Statistical Analysis. All data were analyzed using the SPSS version 11.0 (SPSS Inc, Chicago, Ill) statistical software. Normality of data in each group was confirmed by normal probability plots. Paired *t* test for parametric data and Wilcoxon signed ranks test for nonparametric data were used to analyze each parameter before and after laser refractive surgery. The Mann-Whitney *U* test and Kruskal-Wallis test were used to compare parameters between groups. Multiple comparison test was used to compare differences among parameters of more than two when there was significance using the Kruskal-Wallis test.[20] The association between ΔBSCVA and the clinical outcomes were tested using Spearman rank correlation (for nonparametric data) and Pearson correlation and regression analysis (for parametric data). A *P* value <.05 was considered statistically significant.

RESULTS

The mean age of the patients with improved BSCVA was 30.8±7.2 years (range: 21 to 53 years). In this group, there were 22 eyes with amblyopia from 18 patients and 50 eyes without amblyopia from 25 patients. Classification of eyes based on the preoperative refraction and presence of amblyopia is shown Table 1. Ten eyes from 10 patients had anisometropic amblyopia; 3 eyes of 2 patients had ametropic amblyopia; 2 eyes of 1 patient had meridional amblyopia; 2 eyes of 2 patients had ametropic and anisometropic amblyopia; and 5 eyes of 3 patients had anisometropic and meridional amblyopia.

VISION

The mean BSCVA was 0.17±0.15 (range: −0.04 to 0.58) before surgery and 0.01±0.13 (range: −0.20 to 0.40) after surgery. The mean UCVA was 0.99±0.45 (range: 0.06 to 1.80) before surgery and 0.12±0.21 (range: −0.17 to 1.00) after surgery. There was a statistically significant increase in BSCVA ($P<.001$) and UCVA ($P<.001$) 6 months after surgery.

REFRACTIVE STATUS

Preoperatively, the mean spherical equivalent refraction was −3.75±4.82 D (range: −13.88 to 6.00 D); the mean cylinder was −1.45±1.87 D (range: −5.00 to 4.00 D) (J_0: −0.11±0.79 [range: −2.27 to 2.23], J_{45}: 0.04±0.88 [range: −2.03 to 1.93]); and the mean blur strength of the refractive error was 5.38±3.08 (range: 0.95 to 13.89). Postoperatively, mean spherical equivalent refraction was −0.44±1.30 D (range: −4.50 to 2.50 D); mean cylinder was −0.22±1.09 D (range: −2.25 to 3.75 D) (J_0: 0.03±0.34 [range: −0.79 to 0.99], J_{45}: −0.05±0.43 [range: −1.83 to 0.80]); and blur strength of the refractive error was 1.17±0.90 (range: 0.00 to 4.56). There was a statistically significant decrease in spherical equivalent refraction ($P<.001$), cylinder ($P<.001$) (J_0 [$P<.05$], J_{45} [$P=.59$] [the significance was low]), and blur strength of the refractive error ($P<.001$) postoperatively. Table 2 shows the mean pre- and postoperative refractive status in eyes with and without amblyopia, and Table 3 shows the mean pre- and postoperative re-

TABLE 2

Pre- and Postoperative Vectorial Refractive Status in Eyes With and Without Amblyopia*

	Amblyopia (n=22)			No Amblyopia (n=50)		
Vector	**Preop**	**Postop**	***P*†**	**Preop**	**Postop**	***P*†**
M (SE)	−3.96±6.14	−0.65±1.85	<.01	−3.66±4.18	−0.35±0.97	<.001
J_0	−0.32±0.84	0.12±0.42	<.05	−0.06±0.76	0.00±0.30	.402
J_{45}	0.20±1.11	0.01±0.52	.394	−0.03±0.75	−0.08±0.39	.434
B	6.09±4.16	1.66±1.21	<.001	5.07±2.45	0.96±0.62	<.001

M (SE) = spherical equivalent refraction, J_0 = power of Jackson cross cylinder at 180°, J_{45} = power of Jackson cross cylinder at 45°, B = overall blur strength of the refractive error
**All values are represented as mean±standard deviation.*
†Wilcoxon signed ranks test.
(S [sphere], C [cylinder] × ϕ [axis]) is written as a set of three dioptric powers: M, J_0, J_{45}, using the following formulas: M = S + C/2; $J_0 = (-C/2) \cos(2\phi)$; $J_{45} = (-C/2) \sin(2\phi)$; $B = (M^2 + J_0^2 + J_{45}^2)^{1/2}$, where C = mean cylinder.

TABLE 3

Pre- and Postoperative Vectorial Refractive Status in Eyes With High Myopia, Moderate Myopia, Hyperopia, and Mixed Astigmatism*

Refractive Status	**M (SE)**	**J_0**	**J_{45}**	**B**
High Myopia (SE <−7.00 D)				
Preop	−10.04±2.30	−0.17±0.52	−0.06±0.48	10.07±2.29
Postop	−1.53±1.53	0.06±0.31	−0.01±0.18	1.67±1.42
*P**	<.001	<.05	.610	<.001
Moderate Myopia (−7.00<SE<0)				
Preop	−4.79±1.34	0.05±0.77	0.08±0.48	4.89±1.30
Postop	−0.57±0.63	−0.04±0.23	0.00±0.14	0.78±0.46
*P**	<.001	.144	.133	<.001
Hyperopia				
Preop	4.52±1.04	−0.38±0.42	0.33±0.95	4.67±0.89
Postop	0.95±1.49	0.12±0.48	−0.24±0.87	1.77±0.88
*P**	<.01	<.05	<.05	<.01
Astigmatism				
Preop	−0.36±1.39	−0.21±1.13	−0.12±1.50	2.22±0.64
Postop	0.07±0.95	0.09±0.44	−0.01±0.50	1.07±0.39
*P**	<.05	<.05	<.05	<.05

M (SE) = spherical equivalent refraction, J_0 = power of Jackson Cross Cylinder at 180°, J_{45} = power of Jackson Cross Cylinder at 45°, B = overall blur strength of the refractive error
**All values are represented as mean±standard deviation.*
†Wilcoxon signed ranks test.
(S [sphere], C [cylinder] × ϕ [axis]) is written as a set of three dioptric powers: M, J_0, J_{45}, using the following formulas: M = S + C/2; $J_0 = (-C/2) \cos(2\phi)$; $J_{45} = (-C/2) \sin(2\phi)$; $B = (M^2 + J_0^2 + J_{45}^2)^{1/2}$, where C = mean cylinder.

fractive status based on the level of preoperative refraction (high myopia [SE <−7.00 D], moderate myopia [−7.00<SE<0], hyperopia, and mixed astigmatism).

Corneal Topography: Asphericity

Preoperatively, the mean corneal power was 43.62±1.57 D (range: 40.82 to 47.74 D), and the mean

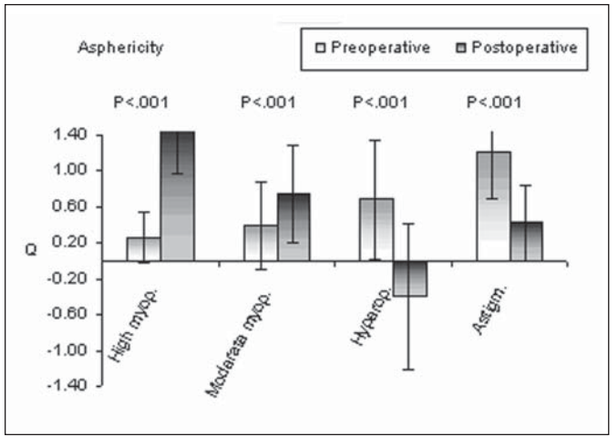

Figure 1. Pre- and postoperative corneal asphericity (Q) for high myopia, moderate myopia, hyperopia, and mixed astigmatism (Astigm). The values for the induced change from preoperative asphericity to postoperative asphericity are shown above each group. *P* values <.05 are statistically significant.

difference between corneal meridians K2 and K1 was 2.28±1.58 D (range: 0.05 to 6.53 D). Postoperatively, the mean K was 40.92±4.02 D (range: 34.16 to 53.33 D), and the mean difference between corneal meridians K2 and K1 was 0.86±0.52 D (range: 0.11 to 2.66 D). A statistically significant decrease was noted in mean corneal power ($P<.001$) after surgery.

The mean Q value was 0.59±0.61 (range: −0.27 to 2.48) preoperatively and 0.70±0.79 (range: −1.39 to 3.07) postoperatively. No significant change was noted between pre- and postoperative Q values ($P<.389$). The mean pre- and postoperative Q values based on preoperative refraction are shown in Figure 1. Analyzed separately, each group showed statistically significant changes in asphericity after surgery. Postoperatively, corneal asphericity became more prolate in mixed astigmatism, whereas it became more oblate in myopia (see Fig 1).

Aberrations

The mean preoperative RMS-3 and RMS-5 were 0.26±0.14 D (range: 0.11 to 0.94 D) and 0.51±0.73 D (range: 0.10 to 5.73 D), respectively. The mean preoperative total wavefront aberration was 6.012±2.575 µm (range: 1.328 to 13.832 µm). Six months after surgery, RMS-3 and RMS-5 were 0.47±0.53 D (range: 0.17 to 4.62 D) and 0.95±1.64 D (range: 0.17 to 13.58 D), respectively. The postoperative total wavefront aberration was 2.064±0.861 µm (range: 0.723 to 4.895 µm). There was a statistically significant increase in RMS-3 ($P<.001$) and RMS-5 ($P<.001$) and a statistically significant decrease in total wavefront aberration ($P<.001$) 6 months after surgery.

TABLE 4

Pre- and Postoperative Higher Order Aberrations For All Groups Treated With NAVEX

	Preoperative (µm)	Postoperative (µm)	P*
HOA	0.452±0.207	0.730±0.319	<.001
TC	0.212±0.159	0.415±0.257	<.001
T3F	0.281±0.161	0.375±0.237	<.001
T4F	0.113±0.119	0.140±0.113	<.001
TSA	0.125±0.108	0.253±0.240	<.001
HiA	0.108±0.063	0.176±0.153	<.001

HOA = higher order aberration, TWA = total wavefront aberrations, TC = total coma, T3F = total trefoil, T4F = total tetrafoil, TSA = total spherical aberration, HiA = total high order astigmatism

The mean pre- and postoperative higher order aberrations and Zernike terms are shown in Table 4. The mean total wavefront aberration/higher order aberration ratio was 9±6% preoperatively and 38±13%, postoperatively. The mean pre- and postoperative higher order aberrations and individual Zernike terms in amblyopia, healthy eyes, and each group (high myopia, moderate myopia, hyperopia, and mixed astigmatism) are shown in Figure 2.

Comparison of Myopia, Hyperopia, and Mixed Astigmatism Groups

The comparison of change in data (Δdata) in amblyopia and healthy eyes and in each refractive group is presented in Tables 5 and 6, respectively. There was no significant change in any of the variables investigated, including change in BSCVA, between the amblyopic and normal groups (Table 5).

The mean increase in BSCVA (ΔBSCVA) was significantly higher in both mixed astigmatism and high myopia compared with moderate myopia ($P<.05$) and hyperopia ($P<.001$) (Table 6). The mean increase in BSCVA in hyperopia was significantly lower than in moderate myopia ($P<.05$). The mean increase in BSCVA in mixed astigmatism was higher than in high myopia without statistical significance ($P=.856$, multiple comparison test) (Table 6). A statistically significant negative correlation was observed between the increase in BSCVA and the preoperative BSCVA ($P<.01$).

Correlations

The correlations between ΔBSCVA and age, $BSCVA_{preop}$, ΔM, ΔB, ΔJ_0, ΔJ_{45}, ΔQ, and ΔK are plotted in Figure 3. The correlations between ΔBSCVA and Δtotal wavefront aberration, Δhigher order aberration, and individual Zernike terms are plotted in Figure 4. Correlations

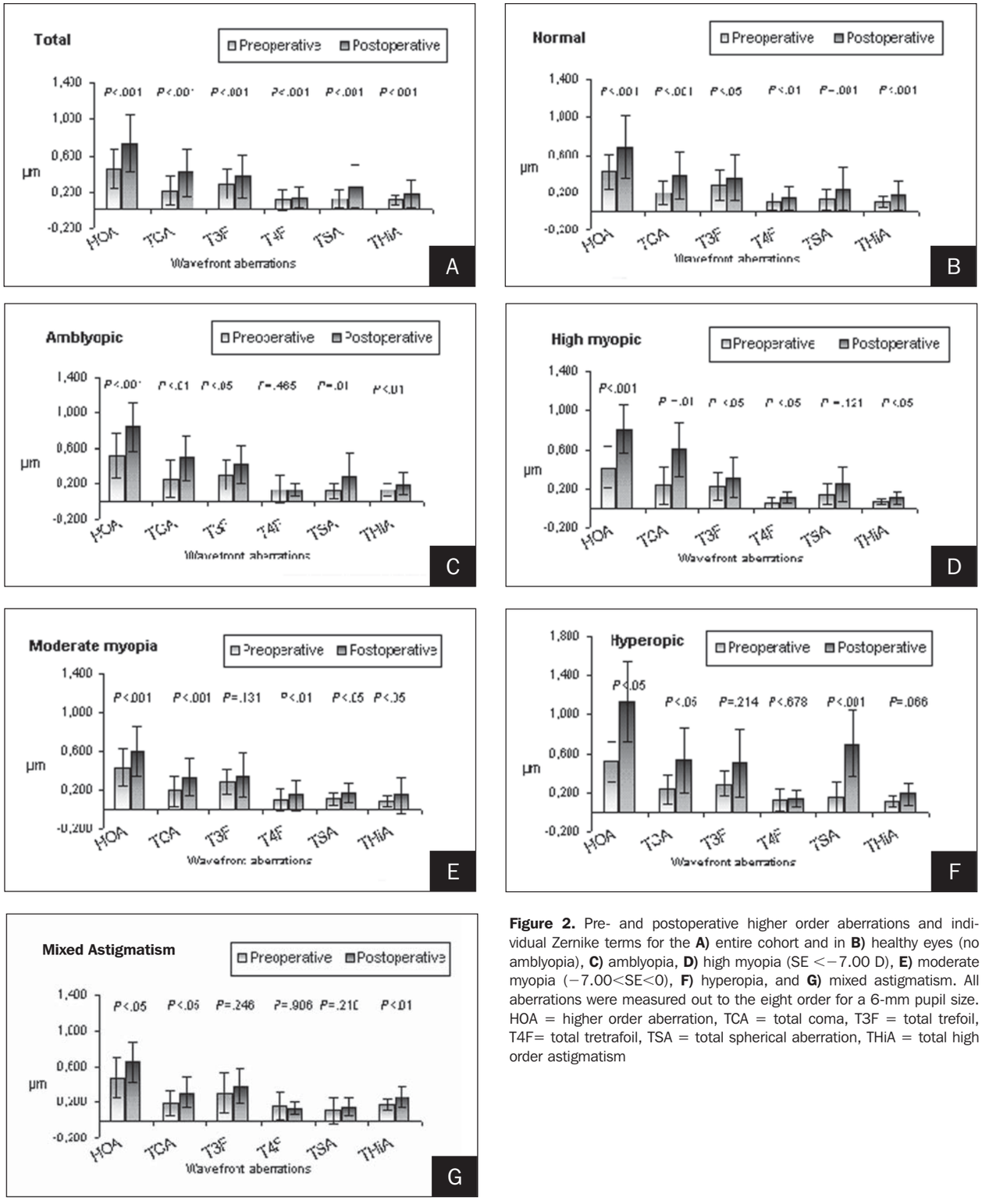

Figure 2. Pre- and postoperative higher order aberrations and individual Zernike terms for the **A)** entire cohort and in **B)** healthy eyes (no amblyopia), **C)** amblyopia, **D)** high myopia (SE <-7.00 D), **E)** moderate myopia ($-7.00<SE<0$), **F)** hyperopia, and **G)** mixed astigmatism. All aberrations were measured out to the eight order for a 6-mm pupil size. HOA = higher order aberration, TCA = total coma, T3F = total trefoil, T4F= total tretrafoil, TSA = total spherical aberration, THiA = total high order astigmatism

TABLE 5

Comparison of Change After LASIK in Refraction, Age, Vision, Pupil Size, Keratometry, Asphericity, and Wavefront Aberration in Eyes With and Without Amblyopia*

	Amblyopia (n=22)	No Amblyopia (n=50)	P†
Age (y)	30.36±6.75	30.96±7.47	.937
ΔBSCVA (logMAR)	−0.19±0.09	−0.15±0.07	.095
ΔBSCVA/ΔB	0.118±0.166	0.079±0.154	.591
ΔPhotopic pupil diameter	−0.017±0.370	−0.044±0.55	.682
ΔMesopic pupil diameter	−0.071±0.440	−0.103±0.660	.458
ΔK (D)	−2.62±3.99	−2.75±3.75	.845
ΔdK (D)	−0.15±1.19	−0.08±1.11	.723
ΔQ	0.03±1.10	0.14±0.91	.545
ΔB	4.43±3.39	4.11±2.61	.912
ΔTWA (μm)	4.024±3.017	3.925±1.857	.616
ΔRMS-3 (D)	0.13±0.19	0.25±0.65	.826
ΔRMS-5 (D)	0.40±0.44	0.44±2.02	.146

BSCVA = best spectacle-corrected visual acuity, TWA = total wavefront aberrations, K = corneal power, dK = difference in keratometry, Q = asphericity value, RMS-3 = wavefront refraction root-mean-square of total aberrations in 3-mm zone, RMS-5 = wavefront refraction root-mean-square of total aberrations in 5-mm zone Note. Negative values of ΔBSCVA indicate increase in BSCVA (logMAR).
**All values are represented as mean±standard deviation.*
†Mann-Whitney U test.

TABLE 6

Comparison of Change After LASIK in Refraction, Age, Vision, Pupil Size, Keratometry, Asphericity, and Wavefront Aberration in Eyes With High Myopia, Moderate Myopia, Hyperopia, and Mixed Astigmatism*

	High Myopia (n=17)†	Moderate Myopia (n=30)‡	Hyperopia (n=9)	Astigmatism (n=16)	P§
ΔBSCVA (logMAR)	−0.19±0.09	−0.14±0.06	−0.09±0.03	−0.20±0.09	.001
ΔBSCVA/ΔB	0.019±0.012	0.052±0.085	0.045±0.051	0.252±0.242	<.001
ΔK (D)	−7.03±1.42	−3.81±1.11	4.52±2.68	−0.51±0.94	<.001
ΔdK (D)	−0.05±1.29	−0.06±0.66	0.88±1.88	−0.93±0.77	<.001
ΔQ	1.28±0.56	0.36±0.46	−1.09±0.43	−0.80±0.48	<.001
ΔB	8.40±1.72	4.10±1.33	−2.91±1.59	1.15±0.61	<.001
ΔTWA (μm)	6.93±1.72	3.93±1.32	3.56±0.77	1.41± 0.70	<.001
ΔRMS−3 (D)	0.23±0.26	0.21±0.81	0.28±0.25	0.15±0.23	<.05
ΔRMS-5 (D)	0.61±0.51	0.59±2.39	0.61±0.54	−0.14±1.25	<.01

BSCVA = best spectacle-corrected visual acuity, TWA = total wavefront aberrations, K = corneal power, dK = difference in keratometry, Q = asphericity value, RMS-3 = wavefront refraction root-mean-square of total aberrations in 3-mm zone, RMS-5 = wavefront refraction root-mean-square of total aberrations in 5-mm zone Note. Negative values of ΔBSCVA indicate increase in BSCVA (logMAR).
**All values are represented as mean±standard deviation.*
†SE <−7.00 D.
‡−7.00<SE<0.
§Kruskal-Wallis test.

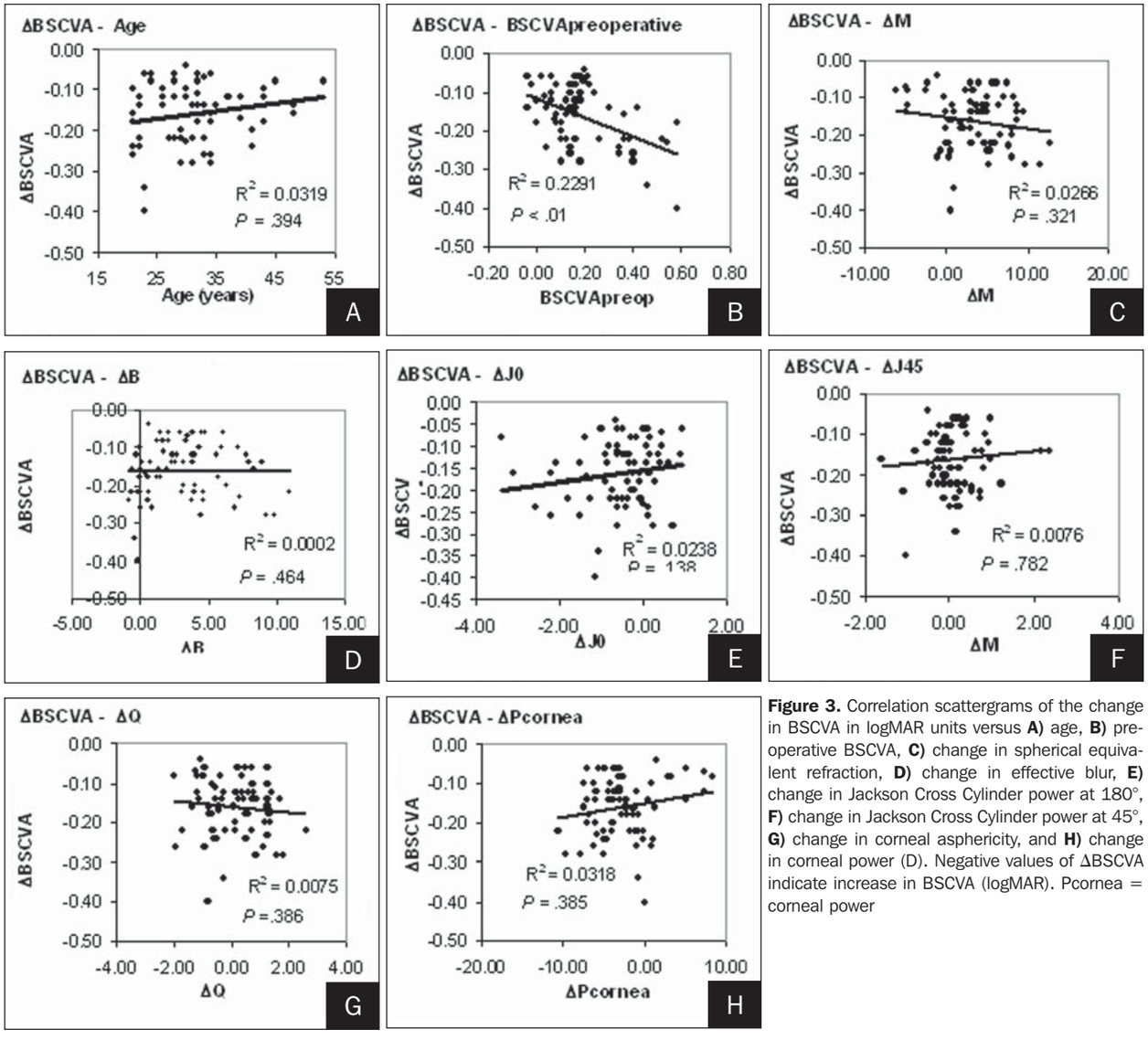

Figure 3. Correlation scattergrams of the change in BSCVA in logMAR units versus **A)** age, **B)** preoperative BSCVA, **C)** change in spherical equivalent refraction, **D)** change in effective blur, **E)** change in Jackson Cross Cylinder power at 180°, **F)** change in Jackson Cross Cylinder power at 45°, **G)** change in corneal asphericity, and **H)** change in corneal power (D). Negative values of ΔBSCVA indicate increase in BSCVA (logMAR). Pcornea = corneal power

between ΔBSCVA and Δdata for each of the myopia, hyperopia, and mixed astigmatism groups are shown in Table 7. In myopia, the amount of BSCVA improvement was correlated with the magnitude of the correction ($P<.05$). The induction of spherical aberration was negatively correlated with the increase in BSCVA ($P<.05$).

DISCUSSION

The increase of BSCVA after laser refractive surgery is reported to be between 0% and 67%.[2-9] This variability may be due to differing patient groups, preoperative refractions, surgical techniques, and microkeratomes and lasers in the studies. In a large series of 300 consecutive myopic eyes, Maldonado-Bas and Onnis[4] observed that BSCVA increase was more likely in eyes with higher preoperative refractive error. However, most studies of refractive surgery primarily report the efficacy and safety of the procedure. Therefore, the presence of amblyopia, the magnitude of the increase in BSCVA, and the cause of this increase are often not investigated.

The results of studies that reported an increase in BSCVA after LASIK in pediatric patients with amblyopia were often suboptimal, because the patients are often unable to fixate.[14,21] Although it is commonly accepted that preventive therapy for amblyopia is effective until 8 to 11 years of age,[14] there are reports of

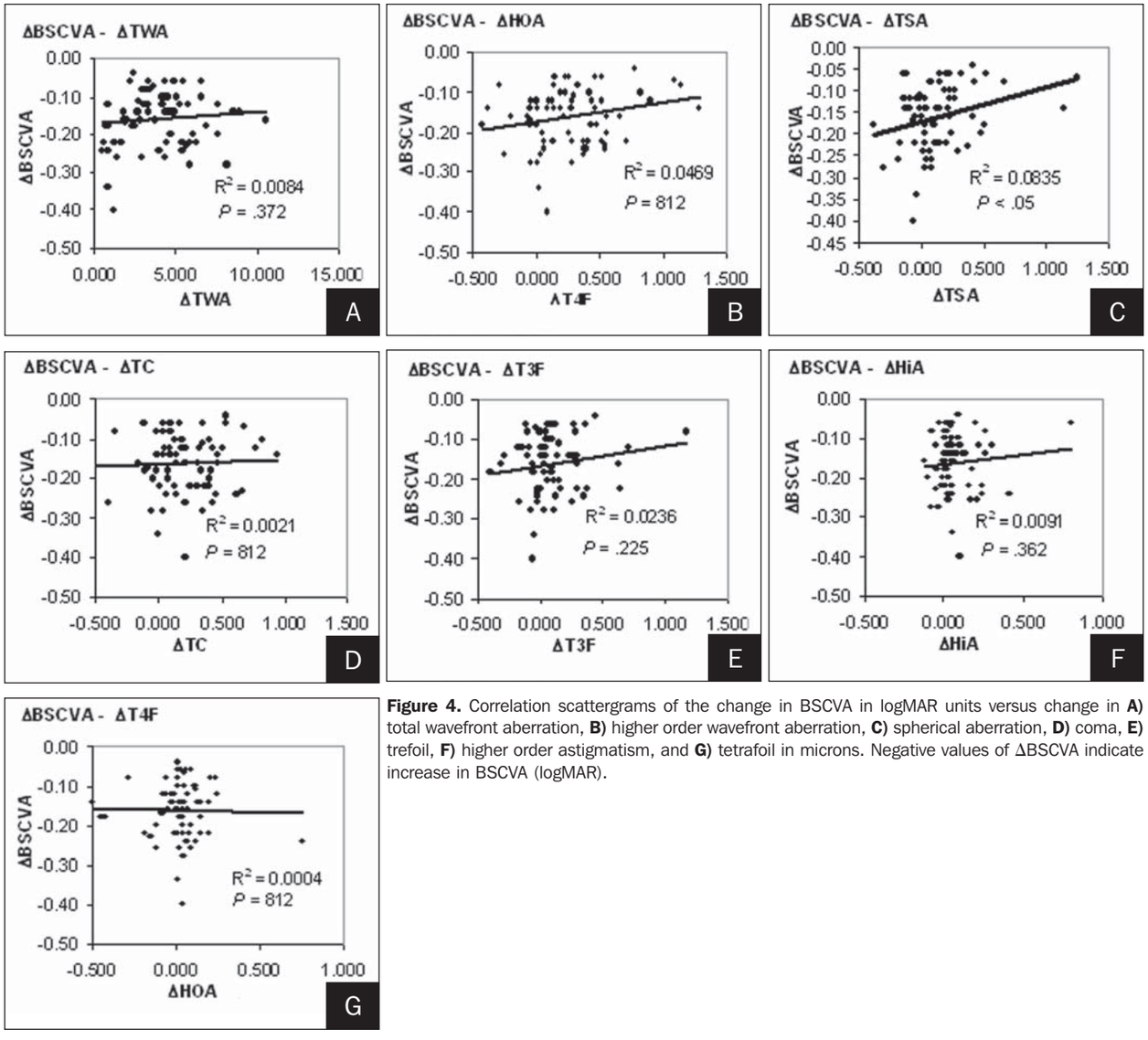

Figure 4. Correlation scattergrams of the change in BSCVA in logMAR units versus change in **A)** total wavefront aberration, **B)** higher order wavefront aberration, **C)** spherical aberration, **D)** coma, **E)** trefoil, **F)** higher order astigmatism, and **G)** tetrafoil in microns. Negative values of ΔBSCVA indicate increase in BSCVA (logMAR).

BSCVA increase after LASIK in autofixating adolescent and adult patients with amblyopia.[11,12] Lanza et al[6] reported results of photorefractive keratectomy in 38 eyes from 36 adult patients with amblyopia comprised mostly (30 of 38 eyes) of compound myopic astigmatism and only 2 eyes with hyperopia.[6] Although not statistically significant, they observed a tendency of greater BSCVA improvement in younger patients, in eyes that were closer to emmetropia, and in eyes that have accurate astigmatic correction.[6]

In the present study, a statistically significant correlation between ΔBSCVA and preoperative BSCVA was found. This implies that patients with worse preoperative BSCVA have more reserve visual capacity. There was no significant correlation found between the increase in BSCVA and age. However, there was a tendency toward greater BSCVA increase in younger patients. Although a significant correlation between increase in BSCVA and the amount of correction (ΔB, Δtotal wavefront aberration, ΔK) was not observed, there were significant correlations between ΔBSCVA and ΔB, Δtotal wavefront aberration, and ΔK in myopia and significant correlation between ΔBSCVA and Δtotal wavefront aberration in hyperopia. However, no such correlation was noted in mixed astigmatism. This suggests that BSCVA increase is related to the magnitude of correction in myopia and aberration correction in hyperopia but not in mixed astigmatism. A significant correlation was not

TABLE 7

Correlation Values for the Change in BSCVA and Change in Data in Eyes With Myopia, Hyperopia, and Mixed Astigmatism

	Myopia		Hyperopia		Mixed Astigmatism	
	r	P	r	P	r	P
BSCVApre	−.381	<.01	.579	.103	−.424	.090
Age	−.130	.391	−.352	.353	.408	.104
ΔB	−.342	<.05	−.288	.452	.060	.818
ΔTWA	−.351	<.05	−.512	<.05	.314	.219
ΔJ_0	−.182	.226	.000	.100	.305	.235
ΔJ_{45}	.160	.287	−.559	.117	.027	.918
ΔK	.406	<.05	−.136	.542	−.120	.647
ΔdK	−.186	.216	−.220	.569	.001	.996
ΔQ	−.396	.064	−.322	.322	.376	.104
Qpostop	−.265	.075	.153	.695	.384	.128
ΔHOA	.062	.682	.017	.965	.112	.668
ΔTC	−.057	.706	−.162	.678	−.038	.884
ΔT3F	.188	.211	.407	.277	.068	.796
ΔT4F	.063	.678	.017	.965	−.455	.066
ΔTSA	.064	.675	.119	.761	.219	.398
ΔHiA	.355	<.05	.220	.569	−.423	.091

B= overall blur strength of the refractive error, TWA = total wavefront aberrations, J_0 = power of Jackson Cross Cylinder at 180°, J_{45} = power of Jackson Cross Cylinder at 45°, K = average central keratometry, dK = difference in keratometry, Q = asphericity value, HOA = higher order aberrations, TC = total coma, T3F = total trefoil, T4F = total tetrafoil, TSA = total spherical aberration, HiA = total high order astigmatism

found between the increase in BSCVA and accurate astigmatic correction (ΔJ_{45}, ΔJ_0, ΔdK) in all eyes and also within each refraction group.

The corneal asphericity (Q value) in the conic equation has been used to describe the corneal surface.[16] Myopic, hyperopic, and astigmatism ablation profiles are different with respect to the ablation pattern and the effect on corneal asphericity.[2,22,23] In this study, although preoperatively the corneal asphericity was the worst for mixed astigmatism, the corneal asphericity improved after bitoric astigmatism correction, whereas it worsened after myopic and hyperopic corrections despite better preoperative asphericities. As in the current study, previous studies have reported that the corneal asphericity was worse after myopic and hyperopic corrections.[22,23] This shows that the bitoric ablation corrects the corneal refractive errors and improves asphericity for patients with mixed astigmatism. Hyperopic and myopic ablation algorithms reshape the cornea to correct refractive errors mostly based on axial length, therefore, adversely affecting corneal asphericity in myopia and hyperopia.[24,25] In this study, there was no significant correlation between ΔBSCVA and change in corneal asphericity or postoperative asphericity. This implies that although the Q value is different in various levels of preoperative refraction, it is not a determinant of postoperative BSCVA.

As in previous reports,[26-29] a significant increase in higher order aberrations after LASIK was found in this study. The mean higher order aberration/total wavefront aberration ratio increased from 9% preoperatively to 38% postoperatively. This suggests that increase in higher order aberrations has a low impact on the increase in BSCVA after LASIK. This finding is also supported by previous reports that could not demonstrate significant effect of higher order aberrations on vision.[17,30-34] One explanation may be that current methods of visual acuity measurements may not be sensitive enough to demonstrate the impact of higher order aberrations on visual acuity. Therefore, development of techniques of vision assessment and new metrics of higher order aberrations may better correlate with clinical measures of visual performance.[31,35]

Although there were significant increases in higher

order aberrations after surgery in all groups, the greatest increase was observed after hyperopic treatments, followed by high myopic treatments, moderate myopic treatments, and finally bitoric ablation treatments. Differences in higher order aberration induction among the groups can be explained by the change in asphericity: eyes treated with bitoric ablation correction had the best postoperative asphericity and least higher order aberration induction, followed by moderate myopia, high myopia, and hyperopia corrections. Previous studies have also reported greater changes in higher order aberrations in hyperopic treatments compared with myopic treatments.[28,36] This greater induction of higher order aberrations in hyperopic treatments may be due to the steeper slope of the hyperopic ablation profile with its three transition points,[37,38] coupled with smaller transition zones, compared with the OATz and CATz myopia profiles that have only two transition points. The greater preponderance of angle kappa in the population with hyperopia makes laser centration difficult, which may also lead to greater induction of higher order aberrations.[39]

A number of studies have reported that myopic or hyperopic LASIK induces spherical aberration in different directions.[25,36,40,41] It has been proposed that the increase in BSCVA after refractive surgery in patients with myopic amblyopia is caused by minimization of spherical aberration.[6,32] In the present study, total spherical aberration increased significantly after myopic and hyperopic correction in eyes with amblyopia and healthy eyes. The greatest induction of spherical aberration was seen in the hyperopic treatments. The use of a large aspheric transition zone to effectively create a large treatment zone, which is the basis of both OATz and CATz treatments, was likely the cause of the reduced spherical aberration induction in myopic eyes. A significant negative correlation was observed between the amount of BSCVA increase and total spherical aberration induction after LASIK. This suggests that total spherical aberration may have more of an impact on visual acuity than the other Zernike terms.

There were significant increases in total coma in all groups. The induced coma had the greatest effect in increasing higher order aberrations after LASIK. Previous studies have also reported significant coma induction after hyperopic and myopic LASIK.[36,42] The increase in total coma in all ablation patterns irrespective of preoperative refractive error suggests that coma induction is due to a common factor. The creation of the lamellar flap or laser ablation itself could be the cause. No significant correlation was found in the present study between BSCVA increase and Δhigher order aberrations or other Zernike terms (total trefoil, total tetrafoil, high order astigmatism).

In contrast to the current study, Sakatani et al[11] stated that amblyopic patients with myopia showed a statistically significant improvement in postoperative BSCVA after LASIK. There are other reports that have proposed that BSCVA increase in amblyopia is seen more often in patients with myopia.[6,19] Better correction of ametropia, elimination of aberrations occurring from the use of spectacles in myopia, and a real recovery from amblyopia were some of the reasons given for this BCSVA increase after myopic LASIK in patients with amblyopia.[6,11,12] However, these studies comprised predominantly patients with myopia with a limited number of patients with hyperopia and mixed astigmatism. Moreover, patients with strabismus, a confounding variable, were included in these studies.

In the current study, postoperative BSCVA was more likely to increase in mixed astigmatic corrections, followed by high myopic, moderate myopic, and hyperopic corrections. Better asphericity and less higher order aberration induction might explain a higher rate of BSCVA increase in patients after mixed astigmatic correction, and worse asphericity and higher higher order aberration induction might explain a lower rate of BSCVA increase after hyperopic correction observed in this study. Previous studies have reported that an increase in BSCVA is common after bitoric ablation.[1,31] The BSCVA increase in these studies may be explained by the fact that spectacle correction for high astigmatism produces a larger distortion of the image than that caused by a lens that corrects for smaller degrees of astigmatism.[2]

Previous reports indicate that patients with amblyopia may have reserve visual capacity that allows for the capability of increased vision after laser refractive surgery.[6,11] However, the improvement in BSCVA observed in patients with and without amblyopia in this study suggests that both groups may have reserve visual capacity. In this study, no significant difference was noted between patients with and those without amblyopia with regard to the change in corneal asphericity and pupil diameter, decrease in total wavefront aberrations, and induction of higher order aberrations and individual Zernike terms. This implies that the optical mechanism of the improved BSCVA increase observed after laser refractive surgery may be similar in both groups. Additional studies are needed to clarify whether this reserve visual capacity is predominantly optical or neurosensorial.

Caution should be taken when comparing the results of this study with those of other studies. The devices and techniques used in the various studies for the measurement of ocular aberrations are not identical.[43,44] The NIDEK OPD-Scan is a relatively new method to detect optical refractive status and wavefront aberrations of the eye. A recent comparison of the OPD-Scan

to other aberrometers found that the OPD-Scan produces similar results.[45,46] Unlike Hartmann-Shack systems, the OPD-Scan uses dynamic retinoscopy to measure aberrations, which makes it unique for measuring the refractive power map over the entire central pupil and measuring highly aberrated eyes and for using significantly more data points to obtain measurements. An additional advantage is that it provides pupillometry, corneal topography, autorefraction, and autokeratometry measurements all on the same axis. However, there is a relative paucity of studies investigating the accuracy and reliability of this instrument.

In the current study, the investigators evaluated the optical factors in eyes with increase in BSCVA after LASIK. These optical factors should also be compared with the results of refractive surgery without improvement in BSCVA. The present results should also be compared with the results of wavefront-guided laser refractive surgery. Previous studies reported that the rate of BSCVA increase after hyperopic correction is low.[47,48] A relatively reduced rate of BSCVA increase after hyperopic correction was also found in this study.

In conclusion, the present study revealed that eyes with poorer preoperative BSCVA and higher myopia are more likely to have an improvement in BSCVA than eyes with better preoperative BSCVA and lower myopia. Although higher order aberrations seem to have a slight influence on the improved BSCVA, different higher order aberration induction patterns between patients treated for myopia, hyperopia, and mixed astigmatism may have an effect on the different rates of improved BSCVA in these groups. In the present study, bitoric ablations for mixed astigmatism were most likely to result in improved BSCVA, improved corneal asphericity, and less induced higher order aberration than myopic and hyperopic ablations. Hyperopic treatments were least likely to result in improved BSCVA and corneal asphericity and most likely to have induction of higher order aberrations of all the treatment groups. Patients with amblyopia were no more likely than those without amblyopia to have improved BSCVA after surgery. Additional studies should be undertaken to investigate the relationship between the optical properties of the eye and wavefront-guided treatment, and new measurement techniques to assess visual performance must be developed.

REFERENCES

1. Duffey RJ, Leaming D. Trends in refractive surgery in the United States. *J Cataract Refract Surg.* 2004;30:1781-1785.
2. Albarran-Diego C, Munoz G, Montes-Mico R, Alio JL. Bitoric laser in situ keratomileusis for astigmatism. *J Cataract Refract Surg.* 2004;30:1471-1478.
3. Chayet AS, Montes M, Gomez L, Rodriguez X, Robledo N, MacRae S. Bitoric laser in situ keratomileusis for the correction of simple myopic and mixed astigmatism. *Ophthalmology.* 2001;108:303-308.
4. Maldonado-Bas A, Onnis R. Results of laser in situ keratomileusis in different degrees of myopia. *Ophthalmology.* 1998;105:606-611.
5. Seward MS, Oral D, Bowman RW, El-Agha MS, Cavanagh HD, McCulley JP. Comparison of LADARVision and Visx Star S3 laser in situ keratomileusis outcomes in myopia and hyperopia. *J Cataract Refract Surg.* 2003;29:2351-2357.
6. Lanza M, Rosa N, Capasso L, Iaccarino G, Rossi S, Romano A. Can we utilize photorefractive keratectomy to improve visual acuity in adult amblyopic eyes? *Ophthalmology.* 2005;112:1684-1691.
7. Gimbel HV, Van Westenbrugge JA, Penno EEA, Ferensowicz M, Feinerman GA, Chen R. Simultaneous bilateral laser in situ keratomileusis. *Ophthalmology.* 1999;106:1461-1468.
8. El-Maghraby A, Salah T, Waring GO III, Klyce SD, Ibrahim O. Randomized bilateral comparison of excimer laser in situ keratomileusis and photorefractive keratectomy for 2.50 to 8.00 diopters of myopia. *Ophthalmology.* 1999;106:447-457.
9. Jaycock PD, O'Brart DPS, Rajan MS, Marshall J. 5-year follow-up of LASIK for hyperopia. *Ophthalmology.* 2005;112:191-199.
10. Von Noorden GK. *Binocular Vision and Ocular Motility: Theory and Management of Strabismus.* 5th ed. St Louis, Mo: Mosby; 1996.
11. Sakatani K, Jabbur NS, O'Brien TP. Improvement in best corrected visual acuity in amblyopic adult eyes after laser in situ keratomileusis. *J Cataract Refract Surg.* 2004;30:2517-2521.
12. Phillips CB, Prager TC, McClellan G, Mintz-Hittner HA. Laser in situ keratomileusis for treated anisometropic amblyopia in awake, autofixating pediatric and adolescent patients. *J Cataract Refract Surg.* 2004;30:2522-2528.
13. Nassaralla BRA, Nassaralla JJ Jr. Laser in situ keratomileusis in children 8 to 15 years old. *J Refract Surg.* 2001;17:519-524.
14. Rashad KM. Laser in situ keratomileusis for myopic anisometropia in children. *J Refract Surg.* 1999;15:429-435.
15. Alio JL, Artola A, Claramonte P, Ayala MJ, Chipont E. Photorefractive keratectomy for pediatric myopic anisometropia. *J Cataract Refract Surg.* 1998;24:327-330.
16. Holladay JT, Janes JA. Topographic changes in corneal asphericity and effective optical zone after laser in situ keratomileusis. *J Cataract Refract Surg.* 2002;28:942-947.
17. Applegate RA, Hilmantel G, Howland HC, Tu EY, Starck T, Zayac EJ. Corneal first surface optical aberrations and visual performance. *J Refract Surg.* 2000;16:507-514.
18. Rosen ES, Gore CL, Taylor D, Chitkara D, Howes F, Kowalewski E. Use of a digital infrared pupillometer to assess patient suitability for refractive surgery. *J Cataract Refract Surg.* 2002;28:1433-1438.
19. Thibos LN, Horner D. Power vector analysis of the optical outcome of refractive surgery. *J Cataract Refract Surg.* 2001;27:31-49.
20. Schwiegerling J. Theoretical limits to visual performance. *Surv Ophthalmol.* 2000;45:139-146.
21. Agarwal A, Agarwal A, Agarwal T, Siraj AA, Narang P, Narang S. Results of pediatric laser in situ keratomileusis. *J Cataract Refract Surg.* 2000;26:684-689.
22. Munnerlyn CR, Koons SJ, Marshall J. Photorefractive keratectomy: a technique for laser refractive surgery. *J Cataract Refract Surg.* 1988;14:46-52.
23. Azar DT, Primack JD. Theoretical analysis of ablation depths

and profiles in laser in situ keratomileusis for compound hyperopic and mixed astigmatism. *J Cataract Refract Surg.* 2000;26:1123-1136.

24. Gatinel D, Hoang-Xuan T, Azar DT. Determination of corneal asphericity after myopia surgery with the excimer laser: a mathematical model. *Invest Ophthalmol Vis Sci.* 2001;42:1736-1742.
25. Chen CC, Izadshenas A, Rana MAA, Azar DT. Corneal asphericity after hyperopic laser in situ keratomileusis. *J Cataract Refract Surg.* 2002;28:1539-1545.
26. Moreno-Barriuso E, Lloves JM, Marcos S, Navarro R, Llorente L, Barbero S. Ocular aberrations before and after myopic corneal refractive surgery: LASIK-induced changes measured with laser ray tracing. *Invest Ophthalmol Vis Sci.* 2001;42:1396-1403.
27. Oshika T, Miyata K, Tokunaga T, Samejima T, Amano S, Tanaka S, Hirohara Y, Mihashi T, Maeda N, Fujikado T. Higher order wavefront aberrations of cornea and magnitude of refractive correction in laser in situ keratomileusis. *Ophthalmology.* 2002;109:1154-1458.
28. Wang L, Koch DD. Anterior corneal optical aberrations induced by laser in situ keratomileusis for hyperopia. *J Cataract Refract Surg.* 2003;29:1702-1708.
29. Llorente L, Barbero S, Merayo J, Marcos S. Total and corneal optical aberrations induced by laser in situ keratomileusis for hyperopia. *J Refract Surg.* 2004;20:203-216.
30. Maeda N. Wavefront technology in ophthalmology. *Curr Opin Ophthalmol.* 2001;12:294-299.
31. Applegate RA, Marsack JD, Ramos R, Sarver EJ. Interaction between aberrations to improve or reduce visual performance. *J Cataract Refract Surg.* 2003;29:1487-1495.
32. Levy Y, Segal O, Avni I, Zadok D. Ocular higher-order aberrations in eyes with supernormal vision. *Am J Ophthalmol.* 2005;139:225-228.
33. Amesbury EC, Schallhorn SC. Contrast sensitivity and limits of vision. *Int Ophthalmol Clin.* 2003;43:31-42.
34. Joslin CE, Wu SM, McMahon TT, Shahidi M. Higher-order wavefront aberrations in corneal refractive therapy. *Optom Vis Sci.* 2003;80:805-811.
35. Marsack JD, Thibos LN, Applegate RA. Metrics of optical quality derived from wave aberrations predict visual performance. *J Vis.* 2004;4:322-328.
36. Kohnen T, Mahmoud K, Bühren J. Comparison of corneal higher-order aberrations induced by myopic and hyperopic LASIK. *Ophthalmology.* 2005;112:1692-1698.
37. Yoon G, Macrae S, Williams DR, Cox IG. Causes of spherical aberration induced by laser refractive surgery. *J Cataract Refract Surg.* 2005;31:127-135.
38. MacRae S. Excimer ablation design and elliptical transition zones. *J Cataract Refract Surg.* 1999;25:1191-1197.
39. Mrochen M, Kaemmerer M, Mierdel P, Seiler T. Increased higher-order optical aberrations after laser refractive surgery; a problem of subclinical decentration. *J Cataract Refract Surg.* 2001;27:362-369.
40. Brown NP, Korets JF, Bron AJ. The development and maintenance of emmetropia. *Eye.* 1993;13:83-92.
41. Shufelt C, Fraser-Bell S, Ying-Lai M, Torres M, Varma R; Los Angeles Latino Eye Study Group. Refractive error, ocular biometry, and lens opalescence in an adult population: the Los Angeles Latino Eye Study. *Invest Ophthalmol Vis Sci.* 2005;46:4450-4460.
42. Qazi MA, Roberts CJ, Mahmoud AM, Pepose JS. Topographic and biomechanical differences between hyperopic and myopic laser in situ keratomileusis. *J Cataract Refract Surg.* 2005;31:48-60.
43. Hieda O, Kinoshita S. Measuring of ocular wavefront aberration in large pupils using OPD-scan. *Semin Ophthalmol.* 2003;18:35-40.
44. Rozema JJ, Van Dyck DEM, Tassignon MJ. Clinical comparison of 6 aberrometers. Part 2. Statistical comparison in a test group. *J Cataract Refract Surg.* 2006;32:33-44.
45. Wang L, Koch DD. Ocular higher-order aberrations in individuals screened for refractive surgery. *J Cataract Refract Surg.* 2003;29:1896-1903.
46. Wang Y, Zhao K, Jin Y, Niu Y, Zuo T. Changes of higher order aberration with various pupil sizes in the myopic eye. *J Refract Surg.* 2003;19:S270-S274.
47. El-Agha MSH, Bowman RW, Cavanagh D, McCulley JP. Comparison of photorefractive keratectomy and laser in situ keratomileusis for the treatment of compound hyperopic astigmatism. *J Cataract Refract Surg.* 2003;29:900-907.
48. Zadok D, Raifkup F, Landau D, Frucht-Pery J. Long-term evaluation of hyperopic laser in situ keratomileusis. *J Cataract Refract Surg.* 2003;29:2181-2188.

LASIK Using the NIDEK EC-5000 for the Correction of Hyperopic Astigmatism

Mahmoud M. Ismail, MD, PhD

ABSTRACT

PURPOSE: To assess the refractive outcomes of LASIK for the surgical correction of hyperopic astigmatism using the NIDEK EC-5000 excimer laser.

METHODS: LASIK was performed on 46 eyes from 26 patients (19 men and 7 women) for the correction of congenital hyperopic astigmatism. The NIDEK EC-5000 excimer laser and the Moria M2 microkeratome were used in all procedures. Cylindrical ablations were performed on the negative axis out to a 6-mm diameter.

RESULTS: The mean preoperative cylindrical refraction was +3.15±0.70 diopters (D) (range: +1.75 to +4.50 D), and the mean 24-month postoperative refraction was +1.27±0.78 D (range: +0.50 to +3.25 D). Vector analysis showed a 2.17±1.27 D reduction in the equivalent cylinder. Preoperative mean uncorrected visual acuity (UCVA) was 20/100, and 24-month postoperative UCVA was 20/30. One eye lost one line of best spectacle-corrected visual acuity at 24 months postoperatively. Complications related to the LASIK flap occurred in 2 (4.3%) eyes. Partial regression of the astigmatic effect began at 4 to 6 months but stabilized by 1 year.

CONCLUSIONS: LASIK is a safe but limited alternative for the correction of astigmatism in eyes with hyperopic astigmatism. Early regression of the astigmatic effect in the first 6 months seems to be the primary disadvantage of this technique. [*J Refract Surg*. 2006;22:S1069-S1072.]

Astigmatism is the most common refractive defect of the human eye.[1] Since the late 1960s, numerous attempts have been made to correct astigmatism using various types of corneal incisions. However, these corneal incisions were effective only for mixed and myopic astigmatism. In the early 1990s, holmium laser thermal keratoplasty was proposed for the correction of hyperopic astigmatism.[2] Thermal keratoplasty was a relatively easy and safe technique; however, partial or often total regression was observed in at least 60% of eyes treated.[2-4]

The introduction of excimer laser technology offers a new alternative for the correction of refractive errors. The ultraviolet rays emitted by the excimer laser are capable of intrastromal ablation during LASIK. Excimer laser ablation modifies the curvature of the corneal surface, changing its refractive power to correct for the refractive error of the eye. Studies have shown LASIK to be a relatively safe and precise surgical technique for the correction of low to moderate myopia up to −12.00 diopters (D).[5-7] Encouraging results using LASIK for the correction of low hyperopia up to +3.00 D have also been reported[8]; however, few studies have reported the outcomes of LASIK for the correction of hyperopic astigmatism.[8-11]

This study presents the refractive outcomes of LASIK for the treatment of primary hyperopic astigmatism using the NIDEK EC-5000 excimer laser (NIDEK Co Ltd, Gamagori, Japan).

PATIENTS AND METHODS

LASIK was performed on 46 consecutive eyes from 26 patients (19 men and 7 women) for hyperopic astigmatism. The NIDEK EC-5000 excimer laser was used in all procedures. Average patient age was 29.9±7.9 years (range: 18 to 47 years). The preoperative mean cylindrical refractive error was +3.15±0.70 D (range: +1.75 to +4.50 D). The preoperative mean spherical equivalent refraction was +1.15±0.27 D (range: +0.50 to +1.75 D). The mean preoperative uncorrected visual acuity (UCVA) was 20/100±1 (range: 20/200 to

From the University of Al-Azhar, El Magrabi Eye Hospital, Cairo, Egypt.

The author has no financial interest in the materials presented herein.

Correspondence: Mahmoud M. Ismail, MD, PhD, PO Box 2, 11811 Cairo, Egypt. E-mail: mahmoud.ismail@magrabi.com

20/30). The mean preoperative best spectacle-corrected visual acuity (BSCVA) was 20/25±1 (range: 20/50 to 20/20). The mean preoperative keratometry reading was 40.28±2.37 for K_1 and 43.39±1.8 for K_2.

Patient Selection Criteria and Examination

Inclusion criteria were age ⩾18 years, a stable refraction for 2 years (defined as a change <0.50 D manifest refraction spherical equivalent in the operative eye for a minimum of 24 months before surgery), and BSCVA of ⩾20/50. Contact lens use had to be discontinued for at least 2 weeks before surgery regardless of contact lens type. Patients were excluded from the study if they had corneal disease, irregular astigmatism, leukoma, previous ocular surgery, or any ocular or systemic diseases, such as a collagen vascular disease or dry eye syndrome, that would interfere with corneal wound healing.

Preoperatively, a complete ocular examination was performed that included UCVA measurement, BSCVA measurement, manifest refraction, cycloplegic refraction, pachymetry, keratometry, videokeratography (Tomey 3.3, Phoenix, Ariz), slit-lamp examination, and a dilated fundus examination. Postoperatively, measurements of UCVA, BSCVA, manifest and cycloplegic refractions, slit-lamp examination, and corneal topography were obtained at 1, 3, 6, 12, 24, and 36 months. Corneal haze, epithelial ingrowth, or flap-related complications were noted at each postoperative visit.

Surgical Procedure

The NIDEK EC-5000 excimer laser system was used in this study. The laser ablation was performed according to the manufacturer's instructions using software for hyperopic astigmatism treatment. Cylindrical ablation was performed on the negative axis of the astigmatism out to a 6-mm diameter, and the hyperopic component was treated out to an 8.5-mm diameter. All procedures were performed by an experienced LASIK surgeon (M.M.I.).

The eyes were prepared for surgery using sterile technique. Topical anesthetic (tetracaine chlorhydrate 0.1%; Laboratory Cusi, Barcelona, Spain) was instilled every 10 minutes for 30 minutes before flap creation. A lid speculum was inserted to allow adequate exposure for placement of the microkeratome. The peripheral cornea was indicated with two pararadial gentian violet marks. The suction ring was centered on the limbus, and the intraocular pressure was verified to be >65 mmHg with a Barraquer tonometer.

The cornea was copiously irrigated before creation of a 160-µm thick corneal flap cut. All flaps were created using the M2 microkeratome (Moria, Antony, France). The flap was reflected back to expose the stromal bed, and the laser was programmed to deliver the astigmatic ablation prior to the spherical ablation. Proper alignment of the eye with the laser was achieved by aligning the microscope cross-hairs and first Purkinje image of the red helium-neon beam in conjunction with cooperative patient fixation. The patient fixation light was coaxial with the surgeon's line of vision and the excimer laser beam. The astigmatic laser ablation was delivered to the cornea using an energy fluence of 160 mJ/cm^2 and 50 Hz frequency. Following ablation, the hinged flap was reflected back onto the stroma using a 23-gauge cannula, and the interface was irrigated using balanced salt solution to remove any debris or epithelial cells. The flap was correctly aligned according to the pararadial gentian violet marks. The keratectomy incision was dried with surgical sponges, and the flap was checked for adhesion by observing the patient blinking through the microscope oculars. The eye was not patched postoperatively.

Postoperatively, patients used topical antibiotic eye drops (Tobrex; Alcon Laboratories, Ft Worth, Tex) four times a day for 6 days. From the second postoperative day, patients began topical treatment with fluorometholone 0.25% (FML Forte; Allergan, Irvine, Calif) four times a day for 1 week, tapering the dose to 1 drop a day for the following 4 weeks.

Data Analysis

Refractive outcomes were analyzed using MS Excel software (Microsoft Corp, Redmond, Wash). Statistical analysis was performed using SAS software (SAS Institute, Cary, NC) and a simple *t* test. A *P* value <0.5 was considered statistically significant.

RESULTS

All patients were followed for at least 24 months postoperatively. Mean preoperative spherical equivalent refraction was +1.35±0.23 D (range: +0.50 to +2.25 D), whereas the mean spherical equivalent refraction at 24 months was 0.63±0.35 D (range: +0.25 to +0.75 D). Preoperative mean cylindrical refraction was +3.15±0.70 D (range: +1.75 to +4.50 D). Residual manifest cylindrical refraction was +0.52±0.38 D at 15 days, +0.78±0.39 D at 1 month, +0.95±0.28 D at 3 months, +1.10±0.20 D at 6 months, +1.12±0.83 D (range: +0.50 to +3.25 D) at 12 months, and +1.27±0.78 D (range: +0.50 to +3.25 D) at 24 months. Vector analysis showed a 2.17±1.27 D change in the equivalent cylinder at 24 months. Postoperatively, the axis of the residual cylinder was within 5° of the preoperative astigmatic axis in all eyes.

The mean preoperative keratometry reading was

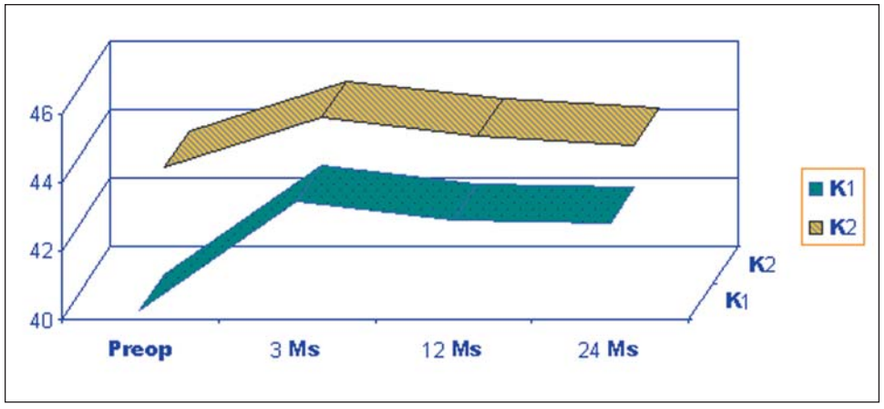

Figure 1. Keratometry of both meridians before and 24 months after LASIK for hyperopic astigmatism.

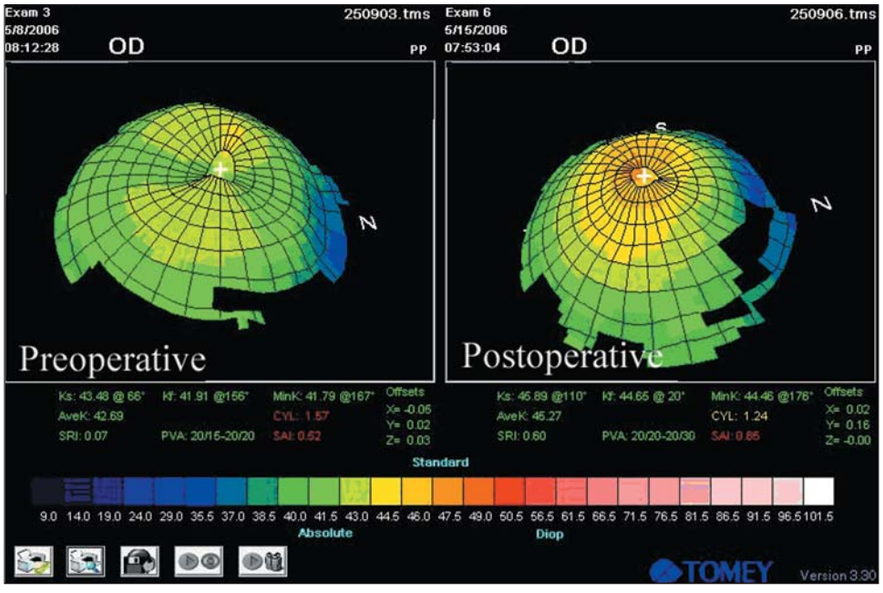

Figure 2. Sample pre- and postoperative corneal topography of a hyperopic eye that underwent LASIK correction.

40.28±2.37 D for K_1 and 43.39±1.80 D for K_2 (range: 39.50 to 45.00 D). At 3 months postoperatively, it was 43.43/44.82 D (K_1/K_2), and at 12 months, it was 42.90/44.30 D, respectively. After 24 months, the mean K_1 reading was 42.80±2.20 D and the mean K_2 reading was 44.09±1.70 D (range: 41.50 to 46.50 D), which was significantly different from the preoperative K readings ($P<.001$) (Fig 1).

Preoperative UCVA showed an average of 20/100±1 (range: 20/200 to 20/40), whereas the preoperative BSCVA was 20/25±1 (range: 20/50 to 20/20). Two years after surgery, the mean UCVA was 20/30±1 Snellen line and the mean postoperative BSCVA was 20/25±1 Snellen line. Comparing the preoperative BSCVA with the 24-month BSCVA, 24 (52.2%) eyes reached preoperative BSCVA levels, 8 (17.4%) eyes gained one or more lines of vision, and 1 (2.2%) eye lost one line of BSCVA. Corneal topography analysis showed no induced irregular astigmatism; sample corneal topographies are shown in Figure 2. Corneal topographic analysis revealed three cases of clinically insignificant decentration (<1 mm from the optical zone). These decentered eyes were not symptomatic; however, one of these eyes lost one line of BSCVA compared with preoperative measures. Flap-related complications occurred in 2 (4.3%) eyes: one case of flap striae and one case of epithelial ingrowth, both requiring surgical intervention, were resolved without sequelae. One year after the LASIK procedure, no astigmatic regression was evident in any of the eyes.

DISCUSSION

LASIK is a rapidly evolving technique for the correction of myopia, myopic astigmatism, and hyperopia. Different investigators have reported their outcomes using LASIK, confirming that it is a reliable, predictable, and potentially safe refractive surgical procedure. However, 2% to 7% of treated eyes can still present

with some complications related to flap creation and laser ablation. In addition, there are reported limitations when attempting treatment of irregular astigmatism and hyperopic astigmatism.[8-11]

The ablation profile used in the correction of hyperopic astigmatism reshapes the cornea by direct flattening of the steep meridian or through an oval paracentral ablation of the flat meridian, countering the effect of the spherical error. Few studies have been reported for the treatment of hyperopic astigmatism with the excimer laser. A preliminary 6-month study was published by Lindstrom et al[8] using the Visx STAR S2 algorithm (Visx Technologies, San Diego, Calif) ablating the steep meridian first.

The results were promising; however, the follow-up was not adequate to determine the effect of regression of the procedure.[8] Barraquer and Gutierrez[9] and Arbelaez and Knorz[10] reported better results for hyperopia up to +5.00 D and hyperopic astigmatism up to +3.00 D by ablating the flat meridian with a laser (Keracor 117; Bausch & Lomb, Rochester, NY) equipped with an eye tracker. However, a significant number of eyes treated for high hyperopia and hyperopic astigmatism experienced loss of BSCVA.[9,10] Ablating the steep meridian, Vinciguerra et al[11] reported significantly better refractive outcomes following a modification of the hyperopic astigmatism algorithm for the NIDEK EC-5000 excimer laser. However, Azar and Primack[12] conducted a similar study and found that two (4.1%) eyes lost two lines of BSCVA. Zaldivar et al[13] recommended a series of surgical refinements to enhance outcomes. Kanellopoulos et al[14] also found limitations to hyperopic astigmatic LASIK using the WaveLight excimer laser (WaveLight Technologies, Erlangen, Germany) and modified their technique to improve the surgical outcomes.

In the current study, the results obtained from the correction of 46 eyes with regular hyperopic astigmatism are presented. Statistically significant differences between pre- and postoperative refraction, keratometry, and visual acuity ($P<.001$) were obtained. Residual cylinder 6 months after surgery was $+1.10\pm0.20$ D and 24 months after surgery was $+1.27\pm0.78$ D, indicating relative stability of astigmatic cylinder regression after the first year. By 24 months after surgery, the study eyes achieved a mean UCVA of 20/30, in comparison to UCVA of 20/100 in the preoperative period. In 38 (82.6%) of the operated eyes, UCVA equal to or greater than that seen preoperatively with correction was obtained. Regarding complications, 2 (4.3%) eyes experienced flap complications requiring additional intervention. No significant decentered ablations (>1 mm from the optical zone) or overcorrections occurred in this series. In one eye, a patient lost one line of preoperative BSCVA.

In conclusion, the visual and refractive outcomes presented indicate that hyperopic astigmatic treatment with the NIDEK EC-5000 excimer laser system is reliable, safe, and relatively predictable but may result in some regression of effect in the first 6 months after surgery.

REFERENCES

1. Barraquer JI. Conducta de la cornea frente a los cambios de espesor (contribucion a la cirugia refractiva). *Arch Soc Am Oftalmol Optom.* 1964;5:81-87.
2. Alio JL, Ismail MM, Sanchez Pego J. Correction of hyperopia 15 months after non-contact holmium laser thermal keratoplasty. *J Refract Surg.* 1997;81:541-543.
3. Ismail MM, Pérez-Santonja JJ, Alio JL. Correction of hyperopia and hyperopic astigmatism by laser thermokeratoplasty. In: Serdarevic O, ed. *Refractive Surgery: Current Techniques and Management.* Tokyo, Japan: IGAKU-SHOIN Medical Publishers; 1996:263-274.
4. Nano HD, Muzzin S. Noncontact holmium:Yag laser thermal keratoplasty for hyperopia. *J Cataract Refract Surg.* 1998;24:751-757.
5. Arbelaez MC, Pérez-Santonja JJ, Ismail MM, et al. Automated lamellar keratoplasty (ALK) and laser in situ keratomileusis (LASIK). In: Serdarevic O, ed. *Refractive Surgery: Current Techniques and Management.* Tokyo, Japan: IGAKU-SHOIN Medical Publishers; 1996:131-150.
6. Ismail MM. Management of overcorrections following LASIK. In: Machat JJ, Slade SG, Probst LE, eds. *The Art of LASIK.* 2nd ed. Thorofare, NJ: SLACK Incorporated; 1998:451-457.
7. Pérez-Santonja JJ, Bellot J, Claramonte P, Ismail MM, Alio JL. Laser in situ keratomileusis to correct high myopia. *J Cataract Refract Surg.* 1997;23:372-385.
8. Lindstrom RL, Hardten DR, Houtman DM, Witte B, Preschet N, Chu YR, Samulson TW, Linebarger EJ. Six-month results of hyperopic and astigmatic LASIK in eyes with primary and secondary hyperopia. *Trans Am Ophthalmol Soc.* 1999;97:241-255.
9. Barraquer C, Gutierrez MA. Results of laser in situ keratomileusis in hyperopic compound astigmatism. *J Cataract Refract Surg.* 1999;9:1198.
10. Arbelaez MC, Knorz M. Laser in situ keratomileusis for hyperopia and hyperopic astigmatism. *J Cataract Refract Surg.* 1999;4:406-414.
11. Vinciguerra P, Epstein D, Azzolini M, Radice P, Sborgia M. Algorithm to correct hyperopic astigmatism with the NIDEK EC-5000 excimer laser. *J Cataract Refract Surg.* 1999;15:S186-S187.
12. Azar DT, Primack JD. Theoretical analysis of ablation depths and profiles in laser in situ keratomileusis for compound hyperopic and mixed astigmatism. *J Cataract Refract Surg.* 2000;26:1123-1136.
13. Zaldivar R, Oscherow S, Bains HS. Five techniques for improving outcomes of hyperopic LASIK. *J Refract Surg.* 2005;21:S628-S632.
14. Kanellopoulos AJ, Conway J, Pe LH. LASIK for hyperopia with the WaveLight excimer laser. *J Refract Surg.* 2006;22:43-47.

Correction of High Astigmatism: Case Studies Using the Mixed-cylinder Approach

Hamza N. Khan, MD, MPH, FRCSC; Geoffrey B. Kaye, MBChB, FCS(SA), FRCSC; Jean Luc Febbraro, MD

ABSTRACT

PURPOSE: To explain the use of the mixed-cylinder approach in treating moderate to high astigmatism with the NIDEK EC-5000 excimer laser system.

METHODS: Retrospective case series report.

RESULTS: Three patients with bilateral moderate to high astigmatism were treated successfully using the mixed cylinder approach.

CONCLUSIONS: The use of the mixed-cylinder approach with the NIDEK EC-5000 excimer laser may be a safe and predictable option for treating moderate to high astigmatism. [*J Refract Surg*. 2006;22:S1073-S1078.]

The treatment of astigmatism >3.00 diopters (D) in the corneal plane has been a challenge compared with similar magnitudes of spherical correction. Excimer laser correction of astigmatism using surface ablation has a tendency to produce greater haze and regression compared with similar degrees of spherical correction.[1,2] Even with LASIK, some undercorrection and regression is seen.[1,3] Results of limbal relaxing incisions are variable and do not demonstrate sufficient efficacy beyond 2.50 D.[4] Astigmatic keratotomy, although effective, can be associated with irregular astigmatism when using smaller optical zones.[5]

The pitfalls associated with treating high degrees of astigmatism can be resolved primarily by using a mixed hyperopic and myopic approach during LASIK or photorefractive keratectomy (PRK). The desired outcome is to steepen the flat meridian and flatten the steep meridian by equal amounts. This produces a spherical corneal profile.[6] Any residual spherical refractive error is treated concurrently. By treating half the cylinder in the steep meridian and half in the flat meridian, the edge profile and effective optical zone are improved. In turn, this has the effect of producing a more stable result with less haze and regression.[7-10] This technique has been described as cross-cylinder or mixed hyperopic and myopic astigmatism correction. The advantage of this approach, particularly in lasers that apply a cylindrical pattern to treat myopic astigmatism, is to reduce the sharp edge profile seen with the ablation in only one meridian. An increase is seen in the effective optical zone compared to results with laser systems that use an elliptical pattern, particularly where the minor axis diameter is not fixed. A tendency toward more stable and rapid visual rehabilitation has been reported.[10]

This report presents three patient studies to highlight the mixed astigmatism method of correcting higher degrees of cylinder and reducing the problems of haze, treatment vari-

From the University of Alberta and the University of British Columbia, British Columbia, Canada (Khan); Gimbel Eye Center, Edmonton, Alberta, Canada (Kaye); and Paris, France (Febbraro).

The authors have no financial interest in the materials presented herein.

Correspondence: Hamza N. Khan, MD, MPH, FRCSC, 400 1120 Yates St, Victoria BC, Canada. Tel: 250.382.3937; Fax: 250.382.3938; E-mail: khan@post.harvard.edu

ability, and regression. In addition, we highlight the apparent reduction of subjective complaints of halos and glare, which may be indicative of a larger functional optical zone.

PATIENTS AND METHODS

Three case studies are used to describe the technique. Specific individual calculations and results are reported along with topographic studies. The sample is a series from the authors' experience and is considered representative of the typical outcomes and findings. All patients were treated at the Gimbel Eye Centre (Edmonton, Canada) by the authors (H.N.K. or G.B.K.) and followed for at least 6 months.

PATIENT EXAMINATIONS AND SURGERY

Baseline examination included uncorrected visual acuity (UCVA), best spectacle-corrected visual acuity (BSCVA), manual keratometry, manifest and cycloplegic refractions, slit-lamp and fundus examinations, Schirmer's test, scotopic pupil assessment, corneal pachymetry, corneal topography (Orbscan; Bausch & Lomb, Rochester, NY), and an epithelial stress test. The epithelial stress test has been reported previously to identify patients at increased risk for epithelial complications during flap creation.[11]

A corneal flap at least 9.0 mm in diameter and 160 or 180 µm in thickness was created with the Hansatome microkeratome (Bausch & Lomb). A NIDEK EC-5000 excimer laser (NIDEK Co Ltd, Gamagori, Japan) with a 40-Hz repetition rate was used to carry out the corneal ablation. At the surgeon's discretion, phototherapeutic keratectomy (PTK) was performed using a viscous masking agent (Laservis; TRB Chemedica, Vouvry, Switzerland) to smooth the surface after the refractive ablation.[12] Postoperative examinations were performed at 1 day, 1 week, and 1, 3, and 6 months. Postoperative examinations included UCVA, BSCVA, manifest refraction, corneal topography, and slit-lamp and fundus examinations. Patients were specifically asked about visual performance and subjective symptoms such as halos at the 1-, 3-, and 6-month postoperative examinations.

NOMOGRAM CALCULATIONS

In this technique, the spherical component of the refractive correction is determined by 1) the spherical equivalent, 2) the PTK effect (hyperopic shift) of the cylindrical treatment, and 3) nomogram adjustment for attempted versus achieved ablation. This last variable depends on patient age and a number of site- and surgeon-specific factors including altitude, humidity, temperature, surgical technique, and specific laser used. The Gimbel nomogram with minor modification was used in this case series.[13] The astigmatic component is determined from the keratometric, manifest, or cycloplegic cylinder. In this study, manifest refraction was used to primarily determine axis and power to be treated. In some cases, an adjustment was made in the axis of treatment based on topography and keratometry.

The calculations to determine laser parameters were:

1. Calculate the spherical equivalent of refraction. This amount, after adjustment for PTK effect and attempted versus achieved ratio, is used in the final laser spherical parameter.
2. Determine the PTK effect of the total astigmatism treatment. Total cylinder × 35% in our nomogram is the expected effect. This produces a hyperopic shift in refraction; therefore, it is added to the sphere.
3. Apply spherical treatment adjustment. Attempted/achieved ratio in our nomogram varies from 70% in patients aged >55 years to 80% in patients aged <30 years.
4. Divide the astigmatism by 2, and write hyperopic (plus) and myopic (minus) components separately. Care must be taken to correctly identify each meridian.
5. Write laser treatment stages:
   a) Hyperopic cylinder with 5.5- to 9.0-mm zone.
   b) Myopic cylinder with 6.5- to 7.5-mm zone.
   —Patients with >2.00 D of myopic cylinder are corrected with this component further divided by 2, and half the cylinder treated at a 6.0-mm optical zone and half at a 6.5-mm optical zone.
   c) Nomogram-adjusted spherical refractive error.
6. For smoothing, four scans of PTK are placed at an 8.0-mm optical zone, using Laservis as a masking agent, prior to replacing the flap in LASIK, or placing a contact lens in PRK.

STEP-BY-STEP NOMOGRAM CALCULATION

Calculations for Mixed Astigmatism Correction

1. Identify desired refractive correction (power and axis) including spherical component.
2. Note spherical equivalent of the refractive error.
3. Calculate the hyperopic shift of total astigmatic correction (PTK effect of central tissue ablation); in this case, 35% of total cylinder.
4. Determine arithmetic sum of the spherical equivalent refraction and hyperopic shift from step 3.
5. Apply nomogram adjustment to spherical correction (varies).
6. Split cylinder into two and write as hyperopic (plus) and myopic (minus) components separately.
7. Note the laser treatment parameters.
   a) Hyperopic cylinder treated at a 5.5- to 9.0-mm zone.
   b) Myopic cylinder treated at a 6.5- to 7.5-mm zone.

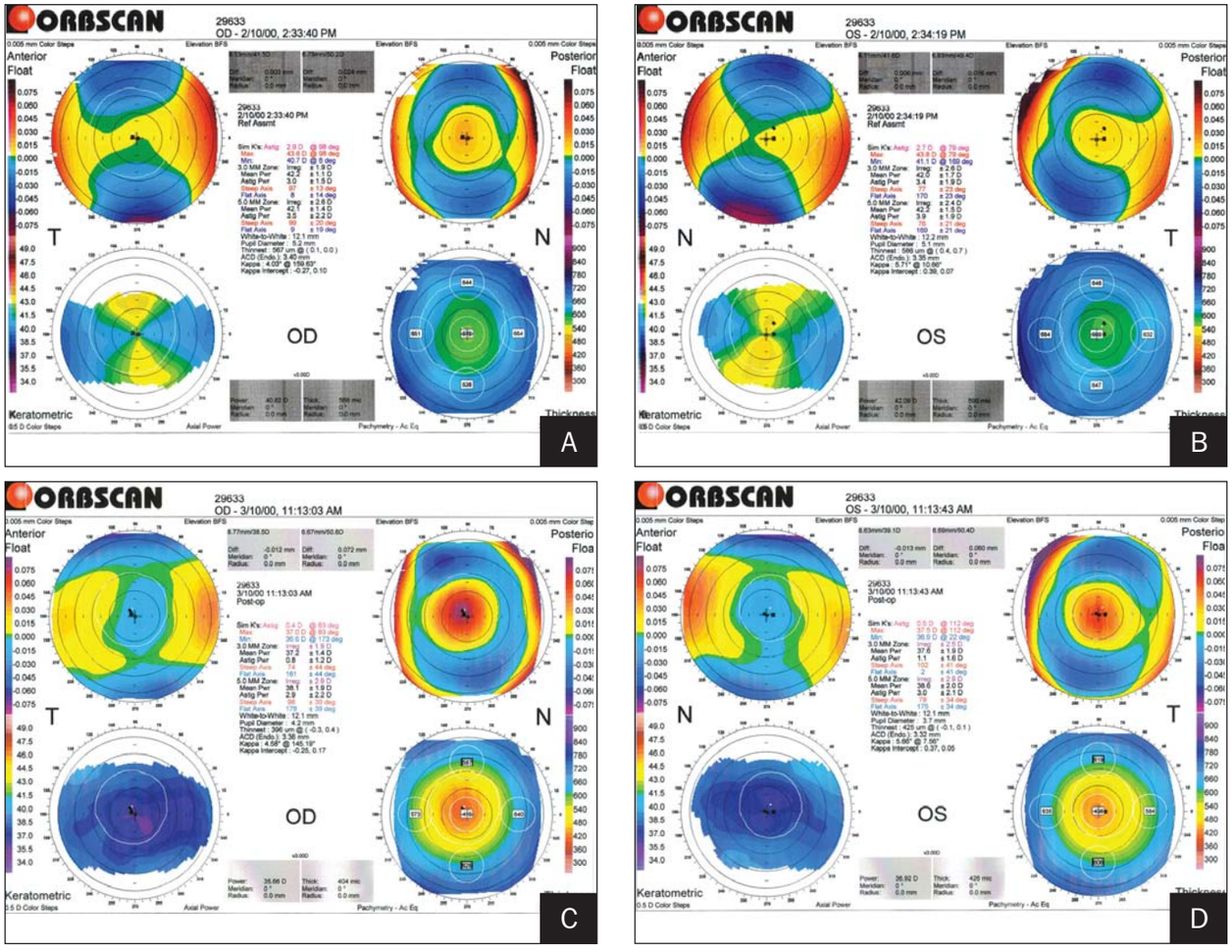

Figure 1. *Case 1.* Preoperative corneal topography of the **A)** right and **B)** left eyes showing significant symmetrical with-the-rule astigmatism. Postoperative corneal topography of the **C)** right and **D)** left eyes.

c) If myopic cylinder is >2.00 D, treat half of this amount at a smaller zone of 6.0- to 7.0-mm to conserve corneal tissue along with half at the zone in step 7(b).
d) Residual nomogram-adjusted sphere treatment.

8. A smoothing treatment can be applied with a few pulses in PTK mode at an 8.0-mm zone using Laservis as a masking agent.

Note: Adequate stromal bed tissue should remain after the ablation to ensure tectonic integrity of the cornea. In patients with large pupils, the myopic transition zone can be expanded to 8.0 mm.

RESULTS

CASE 1

A 34-year-old man presented with manifest refraction of -5.50 $-4.00 \times 10°$ ($20/20^{-1}$) in the right eye and -4.75 $-3.50 \times 165°$ ($20/20^{-1}$) in the left eye. Manual keratometry was 40.75/43.75 in the right eye and 40.75/43.50 in the left eye. Preoperative corneal topography is shown in Figures 1A and 1B.

LASIK was performed in both eyes using the nomogram outlined above without PTK smoothing.

Six months postoperatively UCVA was 20/15 in the right eye and 20/40 in the left eye. Manifest refraction was plano in the right eye and $+0.50$ $-1.50 \times 60°$ (20/25) in the left eye.

Postoperative corneal topography is shown in Figures 1C and 1D. A reduction of one line of BSCVA in the nondominant eye occurred, which was well tolerated. The patient was pleased with the outcome. Subjectively, the patient noted dry eye symptoms, which resolved by 6-month follow-up.

CASE 2

A 51-year-old man presented with manifest refraction of -2.00 $-4.50 \times 12°$ ($20/20^{+2}$) in the right eye and -2.00 $-5.50 \times 180°$ ($20/20^{-1}$) in the left eye. Manual

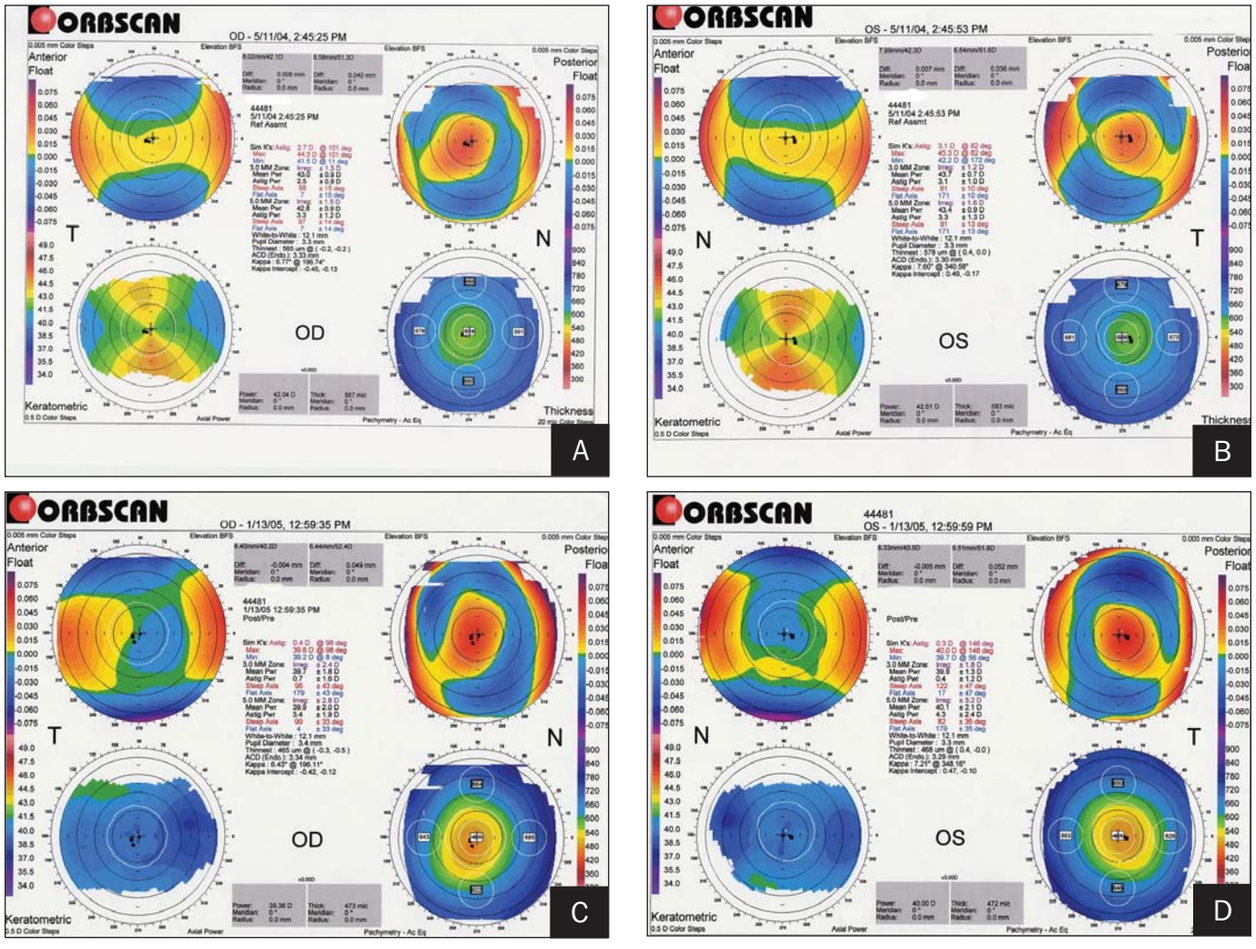

Figure 2. *Case 2.* Preoperative corneal topography of the **A)** right and **B)** left eyes showing significant symmetrical with-the-rule astigmatism. Postoperative corneal topography of the **C)** right and **D)** left eyes.

keratometry was 42.0/45.0 × 96° in the right eye and 42.25/45.37 × 79° in the left eye. Corneal topography is shown in Figures 2A and 2B.

LASIK was performed in both eyes using the nomogram outlined above with PTK smoothing.

The spherical component of the treatment nomogram was adjusted to −2.06 D in the right eye and −2.17 D in the left eye. Based on the planned astigmatic correction of 4.25 D in the right eye and 5.25 D in the left eye, the refractive treatment was divided into three components. In the right eye, plano +2.13 × 100° was treated with a 5.5-mm optical zone and a 9.0-mm transition zone; −2.06 −1.06 × 10° was treated with a 6.5-mm optical zone and a 7.5-mm transition zone; and plano −1.06 × 10° was treated with a 6.0-mm optical zone and a 7.0-mm transition zone. In the left eye, plano +2.63 × 85° was treated with a 5.5-mm optical zone and a 9.0-mm transition zone; −2.17 −1.31 × 175° was treated with a 6.5-mm optical zone and a 7.5-mm transition zone; and plano −1.31 × 175° was treated with a 6.0-mm optical zone and a 7.0-mm transition zone.

At 7 months postoperatively, UCVA was $20/25^{-2}$ in the right eye and 20/15 in the left eye. Manifest refraction was +1.25 sphere (20/20) in the right eye and +0.50 −0.50 × 180° (20/15) in the left eye.

Postoperative topography is shown in Figures 2C and 2D. The patient underwent enhancement for residual hyperopia in the right eye.

Case 3

A 44-year-old man presented with manifest refraction of −4.75 −4.50 × 2° in the right eye and −4.75 −6.00 × 164° in the left eye. Manual keratometry was 42/45 × 95° in the right eye and 42/45.5 × 80° in the left eye. Preoperative corneal topography is shown in Figures 3A and 3B.

LASIK was performed in both eyes using the nomogram outlined above with PTK smoothing.

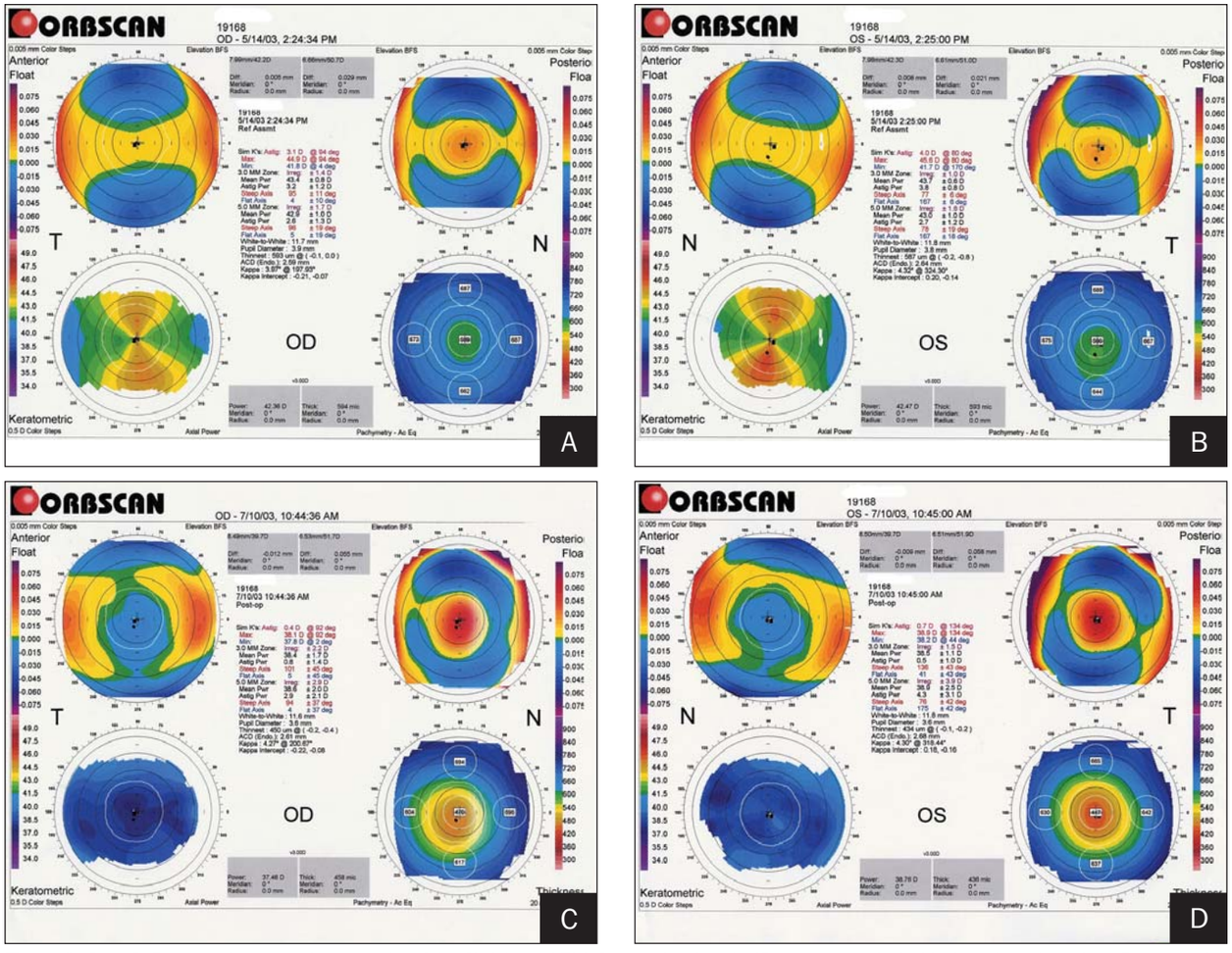

Figure 3. *Case 3.* Preoperative corneal topography of the **A)** right and **B)** left eyes showing significant symmetrical with-the-rule astigmatism. Postoperative corneal topography of the **C)** right and **D)** left eyes showing a significant reduction of astigmatism, with a well-centered, flatter optical zone.

The spherical component of the treatment nomogram was adjusted to −4.09 D in the right eye and −4.24 D in the left eye. Based on planned astigmatic correction of 4.25 D and 5.75 D in the right and left eyes, respectively, treatment was divided into three components. In the right eye, plano +2.25 × 91° was treated with a 5.5-mm optical zone and a 9.0-mm transition zone; −4.09 −1.13 × 1° was treated with a 6.5-mm optical zone and a 7.5-mm transition zone; and plano −1.13 × 1° was treated with a 6.0-mm optical zone and a 7.0-mm transition zone. In the left eye, plano +2.88 × 76° was treated with a 5.5-mm optical zone and a 9.0-mm transition zone; −4.24 −1.44 × 166° was treated with a 6.5-mm optical zone and a 7.5-mm transition zone; and plano −1.44 × 166° was treated with a 6.0-mm optical zone and a 7.0-mm transition zone.

At 8 months postoperatively, UCVA was 20/25 in the right eye and 20/30 in the left eye. Manifest refraction was plano −0.50 × 175° (20/20) in the right eye and −1.00 −0.25 × 25° (20/20) in the left eye.

Postoperative corneal topography is shown in Figures 3C and 3D. The patient was pleased with the monovision result, and no further treatment was performed.

DISCUSSION

Previous studies have shown a reduced level of efficacy compared with spherical treatments in patients with high degrees of astigmatism.[6,14,15] This reduced level of efficiency is based on the loss of a physiologic surface profile that results from ablation in a single meridian. In PRK, this can lead to increased haze and regression of clinical effect. In LASIK, there is a delay in refractive stability, followed by mild regression. In both cases, there is a tendency toward undercorrection.

To produce a better ablation profile, the astigmatic correction can be applied to both meridians. The effect

is to ablate a cylindrical profile in the steeper meridian to flatten it. A midperipheral ablation in the flat meridian causes the flat meridian to steepen. Optically, this combination leads to a nearly spherical cornea.

Using a combined hyperopic and myopic cylinder correction, high astigmatic refractive errors can be corrected predictably with stable results. The goal of reducing optical aberrations from a small optical zone is addressed using this method of treatment. In addition, the rapid visual rehabilitation of these patients, along with refractive stability, suggests a better corneal surface profile. Over time this has become our standard approach for all patients with >1.50 D of astigmatism. Studies to evaluate spherical, coma, trefoil, and other higher order aberrations are required to determine whether the eye has an optimal pattern. Benefit in terms of improved low contrast acuity and subjective outcomes remains to be determined.

In addition to the corneal flattening resulting from the treatment of the original spherical refractive error (spherical equivalent), some overall flattening of the cornea occurs due to central ablation of tissue or PTK effect. This is analogous to coupling that is seen in astigmatic keratotomy. However, this coupling is not a 1:1 ratio and does not operate in the same direction as seen in astigmatic keratotomy. In our nomogram, a rate of 35% is used as a hyperopic shift from total cylinder correction. This shift is then added to the spherical correction to reduce myopia (or increase hyperopia). Phototherapeutic keratectomy smoothing was added as final step because of its reported benefits. Vinciguerra et al[16,17] have shown in two separate studies that PTK smoothing leads to better surface quality and reduced haze. Four scans of PTK, in conjunction with a masking agent, do not produce any observable refractive effect in our experience.

We have demonstrated the steps in performing the calculation of mixed astigmatism correction for high degrees of astigmatism and reviewed case studies. Further determination of efficacy, stability, and safety requires long-term cohort studies. Evaluation is needed in a prospective cohort study of astigmatic effect using vector analysis and patient outcome measures of contrast acuity, quality of vision, and patient satisfaction. Treatment of mixed astigmatism with the NIDEK EC-5000 excimer laser using a combination of hyperopic and myopic ablation profiles appears to improve the refractive options available to surgeons and their patients.

REFERENCES

1. Van Gelder RN, Steger-May K, Yang SH, Rattanatam T, Pepose JS. Comparison of photorefractive keratectomy, astigmatic PRK, laser in situ keratomileusis, and astigmatic LASIK in the treatment of myopia. *J Cataract Refract Surg.* 2002;28:462-476.
2. Pop M, Aras M. Photorefractive keratectomy retreatments for regression. One-year follow-up. *Ophthalmology.* 1996;103:1979-1984.
3. Condon PI, Mulhern M, Fulcher T, Foley-Nolan A, O'Keefe M. Laser intrastromal keratomileusis for high myopia and myopic astigmatism. *Br J Ophthalmol.* 1997;81:199-206.
4. Budak K, Friedman NJ, Koch DD. Limbal relaxing incisions with cataract surgery. *J Cataract Refract Surg.* 1998;24:503-508.
5. McDonnell PJ, Caroline PJ, Salz J. Irregular astigmatism after radial and astigmatic keratotomy. *Am J Ophthalmol.* 1989;15;107:42-46.
6. Vinciguerra P, Camesasca FI. Mixed astigmatism: theory and technique. *Int Ophthalmol Clin.* 2002;42:31-40.
7. Vinciguerra P, Sborgia M, Epstein D, Azzolini M, MacRae S. Photorefractive keratectomy to correct myopic or hyperopic astigmatism with a cross-cylinder ablation. *J Refract Surg.* 1999;15:S183-S185.
8. Hassaballa MA, Ayala MJ, Alio JL. Laser in situ keratomileusis correction of mixed astigmatism by bitoric ablation. *J Cataract Refract Surg.* 2003;29:1889-1895.
9. El-Agha MS, Bowman RW, Cavanagh D, McCulley JP. Comparison of photorefractive keratectomy and laser in situ keratomileusis for the treatment of compound hyperopic astigmatism. *J Cataract Refract Surg.* 2003;29:900-907.
10. Chayet AS, Magallanes R, Montes M, Chavez S, Robledo N. Laser in situ keratomileusis for simple myopic, mixed, and simple hyperopic astigmatism. *J Refract Surg.* 1998;14:S175-S176.
11. Khan HN, Mann GS, Kaye GB. Prospective evaluation of epithelial complications during LASIK: prevention by preoperative assessment. Presented at: American Society of Cataract and Refractive Surgery Annual Meeting; April 28-May 2, 2001; San Diego, Calif.
12. Kremer F, Aronsky M, Bowyer B, Stevens SX. Treatment of corneal surface irregularities using biomask as an adjunct to excimer laser phototherapeutic keratectomy. *Cornea.* 2002;21:28-32.
13. Gimbel HV, Anderson Penno EE. *LASIK Complications: Trends and Techniques.* 3rd ed. Thorofare, NJ: SLACK Incorporated; 2004.
14. Seiler T, Kaemmerer M, Mierdel P, Krinke HE. Ocular optical aberrations after photorefractive keratectomy for myopia and myopic astigmatism. *Arch Ophthalmol.* 2000;118:17-21.
15. Nagy ZZ, Munkacsy G, Popper M. Photorefractive keratectomy using the Meditec MEL 70 G-scan laser for hyperopia and hyperopic astigmatism. *J Refract Surg.* 2002;18:542-550.
16. Vinciguerra P, Azzolini M, Airaghi P, Radice P, De Molfetta V. Effect of decreasing surface and interface irregularities after photorefractive keratectomy and laser in situ keratomileusis on optical and functional outcomes. *J Refract Surg.* 1998;14:S199-S203.
17. Vinciguerra P, Camesasca FI. Treatment of hyperopia: a new ablation profile to reduce corneal eccentricity. *J Refract Surg.* 2002;18:S315-S317.

Corneal Astigmatism, High Order Aberrations, and Optical Quality After Cataract Surgery: Microincision Versus Small Incision

Ke Yao, MD; Xiajing Tang, MD; Panpan Ye, MD

ABSTRACT

PURPOSE: To compare the astigmatism, high order aberrations, and optical quality of the cornea after microincision (~1.7 mm) versus small incision (~3.2 mm) cataract surgery at Eye Center, Zhejiang University, Hangzhou, China.

METHODS: This prospective, randomized clinical study included microincision cataract surgery and small incision cataract surgery performed on 60 eyes. Corneal astigmatism and higher order aberrations to the sixth order were measured using the NIDEK OPD-Scan aberrometer/topographer 1 month after surgery. To evaluate the optical quality of the cornea, the 0.5 modulation transfer function (MTF) value and 0.1 MTF value within a 5-mm pupil were calculated using OPD-Station software. Statistical analysis assessing the difference between groups was carried out using the independent *t* test.

RESULTS: The mean corneal astigmatism was significantly lower after microincision cataract surgery compared with small incision cataract surgery (0.78±0.38 diopters [D] vs 1.29±0.68 D, respectively; P=.001). No significant differences were found between the two groups for the root-mean-square value of total high order aberrations or individual high order aberrations for spherical aberration, coma, and trefoil. However, eyes that underwent microincision cataract surgery showed statistically significantly better optical performance with a 0.5 MTF value than eyes that underwent small incision cataract surgery (3.13±0.30 cycles per degree [cpd] vs 2.75±0.63 cpd, respectively; P=.005). The 0.1 MTF values for the two groups were 9.37±3.72 cpd for microincision cataract surgery and 7.24±3.43 cpd for small incision cataract surgery, which was not significantly different (P=.136).

CONCLUSIONS: Microincision cataract surgery generates statistically significantly less corneal astigmatism and better optical quality of the cornea by MTF evaluation compared with small incision cataract surgery. However, microincision cataract surgery shows no significant advantage in reducing corneal high order aberrations over small incision cataract surgery. [*J Refract Surg*. 2006;22:S1079-S1082.]

The human eye is a complex structure, and each of its elements contributes to visual function. Degraded optical performance of the cornea after incisional cataract surgery would limit the visual quality of the pseudophakic eye. In conventional, coaxial phacoemulsification, or small incision cataract surgery, anterior chamber infusion is supplied through a flexible silicone sleeve surrounding the phaco needle. Typical phaco tips have diameters of approximately 1 mm. Coaxial systems, which are used in traditional small incision cataract surgery, require corneal incisions ranging from 2.5 to 3.2 mm to accommodate infusion sleeves large enough to provide adequate inflow. Although these incisions are smaller compared with those in earlier techniques, they are still large enough to increase corneal astigmatism and induce aberrations that degrade the optical quality of the cornea.[1-3]

The improvements in ultrasound technology, phaco instrumentation, and new intraocular lens (IOL) materials have accompanied the evolution of new surgical techniques, resulting in the development of microincision cataract surgery.[4] Microincision cataract surgery was defined as cataract surgery performed through a <2-mm incision using a bimanual technique. In bimanual microincision cataract surgery, anterior chamber infusion is accomplished with an instrument separate from the phacoemulsification/aspiration unit. Ultrasound power is provided by a sleeveless, bare phaco needle on a standard handpiece with the irrigation port capped. The infusion line is connected to a second instrument, usually a 19- or 20-gauge irrigating chopper, which provides fluid inflow and assists in nuclear manipulation. Each instrument is inserted through clear corneal incisions of approximately 0.9 to 1.5 mm. In addition, the advent of newer IOL technology has made it possible to inject an IOL through an incision >1.5 mm. Advanced microincision cataract surgery may have

From Eye Center, Affiliated Second Hospital, College of Medicine, Zhejiang University, Hangzhou, China.

The authors have no financial interest in the materials presented herein.

Correspondence: Ke Yao, MD, Eye Center, Affiliated Second Hospital, College of Medicine, Zhejiang University, 88 Jiefang Rd, Hangzhou 310009, China. Tel/Fax: 86 571 87783908; E-mail: xlren@zju.edu.cn

TABLE 1

Preoperative Data of 60 Eyes That Underwent Microincision or Small Incision Cataract Surgery

Demographic	Microincision	Small Incision	*P* Value
No. patients (eyes)	30	30	
Age (y)	70.07±10.89	71.20±9.05	.815
ΔSimK (D)	0.70±0.34	0.66±0.38	.669
Corneal power (D)	44.89±1.44	44.32±1.27	.710

Note. *ΔSimK denotes the difference in power between the steep and flat meridians.*

some advantages over coaxial small incision cataract surgery, such as inducing less astigmatism, improving anterior chamber stability, and reducing the incidence of endophthalmitis.

Although the outcomes of microincision cataract surgery have been reported by many authors,[5,6] no studies have evaluated the postoperative corneal properties and optical quality after microincision cataract surgery compared with small incision cataract surgery. This study assesses the potential advantages of microincision cataract surgery over small incision cataract surgery in reducing astigmatism, aberrations, and improving optical quality of the cornea after surgery.

PATIENTS AND METHODS

Sixty eyes from patients scheduled for cataract surgery were randomly assigned to undergo microincision cataract surgery (group 1) or coaxial small incision cataract surgery (group 2). Patient inclusion criterion was the presence of a visually significant cataract. Patient exclusion criteria for the study were a history of ocular surgery including laser surgery, corneal disease, ocular media opacification other than cataract, and retinal disease. All clinical examinations and surgeries were conducted at Eye Center, Affiliated Second Hospital of Zhejiang University, Hangzhou, China. The same surgeon performed all surgeries, and an independent ophthalmologist who did not perform any of the surgeries in this study conducted follow-up. Data from 1-month postoperative follow-up are presented.

SURGICAL TECHNIQUE

Surgery was performed under topical or retrobulbar anesthesia. In microincision cataract surgery, two microincisions, each 1.5-mm long, were created on the superior cornea. One incision was an irrigation channel and the other an aspiration channel. Once the anterior chamber was filled with viscoelastic material, a capsulorrhexis was performed using microincision cataract surgery capsulorrhexis forceps. After hydrodissection, manual prechopping was performed using the microincision cataract surgery prechoppers, followed by low ultrasound phacoemulsification. The residual cortex was eliminated and posterior capsule cleaning performed at the end. Prior to IOL implantation, the capsular bag was filled with viscoelastic material. The IOLs were implanted using an injection system through a 1.6- to 1.8-mm incision.

For small incision cataract surgery, a 3.2-mm clear corneal tunnel incision was created superiorly, and the side puncture was made at the 2-o'clock position. After the capsulorrhexis was completed, hydrodissection, nucleus rotation, and prechopping were performed using a technique similar to that used in group 1. Phacoemulsification was carried out using the "divide-and-conquer" or "stop-and-chop" technique. Finally, the cortex was aspirated with an irrigation/aspiration tip, the IOL implanted, and the viscoelastic removed at the end surgery.

CORNEAL ASTIGMATISM AND OPTICAL QUALITY EVALUATION

Corneal topography, wavefront aberrations, and modulation transfer function (MTF) were measured to evaluate the corneal properties and optical performance after microincision cataract surgery or small incision cataract surgery. The measurement was carried out using the NIDEK OPD-Scan aberrometer and topographer equipped with the OPD-Station software, version 1.02 (NIDEK Co Ltd, Gamagori, Japan). The OPD-Scan device is an aberrometer that uses dynamic skiascopy, an automated form of retinoscopy, to measure the aberrations of the eye. The OPD-Scan plots the total aberrations of the eye, corneal aberrations, and internal aberrations. In addition, the capability of this instrument to measure normal to extremely aberrated eyes made it the instrument of choice for this investigation. The integrated corneal topographer provides a number of corneal topography maps that allow extensive evaluation of the cornea. The OPD-Station software allows isolation of corneal or internal aberrations and total aberration to determine the effect of each optical component of the eye on visual function and quality. The OPD-Station software can simulate MTF and plot MTF graphs using the Holladay Summary. In this study, corneal astigmatism was measured using the change in simulated keratometry (ΔSimK) values, the difference in power between the steep and flat meridians, which were obtained from the OPD-Scan. Corneal wavefront aberration to the sixth order and a 5-mm optical zone of the cornea were analyzed. The spatial frequencies at 0.5 MTF and 0.1 MTF of the cor-

TABLE 2

Wavefront Error Values (μm) of Corneal High Order Aberrations After Microincision Cataract Surgery and Small Incision Cataract Surgery Measured to the Sixth Order for a 5-mm Pupil Size

Cataract Surgery	HOA	Total Sphere	Total Coma	Total Trefoil	Total Quadrafoil
Microincision	2.04±1.23	0.26±0.23	0.85±0.68	1.30±0.95	0.74±0.52
Small incision	1.80±0.87	0.28±0.23	0.67±0.38	1.06±0.63	0.80±0.50
P value	.408	.680	.260	.265	.645

Note. High order aberration (HOA) denotes total higher order aberration excluding lower order aberrations such as sphere and cylinder.

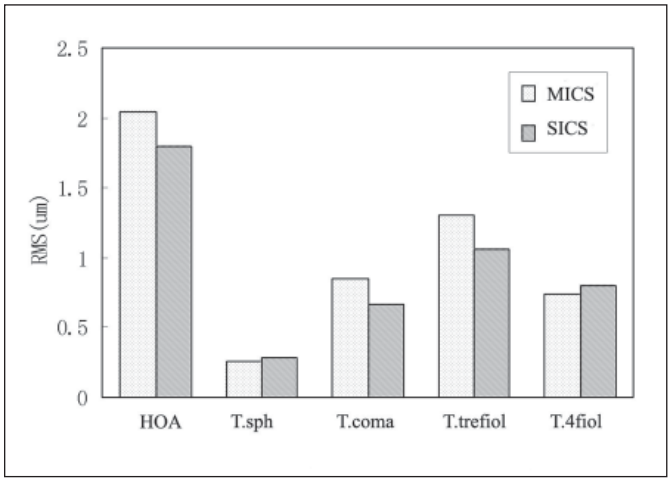

Figure 1. Corneal high order aberrations following microincision cataract surgery (MICS) performed through an ~1.7-mm incision and small incision cataract surgery (SICS) performed through an ~3.2-mm incision.

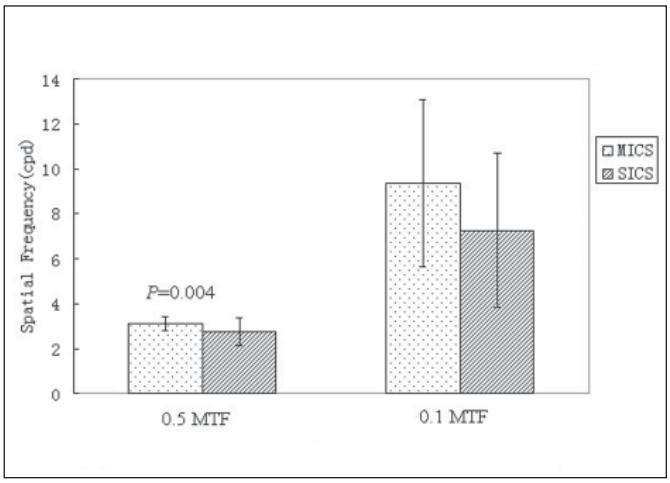

Figure 2. Spatial frequency (cpd) for 0.5 modulation transfer function (MTF) and 1.0 MTF. The difference in 0.5 MTF values was statistically significant (*P*=.004).

nea for a 5-mm pupil size were analyzed as parameters of optical quality.

Statistical Analysis

Analyses were performed using SPSS 11.0 for Windows (SPSS, Chicago, Ill). All values are presented as mean±standard deviation (SD). The comparison between microincision cataract surgery and small incision cataract surgery was established by the independent *t* test. A *P* value <.05 was considered statistically significant.

RESULTS

Microincision cataract surgery was performed on 30 eyes, and small incision cataract surgery was performed on 30 eyes. The baseline data for both groups including age, ΔSimK, and corneal power values are shown in Table 1. There was no statistically significant difference between the two groups for age, ΔSimK, and corneal power preoperatively.

The mean postoperative ΔSimK value was 0.78±0.38 D for group 1 and 1.29±0.68 D for group 2. The difference between the two groups was statistically significant (*P*=.001).

The mean postoperative total corneal high order aberration values were 2.04±1.23 μm for group 1 and 1.80±0.87 μm for group 2. The difference between groups was not significant (*P*=.408). Analyses of some individual Zernike terms such as total spherical aberrations, total coma aberrations, total trefoil, and total quadrafoil aberrations showed no significant difference between groups (Table 2; Fig 1).

Figure 2 plots the 0.5 MTF and 0.1 MTF values. For group 1, the mean 0.5 MTF value was 3.13±0.30 cycles per degree (cpd); for group 2 it was 2.75±0.63 cpd. The difference in 0.5 MTF values between groups was statistically significant (*P*=.004). For group 1, the mean 0.1 MTF value was 9.37±3.72 cpd; for group 2 it was 7.24±3.43 cpd. This difference in 0.1 MTF values was not statistically significant (*P*=.134).

DISCUSSION

Cataract surgery techniques and technology have been evolving over the past two decades, and efforts

to reduce incision size have led to a new generation of microincision cataract surgery. Any incision on the cornea can potentially alter the optical power of the cornea; thus, it is assumed that smaller incisions will likely produce less surgically induced astigmatism. In this investigation of microincision cataract surgery and small incision cataract surgery, the smaller incision size associated with microincision cataract surgery resulted in significantly less postoperative corneal astigmatism. The results of this study confirm previous reports that used vectorial analysis to compare changes in astigmatism of eyes following microincision cataract surgery versus coaxial phacoemulsification.[5] Although traditional small incision cataract surgery is an excellent procedure, which induces low levels of astigmatism, microincision cataract surgery offers the potential for true astigmatically neutral incisions.

The optical quality of the cornea may be degraded not only because of low order aberrations such as astigmatism and defocus but also because of high order aberrations, which cannot be corrected effectively with spectacles.[7] The recent development of wavefront aberrometers for clinical use presents a tool to measure the various optical elements of the eye, separately and collectively. Previous studies have reported decreased optical performance in pseudophakic eyes, with increased astigmatism and high order aberrations such as coma and trefoil generated on the cornea.[3] In the present study, no statistically significant difference was noted between microincision cataract surgery and small incision cataract surgery with respect to generating total high order aberrations. Furthermore, there was no significant difference in individual higher order aberrations such as spherical aberration, coma, and trefoil. This study demonstrates that microincision cataract surgery has no significant advantage over traditional small incision cataract surgery with respect to minimizing the induction of corneal high order aberrations.

The corneal aberration data obtained by the OPD-Scan can be simulated as point spread function (PSF) and MTF values using the OPD-Station software. The PSF and MTF are metrics that indicate the retinal image quality from an incoming object. Data at 0.5 MTF represent the spatial frequency (cpd) at which the image contrast is degraded by 50% compared with the object contrast. Data at 0.1 MTF represent the spatial frequency in which the image contrast is degraded by 90% compared with the object contrast and correspond to the maximum resolution of the optical system.[6] Results of the current study show that microincision cataract surgery has a better MTF performance at 0.5 MTF than small incision cataract surgery, suggesting that microincision cataract surgery may improve the corneal optical quality to some degree over traditional surgery.

In conclusion, microincision cataract surgery minimized surgically induced astigmatism and showed a tendency toward improved optical quality of cornea compared with small incision cataract surgery. However, no difference was found in induction of total or high order aberrations between the techniques.

REFERENCES

1. Naeser K, Knudse EB, Hansen MK. Bivariate polar value analysis of surgically induced astigmatism. *J Refract Surg*. 2002;18:72-78.
2. Guirao A, Redondo M, Geraghty E, Piers P, Norrby S, Artal P. Corneal optical aberrations and retinal image quality in patients in whom monofocal intraocular lenses were implanted. *Arch Ophthalmol*. 2002;120:1143-1151.
3. Guirao A, Tejedor J, Artal P. Corneal aberrations before and after small-incision cataract surgery. *Invest Ophthalmol Vis Sci*. 2004;45:4312-4319.
4. Weikert MP. Update on bimanual microincisional cataract surgery. *Curr Opin Ophthalmol*. 2006;17:62-67.
5. Alio J, Rodriguez-Prats JL, Galal A, Ramzy M. Outcomes of microincision cataract surgery versus coaxial phacoemulsification. *Ophthalmology*. 2005;112:1997-2003.
6. Alio JL, Schimchak P, Montes-Mico R, Galal A. Retinal image quality after microincision intraocular lens implantation. *J Cataract Refract Surg*. 2005;31:1557-1560.
7. Holladay JT. Optical quality and refractive surgery. *Int Ophthalmol Clin*. 2003;43:119-136.

Changes in Corneal Astigmatism and High Order Aberrations After Clear Corneal Tunnel Phacoemulsification Guided by Corneal Topography

Yongxiang Jiang, PhD; Qihua Le, PhD; Jin Yang, MD; Yi Lu, MD

ABSTRACT

PURPOSE: To study changes in corneal astigmatism and high order aberrations after clear corneal tunnel phacoemulsification guided by corneal topography.

METHODS: All patients were randomly assigned to the test group or the control group. Corneal topography-guided clear corneal tunnel phacoemulsification followed by intraocular lens (IOL) implantation was performed on 22 eyes of 16 patients in the test group and conventional temporal corneal tunnel phacoemulsification and IOL implantation were performed on 22 eyes of 21 patients in the control group. The corneal astigmatism and high order aberrations were measured using the NIDEK OPD-Scan aberrometer and topographer preoperatively and up to 3 months after surgery. The corneal astigmatism and sixth order root-mean-square (RMS) for corneal coma, trefoil, spherical, secondary coma, and secondary spherical aberrations at 4-mm pupil diameters were compared.

RESULTS: Fifteen (69%) eyes in the test group and 8 (36%) eyes in the control group achieved ⩾20/25 uncorrected visual acuity 3 months after surgery, which was statistically significant ($P<.05$). The best spectacle-corrected visual acuity was ⩾20/20 in 14 (63%) eyes in the test group and 10 (45%) eyes in the control group. The mean surgically induced astigmatism in the test group was 0.58±0.39 diopters (D) compared with 0.73±0.41 D in the control group. The change in corneal astigmatism from preoperative to 3 months after surgery was −0.17±0.32 D for the test group and 0.10±0.41 D for the control group, which was statistically significant ($P<.05$). The RMS value of trefoil aberrations increased, and all other aberrations decreased at 3 months after surgery in the test group. The RMS values of all corneal high order aberrations increased in the control group, with the increase in trefoil being statistically significant. The comparison of surgically induced high order aberrations between the two groups showed that corneal coma, trefoil, and secondary coma were significantly different.

CONCLUSIONS: Clear corneal tunnel phacoemulsification and IOL implantation guided by corneal topography can yield better visual acuity by reducing the pre-existing astigmatism and inducing less corneal aberrations than conventional temporal corneal tunnel phacoemulsification. [*J Refract Surg*. 2006;22:S1083-S1088.]

Cataracts are the leading cause of visual impairment and blindness in the world. Currently, phacoemulsification with intraocular lens (IOL) implantation is the most popular treatment for cataracts. With the improvement in surgical techniques and the development of new technology, the recovery of visual function has improved.[1-6] In recent years, phacoemulsification through a clear corneal tunnel incision has become increasingly popular due to ease of the technique, reduced length of surgery, little to no trauma to the conjunctiva, less surgically induced astigmatism, and quick rehabilitation of vision.[1,7]

Corneal astigmatism plays an important role in the recovery of visual function after cataract surgery. The corneal refractive changes are attributed to the location and size of the corneal incision.[1,8] Conventional temporal corneal tunnel phacoemulsification without sutures can produce with-the-rule astigmatism, because the corneal curvature at the meridian of the incision would be flattened. Such changes are not optimal for all patients with cataracts. Long and Monica[1] reported that the placement of the incision on the steeper meridian of the cornea can be beneficial if preoperative astigmatism was ⩾0.75 diopters (D). The length of the incision is another important factor that may affect the postoperative corneal astigmatism. The shorter the incision, the less the corneal astigmatism.[8] There are various types of IOLs available for implantation in cataract surgery, and efforts are being made to reduce incision size.[2,9] With the shortening of corneal tunnel incisions from 5.5 mm to 4.1 mm, 3.5 mm, 3.2 mm, and 2.8 mm, visual function postoperatively has steadily increased.[1,8,10-12] It is anticipated that the bimanual microincision technique will allow phacoemulsification through a 1.2- to 1.7-mm clear corneal tunnel incision.[5,13-15] However,

From the Department of Ophthalmology, Eye and ENT Hospital of Fudan University, Shanghai, China.

The authors have no financial or proprietary interest in the materials presented herein.

Correspondence: Yi Lu, MD, Dept of Ophthalmology, Eye and ENT Hospital of Fudan University, Shanghai 200031, China. Tel: 86 021 64377134; Fax: 86 021 64377151; E-mail: luyi_eent@yahoo.com.cn

Olson and Crandall[9] and Oshika and Tsuboi[16] found that an incision <2.0 mm had no impact on corneal curvature. The bimanual technique is not yet widely available, especially in developing countries.

To correct pre-existing astigmatism and minimize surgically induced astigmatism, we adopted 2.6-mm clear corneal tunnel phacoemulsification and IOL implantation guided by corneal topography with the incision placed at the steepest corneal meridian. The goal was to evaluate the changes in corneal astigmatism and high order aberrations after surgery compared with those achieved in traditional surgery with the incision placed temporally. The outcomes of the study may assist the surgeon in selecting the optimal surgical plan for individual cataract patients.

PATIENTS AND METHODS

Patient Population

A total of 37 patients (44 eyes) between the ages of 54 and 82 years (mean age: 65.05±9.53 years) were randomly assigned to either the test group or the control group. Each case was numbered and those with odd numbers were assigned to the test group and those with even numbers to the control group. A 2.6-mm clear corneal tunnel phacoemulsification/IOL implantation guided by corneal topography was performed on 22 eyes of 16 patients in the test group, and conventional temporal corneal tunnel phacoemulsification with IOL implantation was performed in 22 eyes of 21 patients in the control group. Selection criteria included good general health, absence of corneal pathology during slit-lamp microscopy examination, no previous corneal or scleral surgery, absence of severe retinal pathology that could affect the infrared ray reflection from the macula during ocular wavefront aberration measurement, and no complications during or after surgery.[2,7] An explanation of the study was given to all patients and informed consent obtained.

Examination

Clinical examinations were conducted preoperatively and at 1 week, 2 weeks, 1 month, and 3 months after surgery. Clinical examination included best spectacle-corrected visual acuity (BSCVA) and uncorrected visual acuity (UCVA), manifest and cycloplegic refractions, intraocular pressure, and anterior and posterior segment evaluation. The corneal astigmatism and high order aberrations were measured using the NIDEK OPD-Scan aberrometer/topographer (NIDEK Co Ltd, Gamagori, Japan), which uses skiascopy-based ocular aberrometry using 1440 infrared points and placido disk corneal topography.[7] The OPD-Station software (NIDEK Co Ltd) was used to isolate corneal aberration out to the sixth order.

Surgical Technique

All surgeries were performed under topical anesthesia by the same surgeon (L.Y.). Conventional temporal corneal tunnel phacoemulsification and IOL implantation were performed on the patients in the control group. A 2.6×2.0- to 2.5-mm temporal clear corneal tunnel incision was used. A 0.6-mm wide paracentesis was carried out for the insertion of the chopper. Subsequently, Duovisc (Alcon Laboratories, Ft Worth, Tex) was used to maintain the anterior chamber, and a continuous curvilinear capsulorrhexis and hydrodissection were performed. Endocapsular phacoemulsification of the nucleus with Phacochop or "stop-and-chop" techniques and cortical aspiration were performed using an Infinite or Legacy phacoemulsifier (Alcon Laboratories). The anterior chamber and the capsular bag were refilled with Duovisc. A foldable IOL was inserted into the capsular bag using an injector cartridge system. The residual viscoelastic material was removed using an irrigation/aspiration handpiece. Balanced salt solution was injected through the paracentesis to maintain the anterior chamber. At the end of surgery, the wound was checked and found to be watertight. All surgeries were completed without sutures. Postoperatively, all patients were treated with topical 0.1% Tobradex (Alcon Laboratories) and 0.1% Pranoprofen (Sumika Finechem, Osaka, Japan) three times a day for 1 month. All patients in the test group underwent the same surgical procedure as those in the control group with the exception that incisions were placed on the steepest corneal meridian, which were determined using the OPD-Scan axial corneal topography.

Statistical Analysis

The mean corneal astigmatism, the surgically induced astigmatism, and the root-mean-square (RMS) of corneal coma, trefoil, spherical aberration, secondary coma, and secondary spherical aberration for a 4-mm pupil diameter before and after surgery were compared. The surgically induced astigmatism was calculated and standardized using Jaffe's vector analysis. The statistics were performed using the STATA 8.0 (Stata Corp, College Station, Tex) statistical software. The chi-square test, *t* test, Scheffe test, nonparametric Wilcoxon signed-rank test, Mann-Whitney test, and Kruskal-Wallis test were used to analyze the variables studied. A P value <.05 was considered statistically significant.

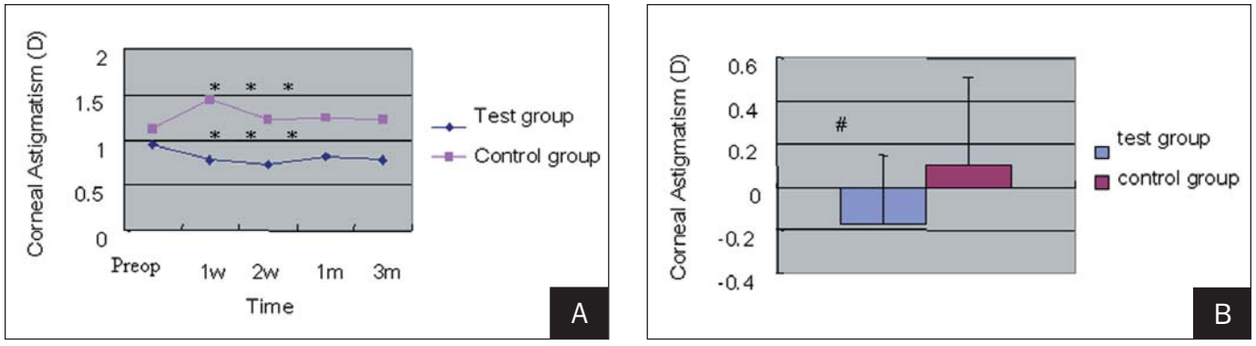

Figure 1. A) The mean values of corneal astigmatism in two groups preoperatively and 1 week, 2 weeks, 1 month, and 3 months after surgery. No statistically significant difference was noted between the mean value of corneal astigmatism at 1 week and 2 weeks, 1 month, and 3 months after surgery. *$P>.05$. **B)** The change in corneal astigmatism induced by cataract surgery 3 months postoperatively. The test group versus the control group, $P<.05$.

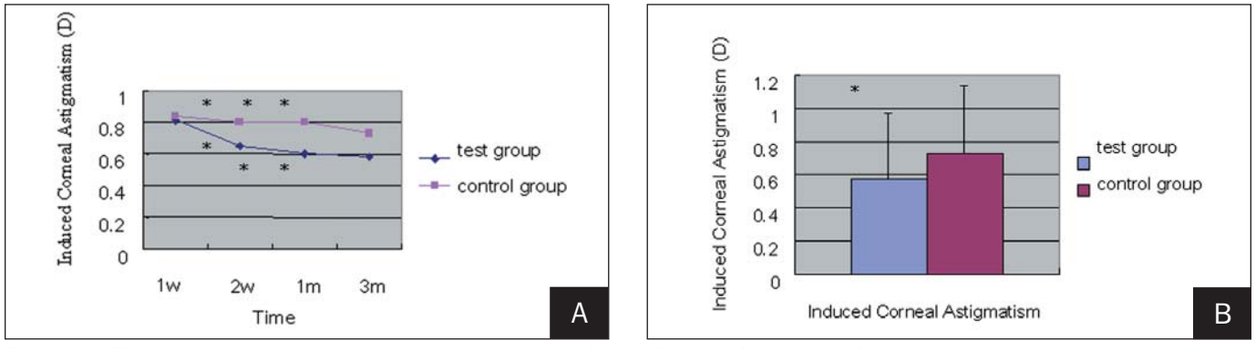

Figure 2. A) The amount of surgically induced corneal astigmatism at 1 week, 2 weeks, 1 month, and 3 months postoperatively in the test and control groups. No statistically significant difference was noted between the mean values of surgically induced corneal astigmatism at each time point. *$P>.05$. **B)** Surgically induced corneal astigmatism 3 months postoperatively in the test group versus control group (*$P>.05$). Surgically induced corneal astigmatism was analyzed using the vector method described by Jaffe.

RESULTS

At 3 months after surgery, 15 (68%) eyes in the test group and 8 (36%) eyes in the control group achieved UCVA ⩾20/25. This difference in postoperative UCVA was statistically significant ($P<.05$). Fourteen (64%) eyes achieved BSCVA ⩾20/20 postoperatively in the test group, and 10 (45%) eyes achieved BSCVA ⩾20/20 postoperatively in the control group. This difference in postoperative BSCVA was not statistically significant ($P>.05$).

Figure 1A shows the mean values of corneal astigmatism in both groups preoperatively and at 1 week, 2 weeks, 1 month, and 3 months after surgery. The mean change in corneal astigmatism preoperatively to 3 months in the test group was -0.17 ± 0.32 D (preoperatively, 0.95 ± 0.60 D and 3 months postoperatively, 0.78 ± 0.56 D). The mean change in corneal astigmatism preoperatively to 3 months in the control group was 0.10 ± 0.41 D (preoperatively, 1.12 ± 0.64 D and 3 months postoperatively, 1.22 ± 0.55 D). The difference in the mean change in corneal astigmatism between both groups was statistically significant ($P<.05$) (Fig 1B). The mean values of surgically induced corneal astigmatism at 1 week, 2 weeks, 1 month, and 3 months after surgery in the test and control groups are shown in Figure 2A. The mean surgically induced astigmatism at 3 months postoperatively was 0.58 ± 0.39 D for the test group and 0.73 ± 0.41 D for the control group. This difference was not statistically significant ($P>.05$) (Fig 2B).

The change of corneal high order aberrations for 4-mm pupil diameters in the test and control groups are shown in Figures 3 and 4, respectively. Trefoil increased at 3 months postoperatively in the test group. Coma, spherical, secondary coma, and secondary spherical aberrations decreased 3 months postoperatively in the test group (see Fig 3). None of the changes in corneal higher order aberrations were statistically significant (see Fig 3). All of the corneal high order aberrations in the control group increased 3 months postoperatively (see Fig 4). The only statistically significant change in individual aberrations from pre- to postoperatively in the control group was trefoil ($P<.05$) (see Fig 4).

Figure 5 demonstrates a typical example of the induced changes in corneal third order aberrations pre-

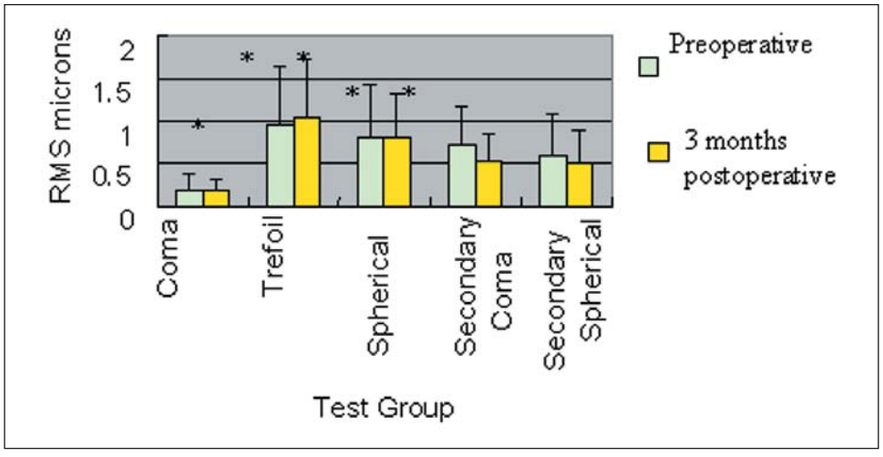

Figure 3. Root-mean-square (RMS) value of corneal high order aberrations at 4-mm pupil diameters in the test group. Preoperative versus postoperative (*P>.05).

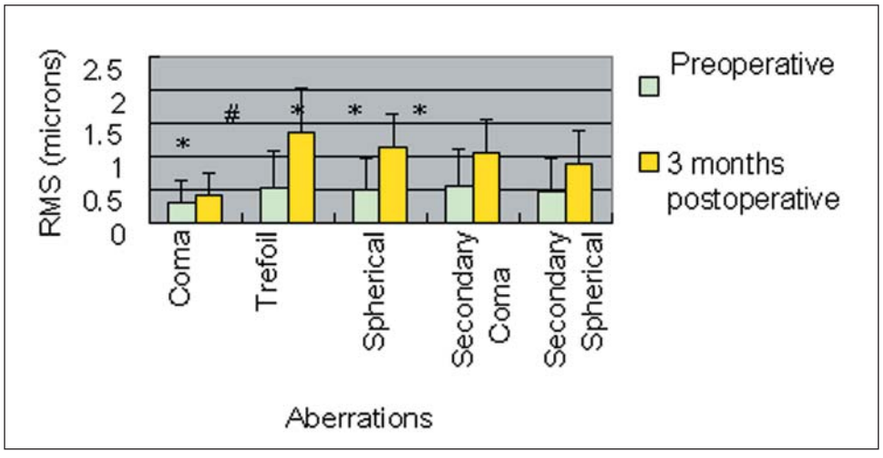

Figure 4. Root-mean-square (RMS) value of corneal high order aberrations at 4-mm pupil diameters in the control group. Preoperative versus postoperative (*P>.05; #P<.05).

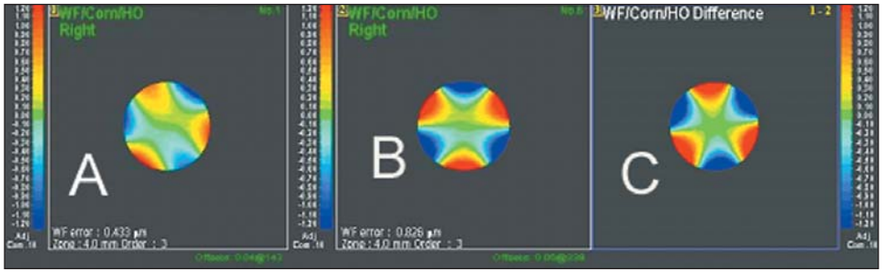

Figure 5. A typical example of changes in third order corneal higher order aberrations for a 4-mm pupil diameter of an eye before and after surgery in the test group. **A)** Coma and trefoil aberrations before surgery. **B)** Aberrations at 3 months after surgery. **C)** Difference map of surgically induced third order aberrations before and after surgery.

and postoperatively in the test group. At 3 months after surgery, a trefoil pattern dominates the third order aberrations, and coma is diminished (see Fig 5). Figure 6 demonstrates a typical example of the induced changes in corneal third order aberrations pre- and postoperatively in the control group. At 3 months after surgery, coma and trefoil dominate the third order aberrations and direction of the trefoil pattern has reversed (see Fig 6).

The comparison of surgically induced corneal higher aberrations between the two groups at 3 months after surgery show that corneal coma, trefoil, and secondary coma were statistically significantly different (P<.05), whereas the spherical and secondary spherical aberrations were not significantly different (P>.05) (Fig 7).

DISCUSSION

The optical quality of the pseudophakic eye is determined by the combination of corneal and internal aberrations generated by the IOL[2] and those induced by surgery. Spherical aberration is determined by the corneal asphericity.[17] In this study, corneal astigmatism and high order aberrations were evaluated as a

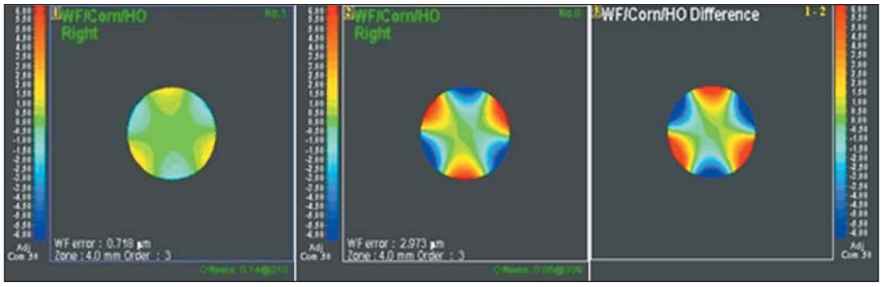

Figure 6. A typical example of changes in third order corneal higher order aberrations for a 4-mm pupil diameter of an eye before and after surgery in the control group. **A)** Coma and trefoil aberrations before surgery. **B)** Aberrations 3 months after surgery. **C)** Difference map showing surgically induced third order aberrations.

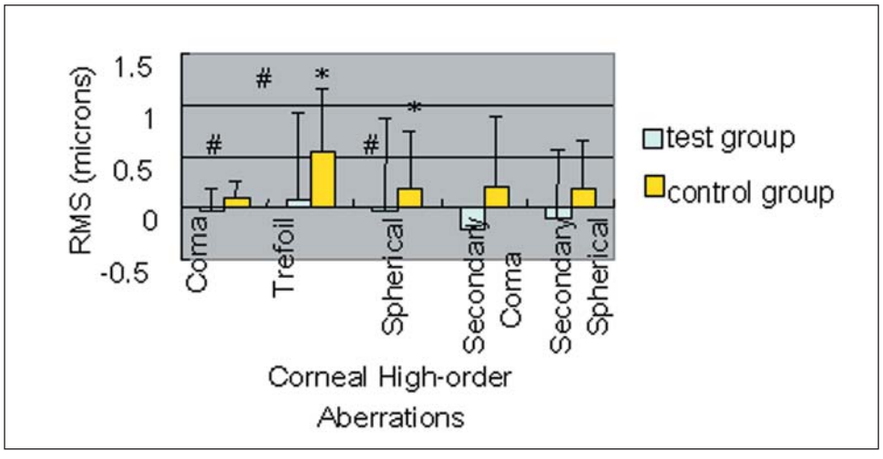

Figure 7. Surgically induced high order aberrations at 3 months after surgery for the test group versus the control group (*P>.05; #P<.05).

measure of change in the cornea after cataract surgery.

A statistically significantly greater number of patients in the test group read ⩾20/25 with correction than in the control group (P<.05). Greater astigmatic correction occurred in the test group shown by the statistically significant change in corneal astigmatism from pre- to postoperatively (P<.05). Based on these data, we believe that a 2.6-mm clear corneal tunnel phacoemulsification and IOL implantation guided by corneal topography can correct astigmatism as low as 0.25 D, resulting in better postoperative visual acuity. For higher preoperative astigmatism, a clear corneal incision placed at the steepest meridian may be beneficial.[10] Although not statistically significant, there were slight differences between groups with respect to surgically induced astigmatism at 1 week, 2 weeks, 1 month, and 3 months postoperatively. However, from 2 weeks to 3 months postoperatively, the corneal astigmatism showed little change, indicating that the 2.6-mm clear corneal tunnel incision was fully stable by 2 weeks postoperatively. This finding is similar to that reported by Masket and Tennen.[18]

The quality of the retinal image is primarily limited by the aberrations of the eye.[4] The total ocular aberrations include corneal aberrations and internal aberrations. One study reported that the average retinal image quality of pseudophakic patients was worse than that in healthy younger subjects because of an increase in aberrations postoperatively.[19] The lower the aberrations, the better the optical quality. Many studies show cataract surgery with IOL implantation can increase corneal aberrations[2,17,20] and internal aberrations.[21-25] However, Marcos et al[2] found that corneal spherical aberration decreased after the surgery. This study reports a similar result.

The present investigators elected to study aberrations for a 4-mm pupil diameter, because pseudophakic eyes rarely dilate to 6 mm without dilating drops.[7] This investigation found no statistically significant change in any of the higher order aberrations postoperatively. This was likely due to the size and location of the incision. Another reason might be the small number of patients; thus sampling error cannot be fully excluded. In the control group, a statistically significant increase was noted in trefoil postoperatively versus preoperatively (P<.05). The comparison of surgically induced higher order aberrations between the two groups shows that corneal coma, trefoil, and secondary coma were significantly different. These changes indicated that 2.6-mm clear corneal tunnel phacoemulsification and IOL implantation guided by topography produced less corneal high order aberration and resulted in better corneal optical quality.

Clear corneal tunnel phacoemulsification and IOL

implantation guided by corneal topography induce less astigmatism and less corneal higher order aberrations compared with temporally placed incisions, both of which can lead to better recovery of visual acuity after surgery.

REFERENCES

1. Long DA, Monica ML. A prospective evaluation of corneal curvature changes with 3.0- to 3.5-mm corneal tunnel phacoemulsification. *Ophthalmology.* 1996;103:226-232.
2. Marcos S, Barbero SP, Jimenez-Alfaro I. Optical quality and depth-of-field of eyes implanted with spherical and aspheric intraocular lenses. *J Refract Surg.* 2005;21:223-235.
3. Kojima T, Kaga T, Watanabe M, Uda K, Naito N, Saito Y, Ichikawa K. Clinical evaluation of the arched blade for cataract surgery. *Ophthalmol Scand.* 2005;83:306-311.
4. Guirao A, Tejedor J, Artal P. Corneal aberrations before and after small-incision cataract surgery. *Invest Ophthalmol Vis Sci.* 2004;45:4312-4319.
5. Assaf A, El-Moatassem Kotb AM. Feasibility of bimanual microincision phacoemulsification in hard cataracts. *Eye.* 2006;Epub.
6. Souza CE, Gerente VM, Chalita MR, Soriano ES, Freitas LL, Belfort R Jr. Visual acuity, contrast sensitivity, reading speed, and wavefront analysis: pseudophakic eye with multifocal IOL (ReSTOR) versus fellow phakic eye in non-presbyopic patients. *J Refract Surg.* 2006;22:303-305.
7. Billucci R, Morselli S, Piers P. Comparison of wavefront aberrations and optical quality of eyes implanted with five different intraocular lenses. *J Refract Surg.* 2004;20:297-306.
8. Hayashi K, Hayashi H, Nakao F, Hayashi F. The correlation between incision size and corneal shape changes in sutureless cataract surgery. *Ophthalmology.* 1995;102:550-556.
9. Olson RJ, Crandall AS. Prospective randomized comparison of phacoemulsification cataract surgery with a 3.2-mm vs 5.5-mm sutureless incision. *Am J Ophthalmol.* 1998;125:612-620.
10. Lever J, Dahan E. Opposite clear corneal incisions to correct pre-existing astigmatism in cataract surgery. *J Cataract Refract Surg.* 2000;26:803-805.
11. Oshika T, Tsuboi S, Yaguchi S, Yoshitomi F, Nagamoto T, Nagahara K, Emi K. Comparative study of intraocular lens implantation through 3.2- and 5.5-mm incisions. *Ophthalmology.* 1994;101:1183-1190.
12. Holladay JT, Piers PA, Koranyi G, van der Mooren M, Norrby NE. A new intraocular lens design to reduce spherical aberration of pseudophakic eyes. *J Refract Surg.* 2002;18:683-691.
13. Prakash P, Kasaby HE, Aggarwal RK, Humfrey S. Microincision bimanual phacoemulsification and Thinoptx implantation through a 1.70-mm incision. *Eye.* 2006;Epub.
14. Weikert MP. Update on bimanual microincisional cataract surgery. *Curr Opin Ophthalmol.* 2006;17:62-67.
15. Hoffman RS, Fine IH, Packer M. New phacoemulsification technology. *Opin Ophthalmol.* 2005;16:38-43.
16. Oshika T, Tsuboi S. Astigmatic and refractive stabilization after cataract surgery. *Ophthalmic Surg.* 1995;26:309-315.
17. Antonoo G, Manuel R, Edward G, Patricia P, Sverker N, Pablo A. Corneal optical aberrations and retinal image quality in patients in whom monofocal intraocular lenses were implanted. *Arch Ophthalmol.* 2002;120:1143-1151.
18. Masket S, Tennen DG. Astigmatic stabilization of 3.0 mm temporal clear corneal cataract incisions. *J Cataract Refract Surg.* 1996;22:1451-1455.
19. Guirao A, Redondo M, Geraghty E, Piers P, Norrby S, Artal P. Corneal optical aberrations and retinal image quality in patients in whom monofocal intraocular lenses were implanted. *Arch Ophthalmol.* 2002;120:1143-1151.
20. Barbero S, Marcos S, Jimenez-Alfaro I. Optical aberrations of intraocular lenses measured in vivo and in vitro. *J Opt Soc Am A Opt Image Vis Sci.* 2003;20:1841-1851.
21. Padmanabhan P, Rao SK, Jayasree R, Chowdhry M. Monochromatic aberrations in eyes with different intraocular lens optic designs. *J Refract Surg.* 2006;22:172-177.
22. Pesudovs K, Dietze H, Stewart OG, Noble BA, Cox MJ. Effect of cataract surgery incision location and intraocular lens type on ocular aberrations. *J Cataract Refract Surg.* 2005;31:725-734.
23. Fabrizio C, Angelo B, Gian Marco T, Flavia M, Gianluca M, Gabriele C, Aldo C. Glare disability and spherical aberration with five foldable intraocular lenses: a prospective randomized study. *Acta Ophthalmol Scand.* 2005;83:20-25.
24. Padmanabhan P, Yoon G, Porter J, Rao SK, Roy J, Choudhry M. Wavefront aberrations in eyes with Acrysof monofocal intraocular lenses. *J Refract Surg.* 2006;22:237-243.
25. Chandhrasri S, Knorz MC. Comparison of higher order aberrations and contrast sensitivity after LASIK, Verisyse phakic IOL, and Array multifocal IOL. *J Refract Surg.* 2006;22:231-236.

Automated Visual Axis Alignment for Refractive Excimer Laser Ablation

Omid Kermani, MD

ABSTRACT

PURPOSE: To describe the use of new laser alignment and delivery software in the NIDEK Advanced Vision Excimer laser platform (NAVEX) that allows centration based on surgeon specification.

METHODS: Descriptive article with a case report.

RESULTS: The software allows specification via numeric entry of the exact placement of the laser tapered to the position of the visual axis or the line of sight.

CONCLUSIONS: The ability to specify the exact location of the laser ablation based on pupil position is fundamental in patients undergoing custom ablation and those with eccentric fixation. A conservative treatment strategy is recommended for initial experience with this alignment software. [*J Refract Surg*. 2006;22:S1089-S1092.]

In refractive excimer laser ablation (LASIK or surface ablation) of hyperopia and myopia, it should be the surgeon who determines which axis to choose for centration—the line of sight, the visual axis, or any point between these two landmarks. The correct alignment of the individually applied laser profile plays a fundamental role in the quality of refractive excimer laser ablation. Even minor lateral misalignments can impair the effect of the treatment.[1-3]

The line of sight is defined by the fixation point at one end and the center of the entrance pupil at the other.[4] The center of the entrance pupil is, in theory, a well-defined point. However, in practical terms, it is variable in position. For example, the entrance pupil center is known to change in position as the pupil size changes.[5] This is one of the reasons why aberrometry is best performed under mesopic conditions. Although the line of sight varies with different illumination conditions, the intercept of the visual axis on the cornea usually does not change its position. The visual axis is defined as the line between the fixation point and the fovea.[4] Clinically, it is difficult to locate the visual axis. However, centering the ablation zone along the intercept of the visual axis on the cornea is thought to ensure an equidistant area of refracted light to be projected around the fovea, minimizing the risk of degradation of vision. Hence, Pande and Hillman[6] recommended the visual axis as the reference axis for centration in corneal refractive procedures. In cases with significant eccentric fixation, it has been proposed, for safety reasons, to center the ablation zone half way between the center of the pupil (line of sight) and the visual axis.[7] The reason for this is the difficulty in determining the exact location of the visual axis once the flap had been reflected to expose stroma. Usually, with the flap in place, the adjustment of the first and second Purkinje images provides a good estimation of the location of the visual axis.

From Augenklinik am Neumarkt, Köln, Germany.

The author has no proprietary interest in the materials presented herein.

Correspondence: Omid Kermani, MD, Augenklinik am Neumarkt, Schildergasse 107 -109, D-50667 Köln, Germany. Tel: 49 221 650 7220; Fax: 49 221 650 72279; E-mail: o.kermani@augenportal.de

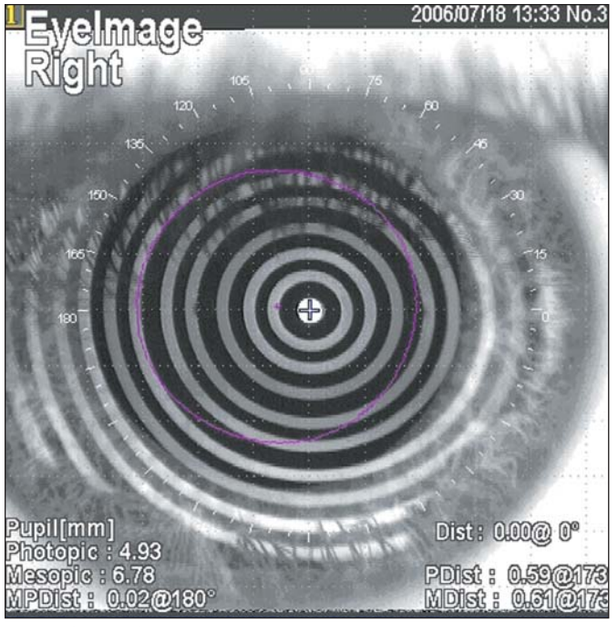

Figure 1. OPD-Scan video image of the eye, depicting the quality of the Placido images and denoting both the central corneal light reflex (blue cross) and the line of sight (purple cross).

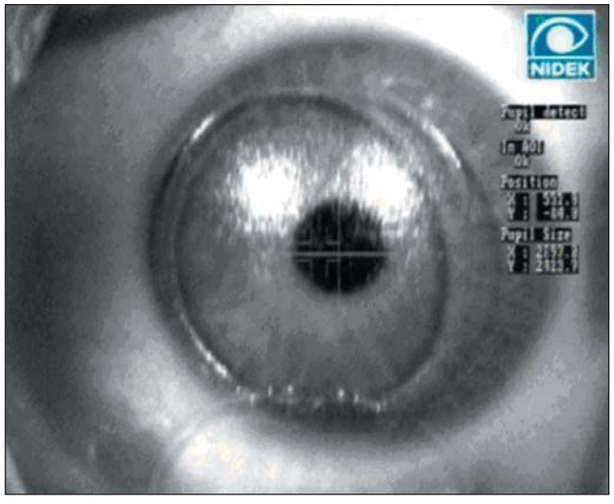

Figure 2. During treatment the center purple cross denotes the actual position of the ablation center, which is in line with the eccentric visual axis in this example. The green cross shows the actual torsional alignment (−1°). Note that the flap with a superior hinge was intentionally centered on the eccentric pupil using a femtosecond surgical laser (IntraLase, Irvine, Calif).

New excimer laser software by NIDEK Co Ltd (Gamagori, Japan) (version 5.27 on CXII or earlier, 8.10 on CXIII models) now allows the automated alignment of the ablation zone on the visual axis during surgery. During the preoperative workup, the OPD-Scan (NIDEK Co Ltd) first identifies and then digitally marks the position of the mesopic and photopic line of sight relative to the coaxial corneal light reflex, which is close to, but not exactly the "visual axis" (Fig 1). The differences between this central corneal reflex and the mesopic or photopic pupil center are computed and given as "MDist" and "PDist" values, respectively. The data are then transferred with all of the other information measured by OPD-Scan into the Final Fit software for preparation of the actual shot data.

For custom ablations, which include multipoint spot ablation (customized aspheric treatment zone and optical path difference customized ablation treatment), the surgeon must determine the centration strategy during the shot file preparation. Selecting the "LOS-Shot Data" function "off" keeps the irregularity ablation (spot ablation) component centered on the corneal reflex (close to the visual axis). With the "LOS-Shot Data" option "on" it will shift the irregularity ablation (spot ablation) component to the pupil center. This option is used in case the surgeon decides to keep the centration for sphere and cylinder on the eye tracker's default position, the pupil center. However, when the surgeon decides to center the sphere and cylinder treatment on the visual axis, MDist/PDist coordinates are used for precise alignment of the ablation zone (Fig 2). With this new software, the surgeon can choose the exact landmark for alignment by entering numerical values into the laser software rather than manually shifting the ablation center with the joystick. Future Final Fit software versions will fully automate this step by processing and transferring the MDist/PDist information automatically with the Final Fit laser shot file. This will likely help improve custom ablation outcomes.

CASE EXAMPLE

A hyperopic patient with differing MDist and PDist values and an OPD-Scan refraction of $+4.28\ -1.75 \times 148$ with a best spectacle-corrected visual acuity (BSCVA) of 20/20, was treated with NAVEX. Figure 1 shows the eye image with differing values of the line of sight and the corneal light reflex. Figure 2 shows that the intraoperative alignment of the laser is designated in a position close to the central corneal reflex and not on the line of sight. The preoperative OPD-Scan map is shown in Figure 3. In this case, the full PDist value of 0.6 mm was entered into the software for laser alignment and delivery (Fig 4). Figure 4A shows that the eye tracker was correctly tracking the predetermined region of the pupil. Figure 4B shows the laser delivery was being delivered to the same region. Postoperatively, the corneal topography shows a mild decentration relative to the area of the central corneal reflex. This is due to the fact that we used 100% PDist as the center offset value

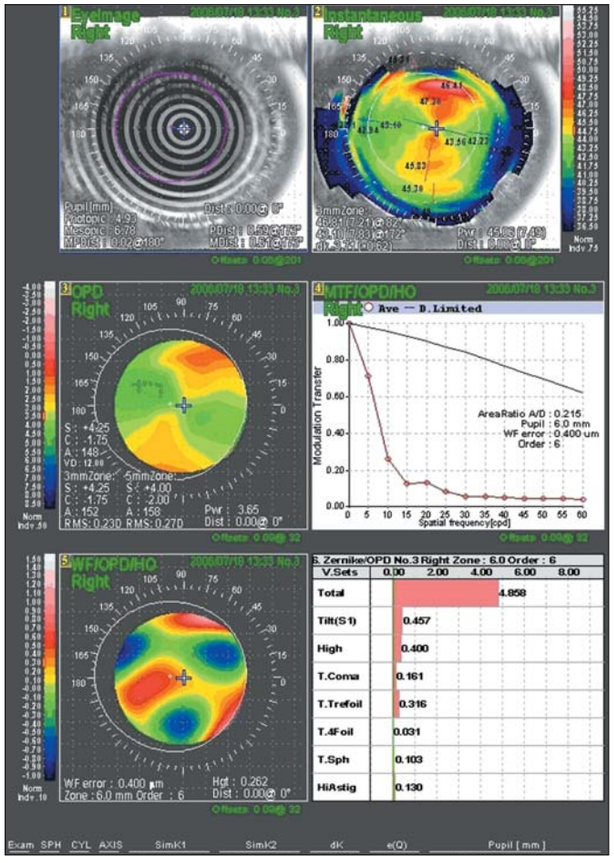

Figure 3. Preoperative diagnostic evaluation using the OPD-Scan. Top left shows the eye image for quality control and iris registration; top right shows instantaneous corneal topography; middle left shows spatially resolved refraction (aberrometry for 6.0 mm) in diopters; middle right shows the modulation transfer function (MTF) with the red line plotting the patient's eye and the blue line plotting the limit of MTF; bottom left shows the higher order (higher order without tilt, sphere, and cylinder) map; bottom right shows a selection of Zernike coefficients.

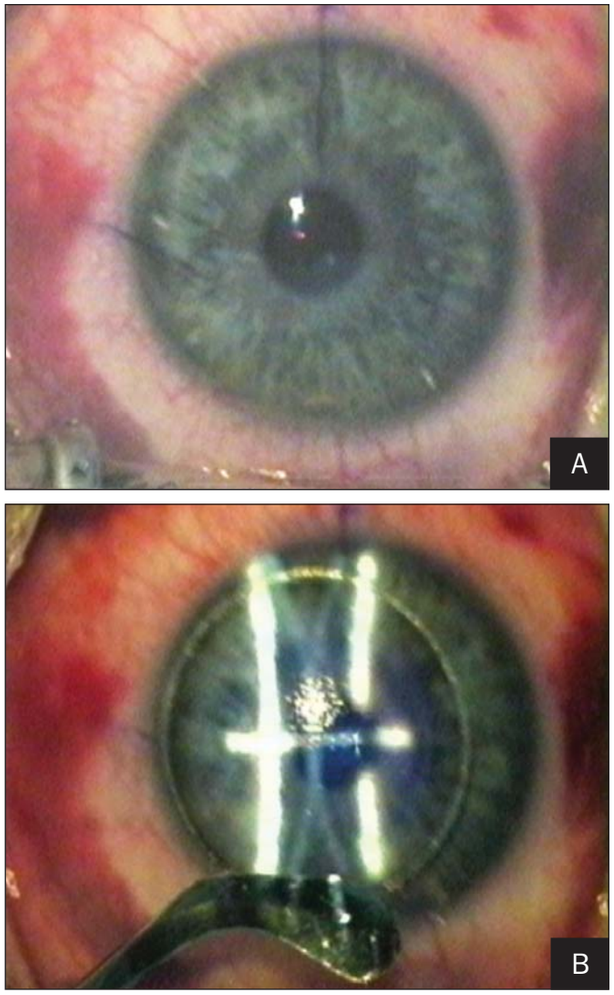

Figure 4. A) Alignment of the laser aiming diode in relation to the pupil. **B)** Laser alignment and delivery to a region of the cornea specified by the NAVEX software. (Note both images show the surgeon's view and are rotated 180° relative to the OPD-Scan images.)

in this case (Fig 5). Subjectively, the patient is asymptomatic postoperatively and uncorrected visual acuity and BSCVA are 20/20.

DISCUSSION

Based on the initial experience with this feature of the NAVEX software, only 50% of the PDist value and an incremental refinement of this value are recommended. The PDist value of the OPD-Scan represents the difference between pupil center and central corneal light reflex and is not the actual location of the visual axis, which may be only 50% to 80% of this value. The location of the intercept of the visual axis on the cornea might change with the change of corneal refraction due to laser ablation (J. Holladay, MD, personal communication, 2006).

Additionally, the change in the line of sight in differing light conditions presents a challenge that has not yet been fully addressed. For example, a change in retinal irradiance between the image and blur circle, and the breakdown of the Stiles-Crawford effect may be accentuated with an alignment strategy that does not account for change in line of sight in differing light conditions.[8]

The alignment of the laser ablation may also have to be specified in each patient taking into account his/her occupation, hobbies, and visual demands in daily life. A truck driver, for example, who does most of his driving at night will likely be more satisfied with the ablation centered on the mesopic pupil center rather

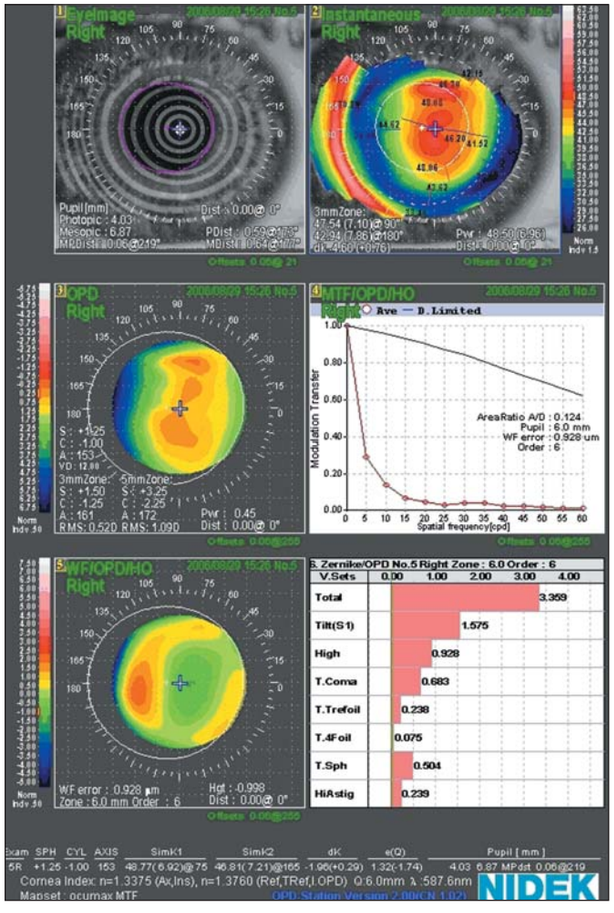

Figure 5. Postoperative diagnostic evaluation using the OPD-Scan. Top left shows the eye image for quality control and iris registration; top right shows instantaneous corneal topography; middle left shows spatially resolved refraction (aberrometry for 6.0 mm) in diopters; middle right shows the modulation transfer function (MTF) with the red line plotting the patient's eye and the blue line plotting the limit of MTF; bottom left shows the higher order (higher order without tilt, sphere, and cylinder) map; bottom right shows a selection of Zernike coefficients.

than the photopic pupil center. The ability to specify the exact center of laser ablation in relation to the pupil will be of fundamental importance for patients who have eccentric fixation such as some hyperopes, patients with significant shift in the line of sight in differing light conditions, and patients undergoing custom ablations. Software now incorporated into the NIDEK NAVEX platform represents a much more accurate method of laser alignment and delivery compared to manual centration over the visual axis.

REFERENCES

1. Bueeler M, Mrochen M, Seiler T. Maximum permissible lateral decentration in aberration-sensing and wavefront-guided corneal ablation. *J Cataract Refract Surg.* 2003;29:257-263.
2. Bueeler M, Mrochen M, Seiler T. Maximum permissible torsional misalignment in aberration-sensing and wavefront-guided corneal ablation. *J Cataract Refract Surg.* 2004;30:17-25
3. Kermani O. Alignment in customized laser in situ keratomileusis. *J Refract Surg.* 2004;20:S651-S658.
4. Thibos LN, Applegate RA, Schwiegerling JT, Webb R, VSIA Standard Taskforce Members. Standards for reporting the optical aberrations of eyes. *J Refract Surg.* 2002;18:652-660.
5. Fay AM, Trokel SL, Myers JA. Pupil diameter and the principal ray. *J Cataract Refract Surg.* 1992;18:348-351.
6. Pande M, Hillman JS. Optical zone centration in keratorefractive surgery. Entrance pupil center, visual axis coaxially sighted corneal reflex, or geometric corneal center? *Ophthalmology.* 1993;100:1230-1237.
7. Seiler T. Refractive surgical problem. *J Cataract Refract Surg.* 2000;26:1111.
8. O'Brart DPS, Lohmann CP, Fitzke FW, Klonos G, Corbett MC, Kerr-Muir MG, Marshall J. Disturbances in night vision after excimer laser photorefractive keratectomy. *Eye.* 1994;8:46-51.